

AD-A090 514

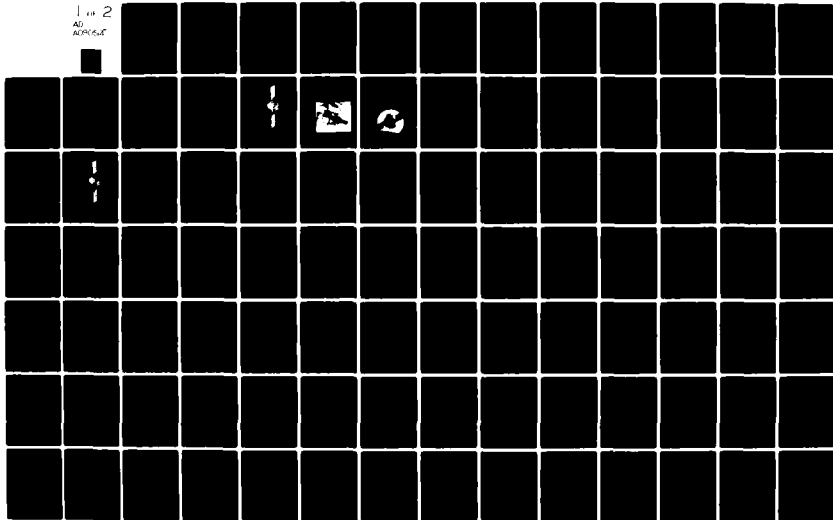
TRW DEFENSE AND SPACE SYSTEMS GROUP REDONDO BEACH CA F/6 21/3
MISSION INTEGRATION STUDY FOR SOLID TEFLON PULSED PLASMA MILLIP--ETC(U)
SEP 80 M N HUBERMAN, S ZAFRAN, M H GRAN F04611-78-C-0064

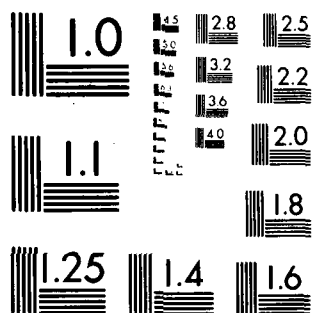
UNCLASSIFIED

AFRPL-TR-80-37

NL

1 of 2
AD
AFRPL-TR





MICROCOPY RESOLUTION TEST CHART
NATIONAL BUREAU OF STANDARDS-1963-A

AFRPL-TR-80-37

LEVEL

2

MISSION INTEGRATION STUDY FOR SOLID TEFLON PULSED PLASMA MILLIPOUND PROPULSION SYSTEM

AD A090514

AUTHORS: M. HUBERMAN
S. ZAFRAN
M.H. GRAN
R. PIEPER
J.M. SELLEN

SEPTEMBER 1980

DTIC
ELECTE
OCT 16 1980
S D C

APPROVED FOR PUBLIC RELEASE;
DISTRIBUTION UNLIMITED

AIR FORCE ROCKET PROPULSION LABORATORY
DIRECTOR OF SCIENCE AND TECHNOLOGY
AIR FORCE SYSTEMS COMMAND
EDWARDS AFB, CALIFORNIA 93523

DDC FILE COPY

TRW

DEFENSE AND SPACE SYSTEMS GROUP
ONE SPACE PARK
REDONDO BEACH • CALIFORNIA

80 10 10 022

NOTICE

When Government drawings, specifications, or other data are used for any purpose other than in connection with a definitely related Government procurement operation, the United States Government thereby incurs no responsibility nor any obligation whatsoever; and the fact that the Government may have formulated, furnished, or in any way supplied the said drawings, specifications, or other data, is not to be regarded by implication or otherwise as in any manner licensing the holder or any other person or corporation, or conveying any rights or permission to manufacture, use, or sell any patented invention that may in any way be related thereto.

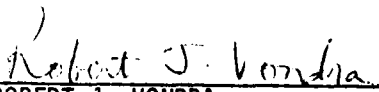
FOREWORD

This final report was prepared by the Defense and Space Systems Group of TRW, Inc., and was sponsored by the Air Force Rocket Propulsion Laboratory under Contract No. FO 4611-78-C-0064.

Work on this contract began in August 1978 and was completed in June 1980 and the pertinent studies of this period are reported herein. This report was submitted by the authors in June 1980.

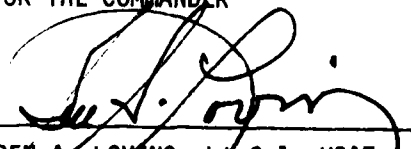
The authors wish to acknowledge the constructive technical comments and suggestions of Dr. R. Vondra of the AFRPL.

This report has been reviewed by the Information Office/XOJ and is releasable to the National Technical Information Service (NTIS). At NTIS it will be available to the general public, including foreign nations. This technical report has been reviewed and is approved for publication; it is unclassified and suitable for general public.


ROBERT J. VONDRA
Project Manager


WALTER A. DETJEN
Chief, Satellite Propulsion Branch

FOR THE COMMANDER


BEN A. LOVING, Lt Col, USAF
Chief, Liquid Rocket Division

Unclassified

Final Rept. Aug 78 - Jun 80

SECURITY CLASSIFICATION OF THIS PAGE (When Data Entered)

REPORT DOCUMENTATION PAGE		READ INSTRUCTIONS BEFORE COMPLETING FORM
1. REPORT NUMBER (18) AFRPL-TR-80-377	2. GOVT ACCESSION NO. AD-A090 514	3. RECIPIENT'S CATALOG NUMBER
4. TITLE (and Subtitle) Mission Integration Study for Solid Teflon Pulsed Plasma Millipound Propulsion System		5. TYPE OF REPORT & PERIOD COVERED Final 8/78 - 6/80
6. PERFORMING ORG. REPORT NUMBER		7. CONTRACT OR GRANT NUMBER(s) (15) F04611-78-C-0064
8. AUTHOR (10) M.N. Huberman, S. Zafran, H. Gran, R. Pieper, J.M. Sellen		9. PROGRAM ELEMENT, PROJECT, TASK AREA & WORK UNIT NUMBERS 62302F (16) 0358 JON 3058 2PV (17) 12
10. PERFORMING ORGANIZATION NAME AND ADDRESS TRW Defense and Space Systems Group One Space Park Drive Redondo Beach, Calif. 90278		11. REPORT DATE (11) September 1980
12. CONTROLLING OFFICE NAME AND ADDRESS Air Force Rocket Propulsion Laboratory Director of Science and Technology Air Force Systems Command Edwards Air Force Base, Calif. 93523		13. NUMBER OF PAGES 181
14. MONITORING AGENCY NAME & ADDRESS (if different from Controlling Office) (12) 182 Same as Item 11 above		15. SECURITY CLASS. (of this report) Unclassified
15a. DECLASSIFICATION/DOWNGRADING SCHEDULE		
16. DISTRIBUTION STATEMENT (of this Report) Approved for public release. Distribution unlimited.		
17. DISTRIBUTION STATEMENT (of the abstract entered in Block 20, if different from Report)		
18. SUPPLEMENTARY NOTES None		
19. KEY WORDS (Continue on reverse side if necessary and identify by block number) Electric Propulsion Auxiliary Propulsion Pulsed Plasma Propulsion Satellite Propulsion		
20. ABSTRACT (Continue on reverse side if necessary and identify by block number) → The objective of this program is to identify, validate and assess advantages to the Air Force of using high performance pulsed plasma electric propulsion technology for satellite stationkeeping, attitude control, drag make-up, and solar pressure compensation and to develop pulsed plasma propulsion system/spacecraft integration and design criteria. ← The application of pulsed plasma propulsion to three specific Air Force missions; the Defense Satellite Communications Systems III (DCSC-III),		

DD FORM 1 JAN 73 1473

Unclassified

over

SECURITY CLASSIFICATION OF THIS PAGE (When Data Entered)

449637

JP

Unclassified

SECURITY CLASSIFICATION OF THIS PAGE(When Data Entered)

Defense Support Program (DSP), and the Global Positioning System (GPS) were studied in detail. The major study conclusions are:

- There are no fundamental obstacles to the use of pulsed plasma propulsion for Air Force Missions.
- Pulsed plasma propulsion provides maximum benefits for functions which require either low impulse bit pulsing or long duration, high total impulse thrusting.
- Significant weight savings can be attained relative to hydrazine for DSCS-III and a 7-year DSP mission.
- Pulsed plasma propulsion can be used to provide in-track orbit control for a GPS/DISCOS (disturbance compensation system) satellite navigation system, but with a slight weight penalty relative to a hydrazine gas generator system.
- Demonstrated reliability, life, and interactive effects characteristics for flight type prototypes are needed before user acceptance can be achieved.

Specific conclusions for each of the detailed mission studies are also included in the report. The report concludes with recommendations for future development needs.

Accession For	
NTIS GRA&I	<input checked="checked" type="checkbox"/>
DTIC TAB	<input type="checkbox"/>
Unannounced	<input type="checkbox"/>
Justification	
By _____	
Distribution/	
Availability Codes	
Avail and/or	
Dist	Special
A	

Unclassified

SECURITY CLASSIFICATION OF THIS PAGE(When Data Entered)

CONTENTS

	Page
I. INTRODUCTION AND SUMMARY.	9
II. MISSION SURVEY.	12
2.1 Background.	12
2.2 Defense Satellite Communications System (DSCS-III).	13
2.3 Defense Support System (DSP).	13
2.4 Global Position System (GPS).	16
2.5 Defense Meteorological Satellite Program (PMSP).	17
2.6 Other Considerations.	17
III. PULSED PLASMA PROPULSION SYSTEM CHARACTERISTICS	19
3.1 Principles of Operation	19
3.2 System Description.	19
IV. DSCS-III MISSION.	24
4.1 Pulsed Plasma Propulsion Subsystem.	26
4.2 Interactions with Attitude Control Subsystem. . .	35
4.2.1 Baseline Configuration	35
4.2.2 Functions Performed.	36
4.2.3 Performance Summary.	41
4.2.4 Propellant Summary	45
4.3 Electric Power.	57
4.3.1 Electric Power Subsystem Description . .	57
4.3.2 Propulsion Power Requirements.	57
4.3.3 Subsystem Impact Assessment.	63
4.4 Interactive Effects	67
4.4.1 Material Deposition on Spacecraft Surfaces	67
4.4.2 Electromagnetic Compatibility.	69
4.4.3 Impact on Communications	69
4.4.4 Spacecraft Charging.	73
4.5 Reliability Analysis.	74
4.6 Configurations Comparison	83
4.7 Cost Analysis	88

CONTENTS (Continued)

	Page
V. DSP MISSION.	96
5.1 Pulsed Plasma Propulsion System.	96
5.2 Propulsion Considerations.	103
5.2.1 Propulsion Functions.	103
5.2.2 DSP Attitude Control and Station-keeping	107
5.2.3 Weight Summary for DSP.	122
5.3 DSP Electric Power Subsystem Analysis.	125
5.3.1 Electric Power Subsystem Description.	125
5.3.2 Propulsion Power Requirements	125
5.3.3 Subsystem Impact Assessment	127
5.4 Interactive Effects.	128
5.4.1 Material Deposition Requirements for Pulsed Plasma Thruster on DSP Spacecraft.	129
5.4.2 Electromagnetic Compatibility of the 1-Millipound Pulsed Thruster on DSP	136
5.4.3 Interaction with DSP Communications	139
5.5 Reliability Analysis for DSP	141
5.6 Cost Analysis.	142
VI. GLOBAL POSITIONING SYSTEM MISSION.	147
6.1 Configuration Studies.	151
6.1.1 Candidate Configurations.	152
6.1.2 GPS/DISCOS Configuration	160
6.2 Propulsion Requirements.	163
6.2.1 Assumptions	164
6.2.2 Solar Pressure Model.	165
6.2.3 Propulsion Requirements for DISCOS.	167
6.2.4 Orbit Plane Precession Due to Misalignment Misalignment.	169
6.2.5 Effects of Mass Shifts within Satellite	169
6.2.6 Attitude Control Consideration.	171
6.3 Propulsion System Comparison	172
6.3.1 Gas Propulsion for GPS/DISCOS	172
6.3.2 Pulsed Plasma Propulsion GPS/DISCOS	175
6.4 Conclusion	177
VII. RECOMMENDATIONS FOR FUTURE DEVELOPMENT	178
REFERENCES	179

ILLUSTRATIONS

		Page
1.	Schematic Diagram of DSCS-III Satellite.	14
2.	Current DSP Satellite.	15
3.	Current GPS Concept (NAVSTAR).	16
4.	Thruster Assembly Schematic Diagram.	21
5.	1 mlb Pulsed Plasma System Envelope.	22
6.	DSCS-III Isometric Diagram	25
7.	Pulsed Plasma Subsystem Schematic Diagram for DSCS-III .	27
8.	Baseline DSCS-III Configuration with Pulsed Plasma Propulsion.	29
9.	DSCS-III Configuration with Body Mounted Thrusters . . .	30
10.	DSCS-III Thruster Configuration.	36
11.	Three Axis Torque Control Capabilities Using Thrusters 1 and 2.	38
12.	Single Point Failure Satationkeeping Strategy.	41
13.	Orbital Efficiency and Thrusting Time for N-S Stationkeeping	45
14.	Roll Torque.	51
15.	Pitch Torque	52
16.	Yaw Torque	53
17.	DSCS-III Electric Power Subsystem.	58
18.	Solar Array Power Time Lines (at PRU at 28 Vdc).	59
19.	Reliability Block Diagram.	75
20.	Markov State Transition Diagram.	80
21.	Schematic Diagram of DSP	97
22.	Thruster Configuration	98
23.	Installation Concept	99

ILLUSTRATIONS (Continued)

	Page
24. Support Structure Concept.	100
25. Hydrazine System Revision - Pulsed Plasma Propulsion . . .	101
26. Example of Combined North and East Stationkeeping Plus Yaw Attitude Control Pulse.	106
27. Average Electrical Power Availability and Requirements for DSP as a Function of Life and Season	108
28. Single Axis Model of DSP Normal Mode Attitude Control Subsystem.	110
29. Histogram of Attitude Error, Control Axis in Orbit Plane.	112
30. Histogram of Attitude Error, Control Axis Normal to Orbit Plane.	113
31. Histogram of Attitude Error, Control Axis 45 Degrees to Orbit Plane	114
32. Solar Disturbance Torque at Equinox.	116
33. Annual Longitude Stationkeeping Velocity Increment	120
34. Electric Power and Distribution Subsystem Block Diagram. .	126
35. Solar Array Output per Half-Orbit, Equinox	128
36. SEMCAP Overview.	138
37. Overview of NAVSTAR GPS.	148
38. Baseline GPS Phase III Space Vehicle Design.	150
39. Single-Axis DISCOS Concept	152
40. NAVSTAR GPS On-Orbit Configuration Incorporating DISCOS Mass and Pulsed Plasma Thrusters	161
41. GN ₂ System Schematic Diagram	162
42. M35 Plenum System Schematic Diagram.	162

TABLES

	Page
1. Performance Summary.	20
2. Mass Properties.	24
3. DSCS-III Design Data Assumed for Study	26
4. Baseline Propulsion Subsystem Weight for DSCS-III.	32
5. Propulsion Subsystem Electrical Interface for DSCS-III	33
6. Propellant Requirements for 7-Year DSCS-III Mission.	46
7. DSCS-III ACS Components Physical Characteristics	47
8. DSCS-III Pointing Performance.	49
9. Fourier Series Coefficients for Solar Torques.	50
10. DSCS-III Load Power Requirements	60
11. Load Requirements with the Chemical Propulsion Subsystem Removed.	61
12. Load Power Requirements with Pulsed Plasma Thruster Subsystem.	62
13. Power Source Performance Characteristics for Thruster Configuration A.	64
14. Power Source Performance Characteristics for Thruster Configuration B	66
15. Weight and Area Impact on Solar Array Size	67
16. Solid Propellant Pulsed Plasma Thruster System Failure Rate Data.	77
17. Solid Propellant Pulsed Plasma Subsystem Thruster Duty Cycle	81
18. Parametric Reliability Assessment, DSCS-III Baseline Configuration.	82
19. DSCS-III Tradeoff Comparisons, 7-Year Mission.	84
20. Candidate DSCS-III Configurations.	85
21. Weight Margin Comparison, 7-Year Mission	87

TABLES (Continued)

	Page
22. Weight Margin Comparison, 10-Year Mission.	89
23. Recurring Cost Breakdown, Hydrazine Propulsion Subsystem for DSCS-III	90
24. Recurring Cost Breakdown, Pulsed Plasma Propulsion Subsystem for DSCS-III	90
25. Recurring Cost Breakdown, Pulsed Plasma/Hydrazine Propulsion Subsystem for DSCS-III.	91
26. Recurring Cost Breakdown, Ion/Hydrazine Propulsion Subsystem for DSCS-III	92
27. Nonrecurring Cost Breakdown, Pulsed Plasma Propulsion Subsystem for DSCS-III	93
28. Recurring Cost Comparison Summary (DSP).	95
29. DSP Design Data Assumed for Study.	97
30. Performance Criteria vs Control Torque (T_c) and DRIM Relay (γ)	111
31. Thruster Activity (Equinox Solar Torques: 0.1% Residual Momentum; E/S Noise = 4 deg).	117
32. Summary of ACS Functions on Thruster Impulse and ΔV Augmentation	119
33. N-S Stationkeeping Impulse Summary	123
34. DSP Propulsion Subsystem Comparison, 7-Year Mission. . . .	124
35. PPT Mass Deposition Requirements	134
36. Parametric Reliability Assessment, Pulsed Plasma Propulsion Subsystem for DSP	143
37. Recurring Cost Breakdown, Hydrazine Propulsion Subsystem for DSP.	144
38. Recurring Cost Breakdown, Pulsed Plasma/Hydrazine Propulsion Subsystem for DSP	145
39. Nonrecurring Cost Breakdown, Pulsed Plasma Propulsion Subsystem for DSP	146

TABLES (Continued)

	Page
40. Recurring Cost Comparison Summary.	146
41 Global Positioning System Mission.	149
42. GPS/DISCOS Propulsion Requirements	172
43. Cold Gas System Weight Summary	173
44. Application Requirements vs Capability Summary for Gas Propulsion for GPS/DISCOS.	174
45. M35 System Weight Summary.	176
46. Upgraded LES-9 Pulsed Plasma Performance for GPS/DISCOS	176
47. Propulsion System Comparison for GPS/DISCOS Application Condidate System	177

I. INTRODUCTION AND SUMMARY

The objective of this program is to identify, validate and assess advantages to the Air Force of using high performance pulsed plasma electric propulsion technology for satellite stationkeeping, attitude control, drag makeup, and solar pressure compensation and to develop pulsed plasma propulsion system/spacecraft integration design criteria.

The simplicity and reliability of the pulsed plasma concept make it especially attractive for a wide variety of spacecraft applications. The ability to produce discrete, repeatable impulse bits for millions of pulses makes the pulsed plasma thruster an attractive candidate for spacecraft requiring long-life, low-level propulsion.

By varying the thruster pulse frequency, the effective steady-state thrust level can be varied by as much as a factor of ten during the mission with no hardware changes. At the same time, by varying the discharge energy, the specific impulse can be tailored from several hundred to several thousand seconds, depending on mission requirements. Potential applications include preapogee burn maneuvers, initial station acquisition, north-south stationkeeping, east-west stationkeeping, repositioning, attitude control, momentum wheel dumping, and drag compensation.

The fact that the thruster uses a solid propellant eliminates the need for tankage, feed lines, seals, or valves, and makes it easily compatible with the space environment. The thruster has zero warm-up time and requires no standby power. Where precise attitude control, spin-axis precision, and stationkeeping are required, these thrusters are especially attractive for both spin-stabilized and three-axis stabilized spacecraft.

To identify specific satellites for this study, a survey was made of potential Air Force missions for the 1985-1990 time frame. Initially, two satellites, Defense Satellite Communications System III (DSCS-III) and the Defense Support Program (DSP), were selected for detailed study. Later in the program the Global Positioning System (GPS) was added as a third satellite for detailed study. The first two missions can be performed using millipound pulsed plasma propulsion systems. The third mission can be accomplished using a modified LES-9 pulsed plasma propulsion system.

This report contains the results, analyses, correlations, conclusions, and recommendations of the Electric Propulsion/Spacecraft Integration Study. The remainder of Section 1 summarizes the study conclusions. The mission survey is summarized in Section 2. Section 3 describes the solid Teflon pulsed plasma millipound propulsion system. Sections 4, 5, and 6, respectively, describe the DSCS-III, DSP, and GPS results. Section 7 summarizes recommendations for future development.

The major study conclusions are:

- There are no fundamental obstacles to the use of pulsed plasma propulsion for Air Force missions.
- Pulsed plasma propulsion provides maximum benefits for functions which require either long duration, high total impulse thrusting or short duration, low impulse bit pulsing.
- Significant weight savings can be attained relative to hydrazine for DSCS-III and a 7-year DSP mission.
- Pulsed plasma propulsion can be used to provide in-track orbit control for a GPS/DISCOS (disturbance compensation system) navigation system, but with a slight weight penalty relative to a hydrazine gas generator system.
- Demonstrated reliability, life, and interactive effects characteristics for flight type prototypes are needed before user acceptance can be achieved.

Specific conclusions pertaining to DSCS-III include:

- The millipound Pulsed Plasma Propulsion System (PPPS) can completely replace an existing hydrazine system if orbit trim and relocation times of the order of weeks are acceptable.
- PPPS can be used as redundant backup or replacement for reaction wheels; ion engines cannot perform this function.
- Weight margin for STS dual launch is a present DSCS-III design concern. PPP can achieve potential weight savings up to 181 pounds for a 7-year mission and 286 pounds for a 10-year mission.
- Excess array power and battery cycle life capability minimize additional array requirement.

- Power required for thermal control is minimized when the power converter is separate from the thruster assembly.
- More data is needed relative to thruster life, failure rates, EMC, and plume effects.

DSP conclusions are:

- The millipound Pulsed Plasma Propulsion System can provide attitude control, E/W and N/S stationkeeping
- Improved inclination control can be achieved relative to 2 deg beginning-of-life (BOL) and 1 deg end-of-life (EOL) capability:
 - 1 deg BOL and 0.1 deg EOL with PPT, no failures first 6 months
 - 1 deg BOL and 0.6 EOL with PPT, failure at launch
- Pulsed plasma propulsion can provide increased payload capability relative to an all hydrazine auxiliary propulsion system:
 - 131 pounds compared with hydrazine requirement for 2 deg BOL, 1 deg EOL
 - 320 pounds compared with hydrazine requirement for 1 deg BOL, 0.1 deg EOL
- Additional pulsed plasma interactions data is needed to insure payload compatibility.

GPS conclusions include:

- More precise orbital control of GPS satellites will provide significant cost benefits for the GPS ground segment; the needed precision can be provided by a DISCOS navigation system.
- The GPS Phase III space vehicle has the potential of being redesigned to accommodate a DISCOS navigation system for precise orbital control.
- DISCOS propulsion functions can be provided by either a gaseous nitrogen, hydrazine gas generator or solid Teflon pulsed plasma propulsion system (upgraded LES-9 configuration).
- For DISCOS propulsion, the pulsed plasma system provides a payload weight advantage of 64 pounds compared with a gaseous nitrogen system and a payload weight penalty of 14 to 21 pounds compared to a hydrazine gas generator.

II. MISSION SURVEY

2.1 BACKGROUND

Before selection could be made of the Air Force satellites to be considered for implementation of the pulsed plasma propulsion subsystem (PPPS), it was necessary to review the current status and future plans of all relevant AFSC/SAMSO space programs. This was accomplished through a series of meetings between TRW, AFRPL personnel, and the various SAMSO program offices (SPOs) supported by Aerospace Corporation engineers. Information obtained during these meetings was supplemented, by available program documentation. Final spacecraft selections (DSCS-III, DSP, and GPS) were based on appraising mission and satellite configuration suitability, availability of detailed satellite design data, program status, and SPO-expressed interest in PPPS.

Visits were made to the following program offices: Defense Support Program (DSP); Global Positioning System (GPS/NAVSTAR); Deep Space Surveillance System (DSSS); Space Test Program (Satellite Infrared Experiment, SIRE); Defense Satellite Communications System, Phase III (DSCS-III); Defense Meteorological Satellite Program (DMSP); Strategic Satellite System (SSS); and a radar satellite study office. Within this group there is great diversity in maturity of the program and, in particular, of the spacecraft. There is also diversity in the pace of technological change and the nature of future plans. A basic problem which became evident during the data gathering phase is that some satellites for which PPPS might be appropriate are not yet well defined. The satellite programs surveyed divide into three groups: mature programs for which gradual or no evolutionary change is programmed; mature programs which will be undergoing major ("block") spacecraft changes but for which the new spacecraft is currently undefined; and new programs for which some preliminary concept formulation has been completed but which remain undefined. Major features of the programs surveyed are summarized below.

2.2 DEFENSE SATELLITE COMMUNICATIONS SYSTEM (DSCS-III)

The DSCS-III satellite is currently undergoing engineering development. The system, scheduled for first launch in the early 1980s, will be a follow-on to the current DSCS-II system which provides communications services in support of the World Wide Military Command Control System (WWMCCS) and other requirements as approved by OJCS. The total space segment will include four active satellites and two on-orbit spares. Satellite dry weight is 1850 pounds. Due to the complex patterns of the beams generated and received by multielement antennas, there are requirements for precision stationkeeping (N/S, 0.1 deg; E/W, 0.1 deg) and attitude control (roll accuracy, 0.06 deg; pitch accuracy, 0.06 deg; yaw accuracy, 0.8 deg; RF beam axis pointing, 0.2 deg). These accuracies, which must be maintained over a long design life (7-10 years) will in the present design be achieved using hydrazine. However, a PPPS used for stationkeeping, momentum dump, and attitude control backup might replace, as a minimum, 266 pounds of hydrazine used for N/S stationkeeping. Figure 1 shows the DSCS-III satellite.

2.3 DEFENSE SUPPORT PROGRAM (DSP)

The current DSP satellite weighs 2400 pounds and is a mature system; the SPO will tolerate only small changes to the spacecraft design. The current satellite has no north-south stationkeeping requirement but requires ± 1 deg east-west precision. The satellite has zero momentum spin, with the spin axis pointing towards the earth's center. At launch, there is a total of 350 pounds of hydrazine propellant weight which provides a capability for major repositioning while on-orbit. Current design life is 3 years (required) with a 5-year goal. Satellite lifetime is now limited by optics and thermal control surface contamination.

An advanced DSP satellite, which will weigh approximately 3300 pounds, will be launched in CY 1982. N/S stationkeeping will be needed for this satellite. However, the N/S accuracy requirement is only 2 degrees for the first year and 1 degree thereafter. This allows the satellite to be injected with a 2 degree bias followed by a passive 3-year inclination drift to 1 degree on the other side of equatorial. Thus, only 2 years of N/S stationkeeping is required for a 5-year mission. However, for a 7-year mission this requirement would double.

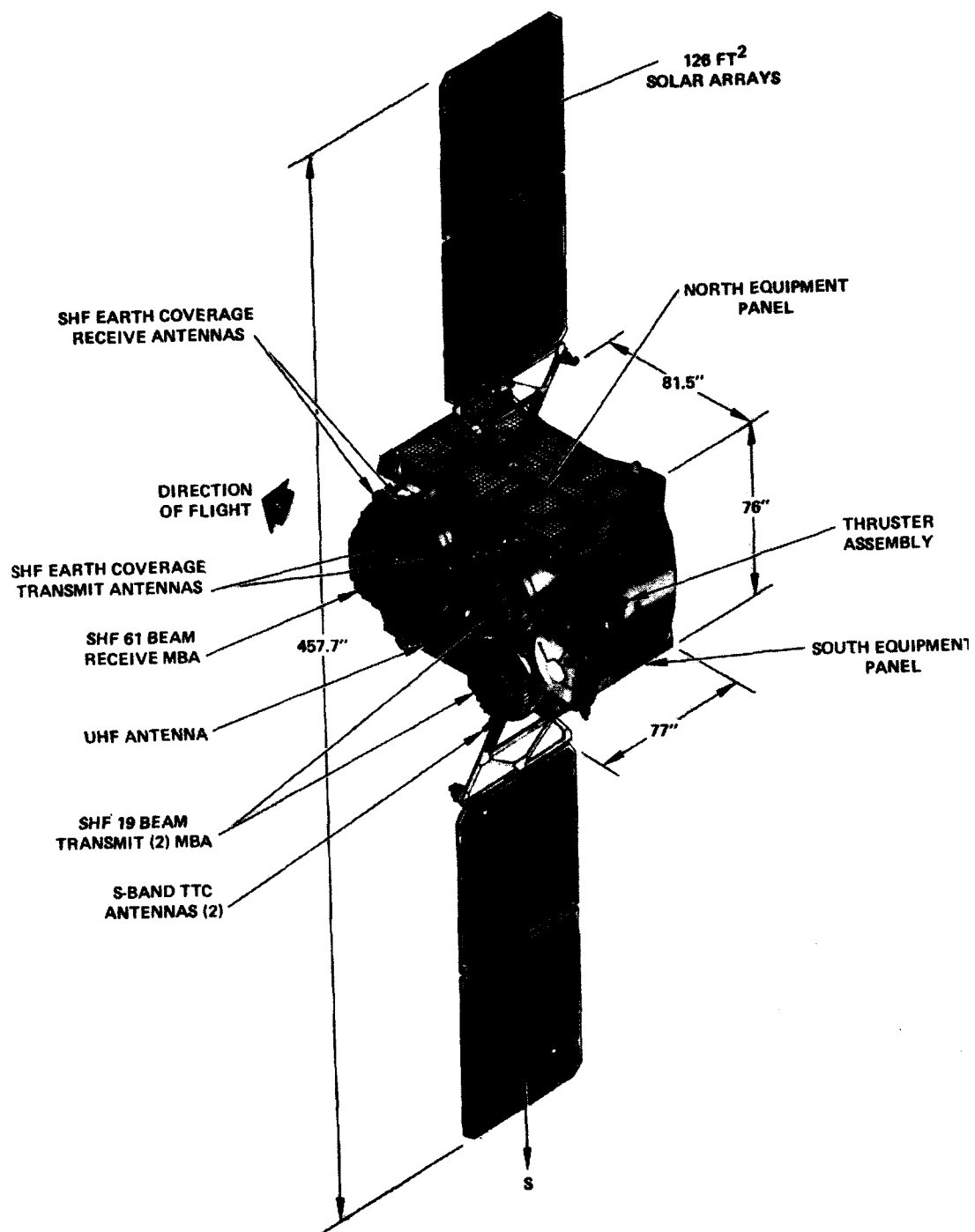


Figure 1. Schematic Diagram of DSCS-III Satellite

The DSP satellite was chosen for further study for several reasons: propulsion requirements for stationkeeping either for a longer lifetime or to a greater precision could make PPPS more attractive than hydrazine; precision pointing accuracy of the new satellite suggests a role for highly controllable low thrust reaction control. Since DSP is a TRW built spacecraft, design data are readily available and the DSP SPO had expressed interest in investigating the applicability of pulsed plasma propulsion for longer life missions. Figure 2 shows the current DSP satellite. The study has been based on a similarly designed hypothetical future DSP with a postulated 7-year stationkeeping requirement.

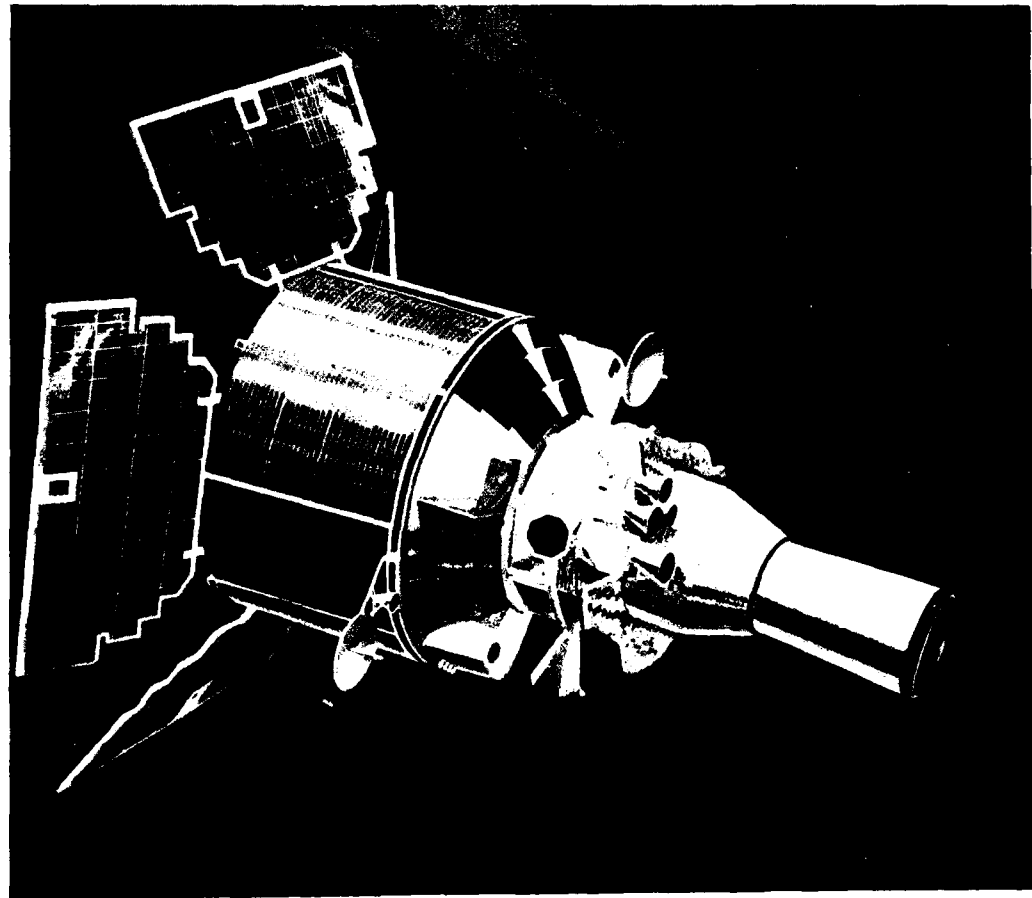


Figure 2. Current DSP Satellite

2.4 GLOBAL POSITIONING SYSTEM (GPS)

The GPS/NAVSTAR system is currently in its first phase, a four satellite (Figure 3) test program, usable several hours each day in the southwestern United States. The ultimate Phase III operational system will include a ground control segment and 18 three-axis stabilized satellites distributed around three half-synchronous altitude, 55-degree inclination orbits. Considerable cost savings for the ground segment can accrue if drag and solar pressure disturbances can be automatically compensated by a disturbance compensation system (DISCOS). The DISCOS system requires a pulsed propulsion system which can operate in a pulsed mode to deliver a repeated low impulse bit thrust increment. Since this application is similar to the TIP-II, TIP-III, and NOVA applications of pulsed plasma propulsion, the GPS application was selected as a third study area for the present program.

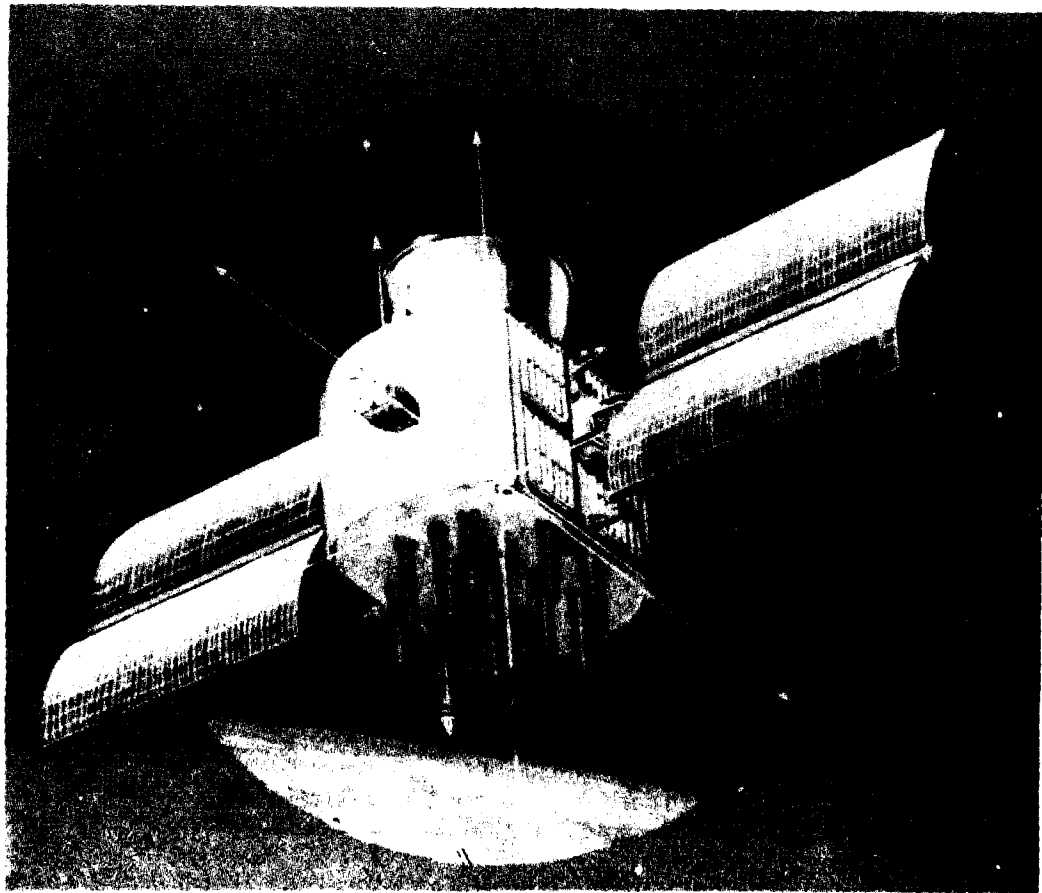


Figure 3. Current GPS Concept (NAVSTAR)

2.5 DEFENSE METEOROLOGICAL SATELLITE PROGRAM (DMSP)

The DMSP satellites are three-axis stabilized in a 450-nautical mile orbit. The satellites are limited to 3-year life and have no requirement for drag makeup or stationkeeping. Because no applicability of PPPS to DMSP could be discerned, the meteorology satellites were eliminated from further consideration.

2.6 OTHER SATELLITES

During the mission survey, it was suggested that the standard Agena vehicle be considered as a prototype low altitude satellite for which PPPS might provide improved drag makeup compared to current methods. The Agena which weighs 1174 pounds, exclusive of mission payload, is adaptable to many combinations of booster, payload, and support equipment. In particular, it has been extensively used for low altitude classified missions. An improved drag makeup capability would enable a satellite to perform its mission longer, at the same altitude, than is now possible. First-order calculations, however, show that PPPS would not be competitive with current technology in the low altitude regime now used for such missions. The generic low altitude mission was therefore rejected as a study candidate.

Consideration was given to selecting for study the SIRE spacecraft, an Agena attached to an experimental sensor payload front end. The idea was to assume that SIRE would closely resemble the eventual DSSS satellite. Although DSSS will probably have nominal stationkeeping tolerances, the need for accurate and repetitive spacecraft attitude control changes might be suitable for PPPS. A major drawback to using PPPS, however, is that the satellite optics will be extremely sensitive to contamination. This problem would compound the difficulty of installing Teflon emitting thrusters. Also, it might be difficult to shield the sensitive payload electronics against the RFI background created by the PPPS high voltage discharges. Because the disadvantages appeared to outweigh the advantages, SIRE (DSSS) was rejected as a candidate.

The SSS, a polar extra-synchronous communications satellite, seemed a plausible choice because of its requirements for precise attitude control and stabilization, as well as for small random maneuvers throughout the

satellite's lifetime. However, this satellite has not yet been defined. (SAMSO intends to solicit bids for a concept formulation study during 1979.) Moreover, DSCS-III is a far better choice in the communications area.

A medium altitude radar surveillance satellite which has been studied under SAMSO funding was rejected on the basis that no PPPS advantages were apparent, little information on satellite configuration is available beyond the radar sensor, and it is unlikely that DoD will authorize development of this system.

III. PULSED PLASMA PROPULSION SYSTEM CHARACTERISTICS

3.1 PRINCIPLES OF OPERATION

The solid propellant pulsed plasma propulsion system produces thrust in the form of discrete impulse bits. The equivalent steady-state thrust is a function of the pulse repetition rate. Equivalent steady-state thrusts of 4 to 4500 μN have been achieved. Specific impulses ranging up to 5100 seconds have been experimentally demonstrated.¹

An impulse bit is generated by producing an electric discharge across the face of the thruster's Teflon propellant. A few surface layers of propellant become ionized and accelerated by gas dynamic forces and the Lorentz force generated by the interaction between the arc current and its self-generated magnetic field. Since the plasma created is electrically neutral, no charge neutralization is required. The cycle can either be repeated or instantly terminated.

Teflon propellant is stored directly in the vacuum of space and requires no tankage. Cross sections of straight propellant rods can be of almost any design (e.g., rectangular, circular, or wedge-shaped). In one design, the rod is in the form of a helical coil.

Thrust is generated simply by charging and discharging a capacitor across a plasma load; no electrical switches, valves, or magnets are required. The simplicity of the entire propulsion system accounts for its high reliability. Furthermore, operational control of the system is inherently compatible with digital logic satellite control systems and, in particular, with autonomous control of a satellite.

3.2 SYSTEM DESCRIPTION

The solid propellant pulsed plasma millipound propulsion system is designed for large total impulse missions such as N-S stationkeeping. The completely integrated system has recently been vacuum tested for an accumulated 4500 hours. The thruster produces 4.45 millinewtons (1 mlb) of

¹D. J. Palumbo and W. J. Guman, "Continuing Development of the Short-Pulsed Ablative Space Propulsion System," AIAA/SAE 8th Propulsion Specialist Conference, New Orleans, LA, 1972.

thrust at a specific impulse of 2200 seconds. Other performance parameters are summarized in Table 1.

Table 1. Performance Summary

Impulse Bit	5 mlb-sec/pulse
Impulse Bit Repeatability	$\pm 5\%$, no degradation with time
Thrust (equivalent steady state)	Nominal - 1 mlb Maximum - 3 mlb
Design Life (total impulse)	50,000 lb-sec
Specific Impulse	2200 sec
System Input Power	170 W (1 mlb)
Efficiency	
Power Processor	0.80
Thruster	0.35
Total System	0.28
Thrust Vector Accuracy	± 0.5 deg
Thrust Vectoring	Gimballing if required

To provide for the large total impulse, the spring-fed propellant is stored in two helical coils and fed independently into the sides of the thruster's electrode nozzle. The helically coiled propellant rods are sufficient for 50,000 pound-seconds of total impulse. The thruster electronics subsystem can be either located within the interior of the propellant loop or relocated to the spacecraft equipment compartment to simplify thermal control. Figure 4 is a schematic of the system.

The complete system, including propellant, weighs about 74 pounds (33.6 kg). Figure 5 shows the thruster envelope and component mass properties are summarized in Table 2.

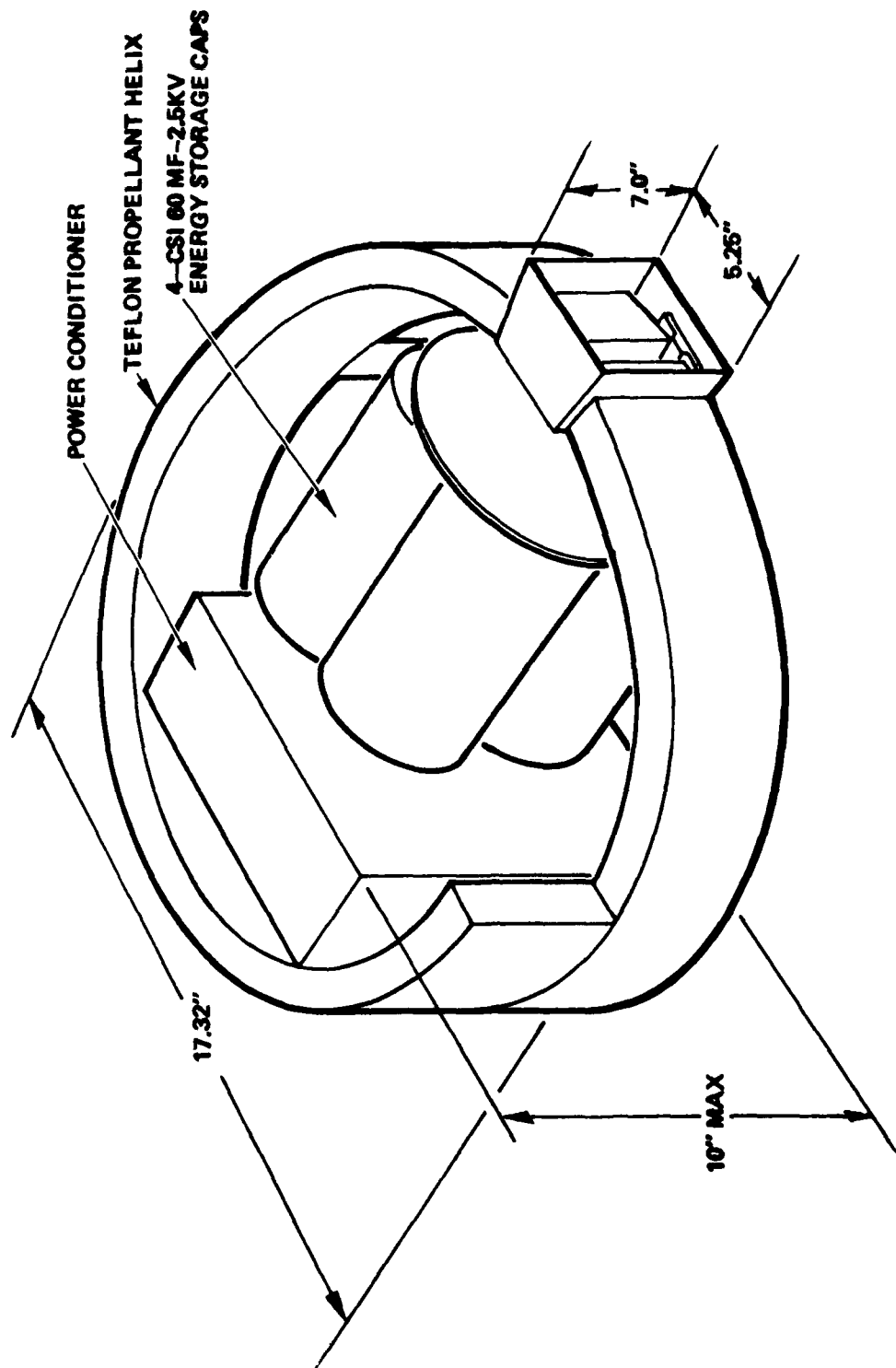


Figure 4. Thruster Assembly Schematic

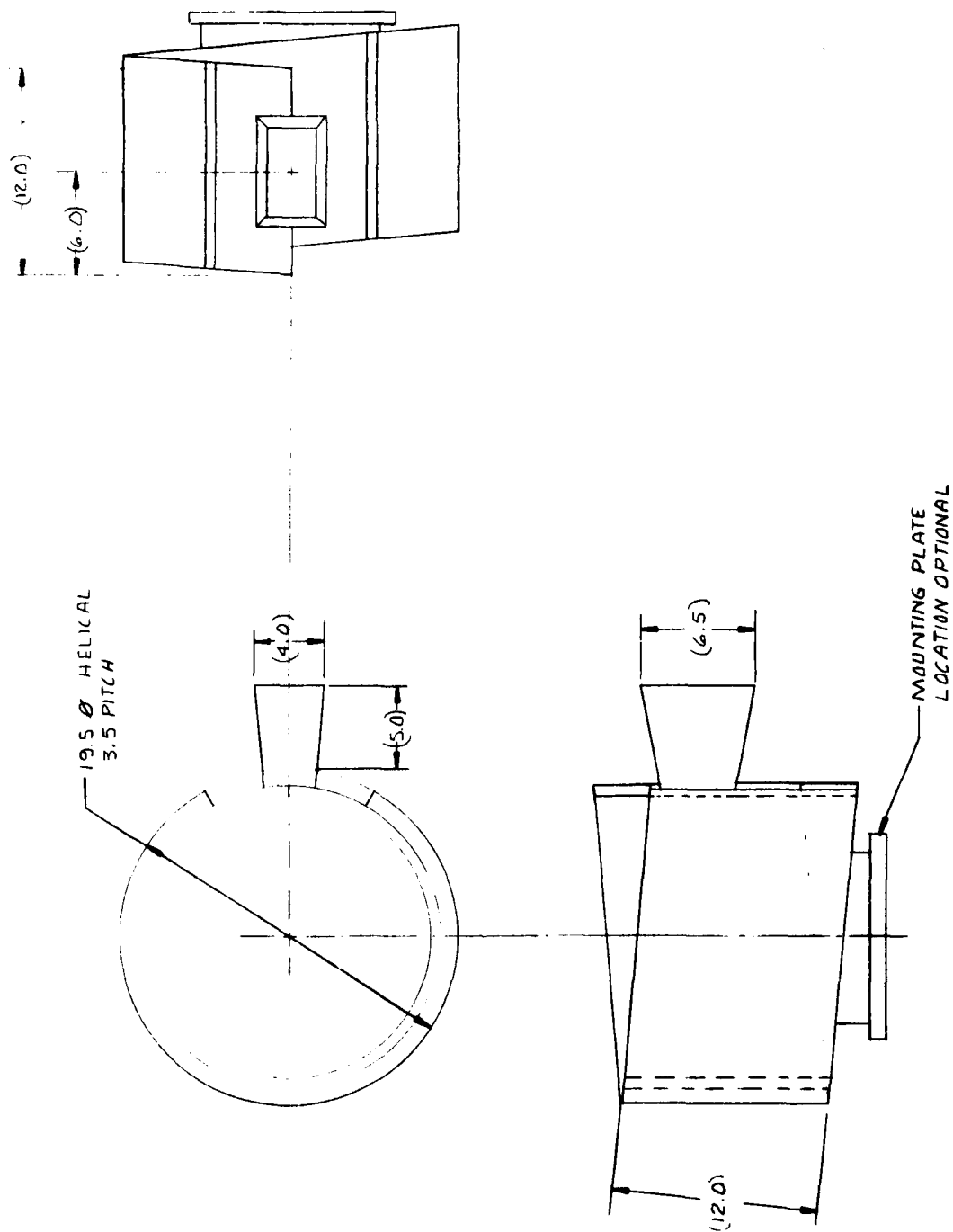


Figure 5. 1 mlb Pulsed Plasma System Envelope

Table 2. Mass Properties

	<u>Mass (lb)</u>
Capacitors	23
Electronics	8
Strip Line and Fuel Housing	8
RFI Structural Enclosure	5
RFI Exhaust Cone	1
Anode, Cathode, Ignitor Plug	1
Gold Plating	2
Propellant	24
Miscellaneous	2
	—
Total	74

Although this study is concerned primarily with the millipound system, pulsed plasma propulsion can be readily scaled to a size and performance which are compatible with a particular application. For example, the GPS/DISCOS application, which requires extremely small impulse bits, can be readily performed by an upgrade of the previously flown LES-9 thruster.

IV. DSCS-III MISSION

The Defense Satellite Communications System-III (DSCS-III) provides the capabilities for effective implementation of worldwide military communications for the next decade. The satellite will be capable of launch from Titan-III or Space Shuttle. For operational use, a constellation of four satellites will be placed in synchronous equatorial orbit and stationed over the Atlantic, East and West Pacific, and Indian Oceans. Table 3 summarizes the DSCS-III design parameters that were planned at the time the study began (late 1978). The satellite uses a monopropellant hydrazine propulsion subsystem.

Figure 6 is an isometric representation of DSCS-III which illustrates the general location of equipment on the spacecraft. Its antenna farm is clustered on the earth pointing face of the central spacecraft body. The solar arrays are gimballed about the north-south axis and the hydrazine thrusters are located on the east-west faces of the central body. Electronic equipment within the spacecraft body is generally mounted from the north and south equipment panels to take advantage of thermal control surfaces (optical solar reflectors) for heat rejection to space.

The first scheduled DSCS-III launch will be performed in tandem with a DSCS-II on board a Titan III system. Subsequent operational flights of DSCS-III communications satellites are scheduled to use the Space Transportation System (STS). Two satellites at a time will be attached to an inertial upper stage (IUS) inside the Space Shuttle that will be implemented for boosting them to geosynchronous altitude. At the present time, the weight margin for a dual launch of this nature is of design concern for the mission. Integration of pulsed plasma thrusters on DSCS-III can provide significant added weight margin. Such margin could compensate for any STS shortfall, permit additional communications equipment on board, or be used for increased component redundancy.

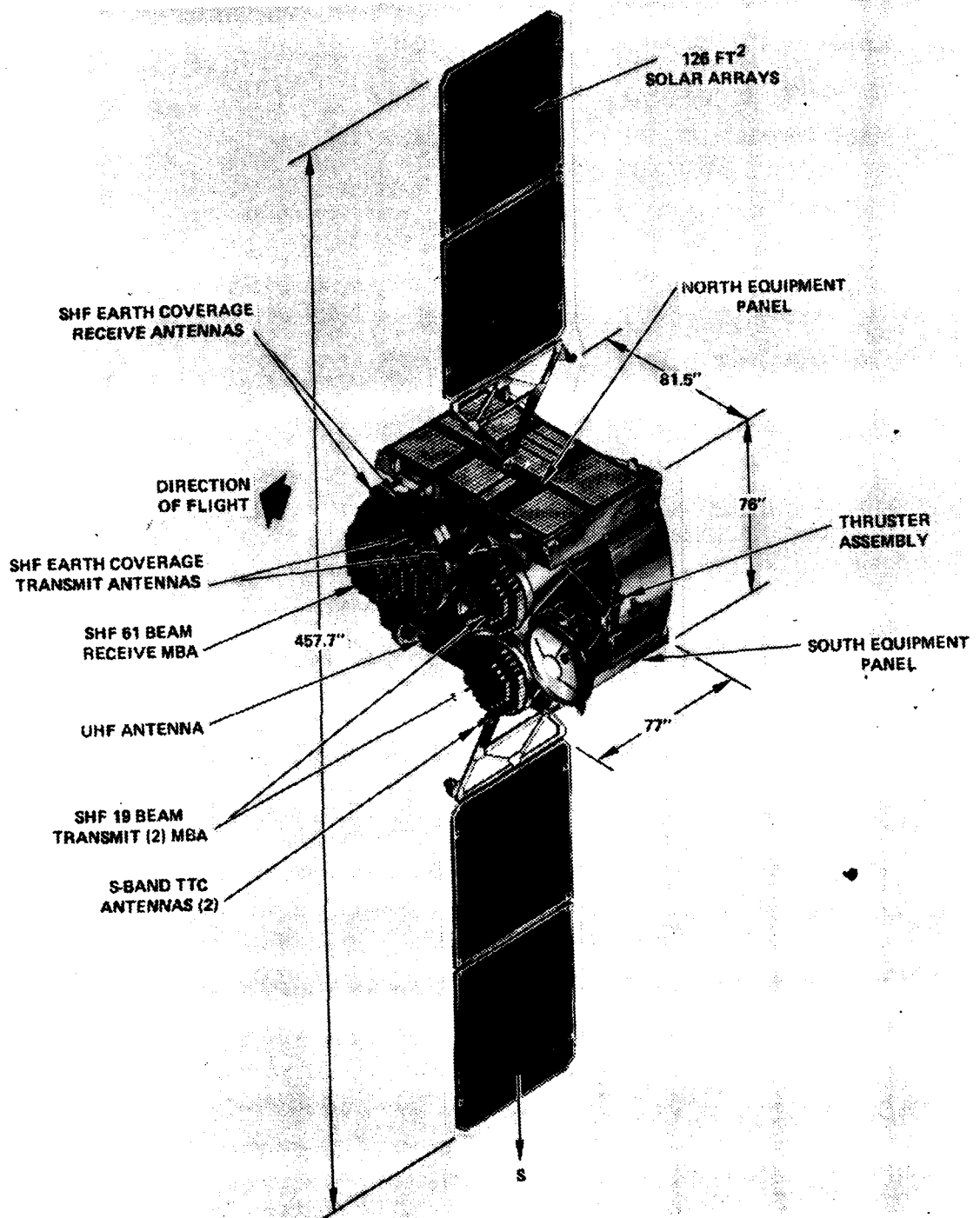


Figure 6. DSCS-III Isometric Diagram

Table 3. DSCS-III Design Data Assumed for Study

Design Life	7-10 years
Spacecraft Weight (Dry)	Approximately 1715 lb
Stabilization	0.2° circular error radius, overall accuracy of RF beam axis pointing $\pm 0.1^\circ$ orbit positioning accuracy
Attitude Control Subsystem	Accuracy - 0.08° roll 0.08° pitch 0.8° yaw
Electrical Power Subsystem	1100 watts array power (beginning of mission) 837 watts array power (10 years) 28 V $\pm 1\%$
Existing Hydrazine Propulsion Subsystem	Thrust levels - 1 lb to 0.3 lb Blow down ratio - 4:1 with full load Specific impulse - 228 sec at initial conditions
Overall reliability	Greater than 0.7 at 7 years

4.1 PULSED PLASMA PROPULSION SUBSYSTEM

The pulsed plasma propulsion system (PPPS) for DSCS-III is shown schematically in Figure 7. It is comprised of four thruster assemblies and four power converters. Each thruster assembly is gimbal mounted and contains a thruster, energy storage capacitors, and Teflon propellant. Electrical interconnections between each piece of equipment and the spacecraft are indicated on the schematic diagram.

Pulsed plasma propulsion can be used for initial stabilization, orbit trim, relocation, stationkeeping, momentum wheel unloading, and attitude control functions on DSCS-III. If the time required to perform these functions is acceptable, then it can completely replace the existing hydrazine subsystem. Accordingly, a number of candidate configurations were evaluated and compared. The principal tradeoffs included those listed below.

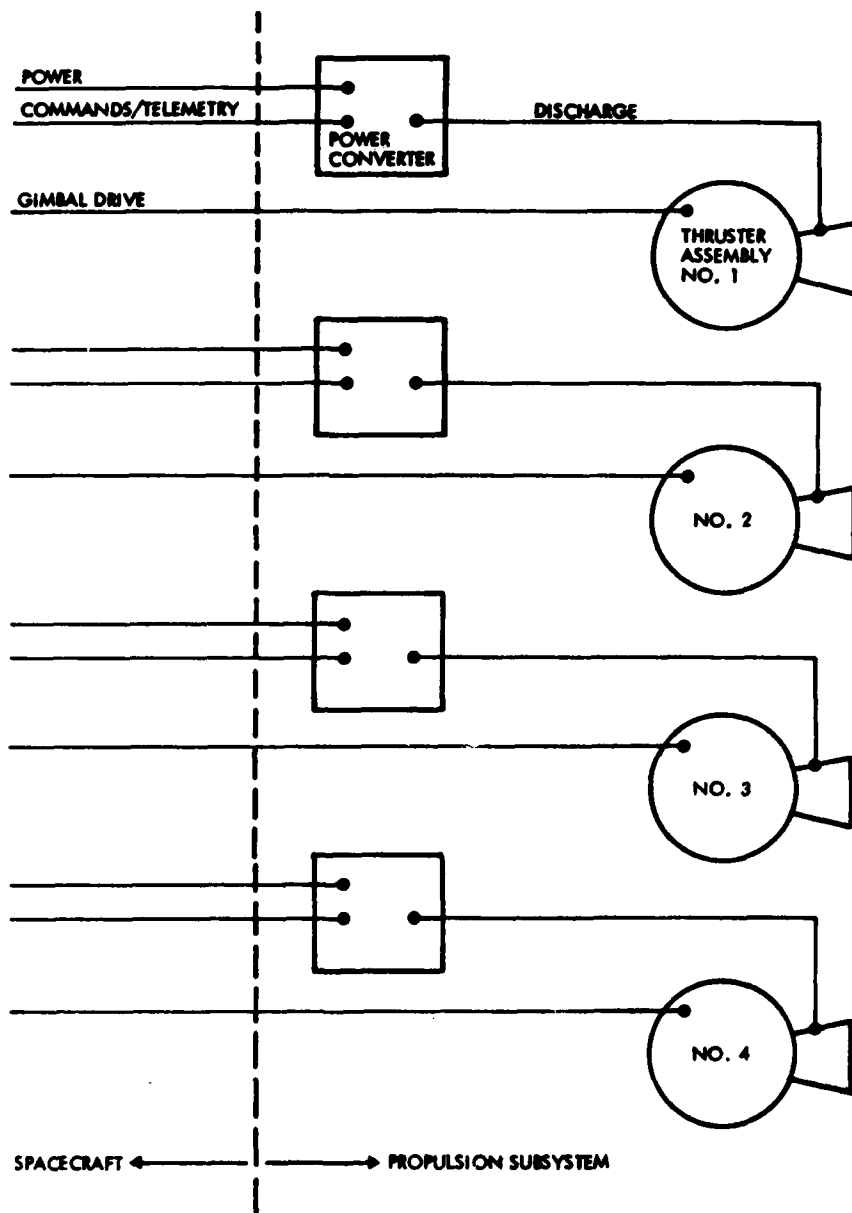


Figure 7. Pulsed Plasma Subsystem Schematic Diagram for DSCS-III

- Boom-Mounted versus Body-Mounted Thrusters. Boom mounted thrusters (Configuration A, Figure 8) provide for minimum plume interactions with the spacecraft. Body mounted thrusters (Configuration C, Figure 9) provide a lighter weight approach while still maintaining good clearances between the thruster plumes and nearby equipment.
- Spacecraft Rotated 90 deg About Y (N/S) Axis for Orbit Trim and Relocation. Maneuver times are reduced by providing a more favorable thrusting direction for orbit trim and relocation functions with thrusters nominally oriented for stationkeeping purposes. However, this maneuver does not allow the earth sensor to be used for attitude control.
- Maximum Number of Thrusters Operating Simultaneously (Configuration B). Maneuver times are reduced by operation at higher thrust levels, i.e., by operating a number of 1 milli-pound thrusters simultaneously in parallel. Power requirements, however, increase linearly with the number of thrusters thus employed, with attendant impact on the spacecraft electrical power subsystem.
- Hydrazine for Orbit Trim and Relocation. Combination hydrazine/pulsed plasma propulsion subsystems yield attractive weight margins, albeit not as large as all plasma propulsion. Hydrazine is used to reduce long maneuver times.
- Active Attitude Control. By using pulsed plasma thrusters for active limit cycle attitude control, the reaction wheels on DSCS-III can be eliminated.
- 245 Days/Year Stationkeeping. By performing stationkeeping functions during favorable seasons when more power is available for propulsion, there is no need to add array or battery capability to existing DSCS-III electrical power subsystem.

Configuration A, Figure 8, was designated as the baseline* design at the onset of the study. In order to minimize plume impingement on the solar array during north-south stationkeeping (the function requiring the greatest thrusting time), the thrusters are canted 30 degrees away from north-south (Y axis) and towards east-west (X axis). The thrusters

*The term "baseline" for this study denotes the initial configuration selected for analysis. It was used as a point of departure for subsequent tradeoffs and subsystem analyses. The preferred configuration for eventual integration was then determined from the detailed configuration and tradeoff studies.

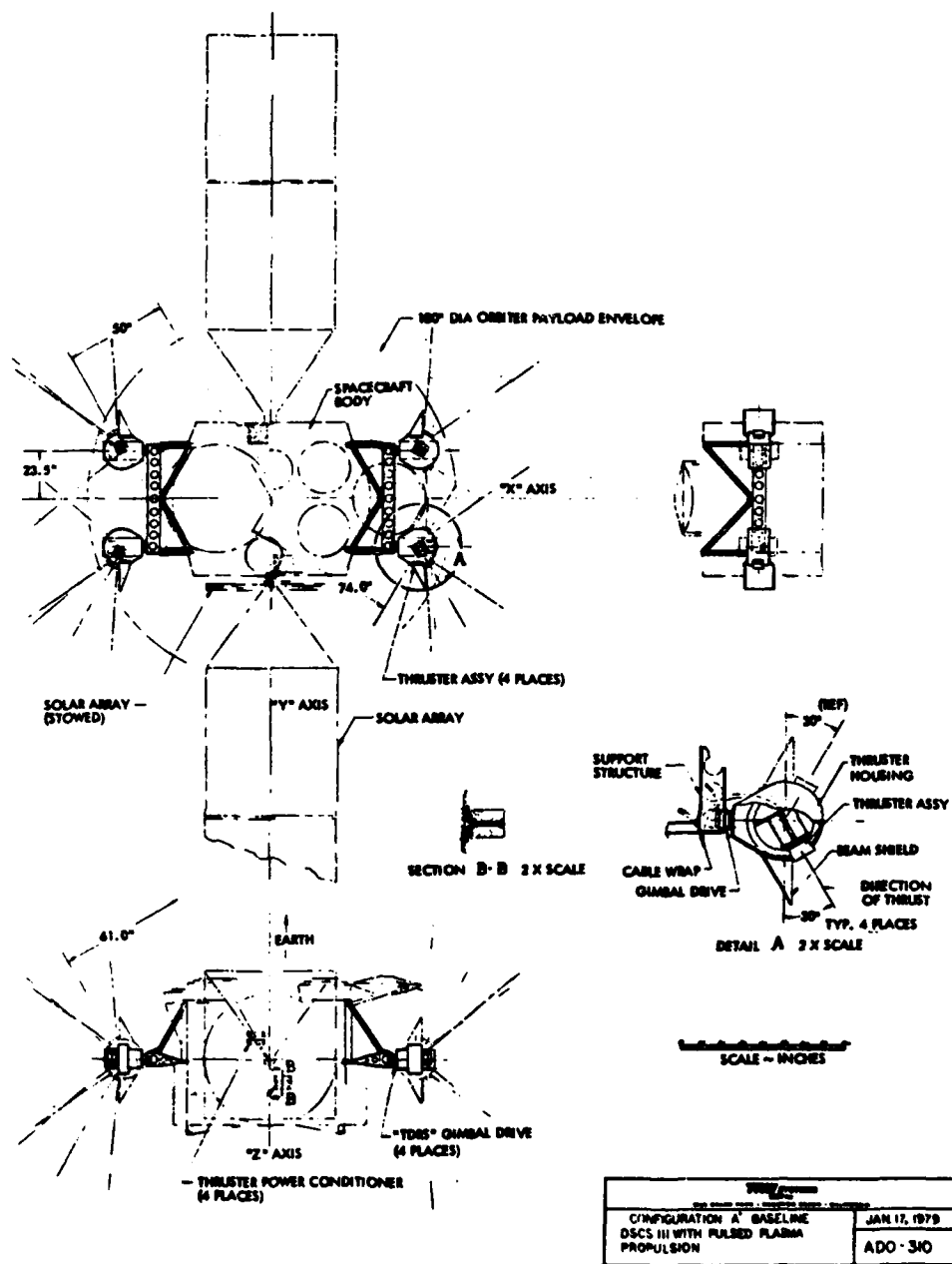


Figure 8. Baseline DSCS-III Configuration with Pulsed Plasma Propulsion

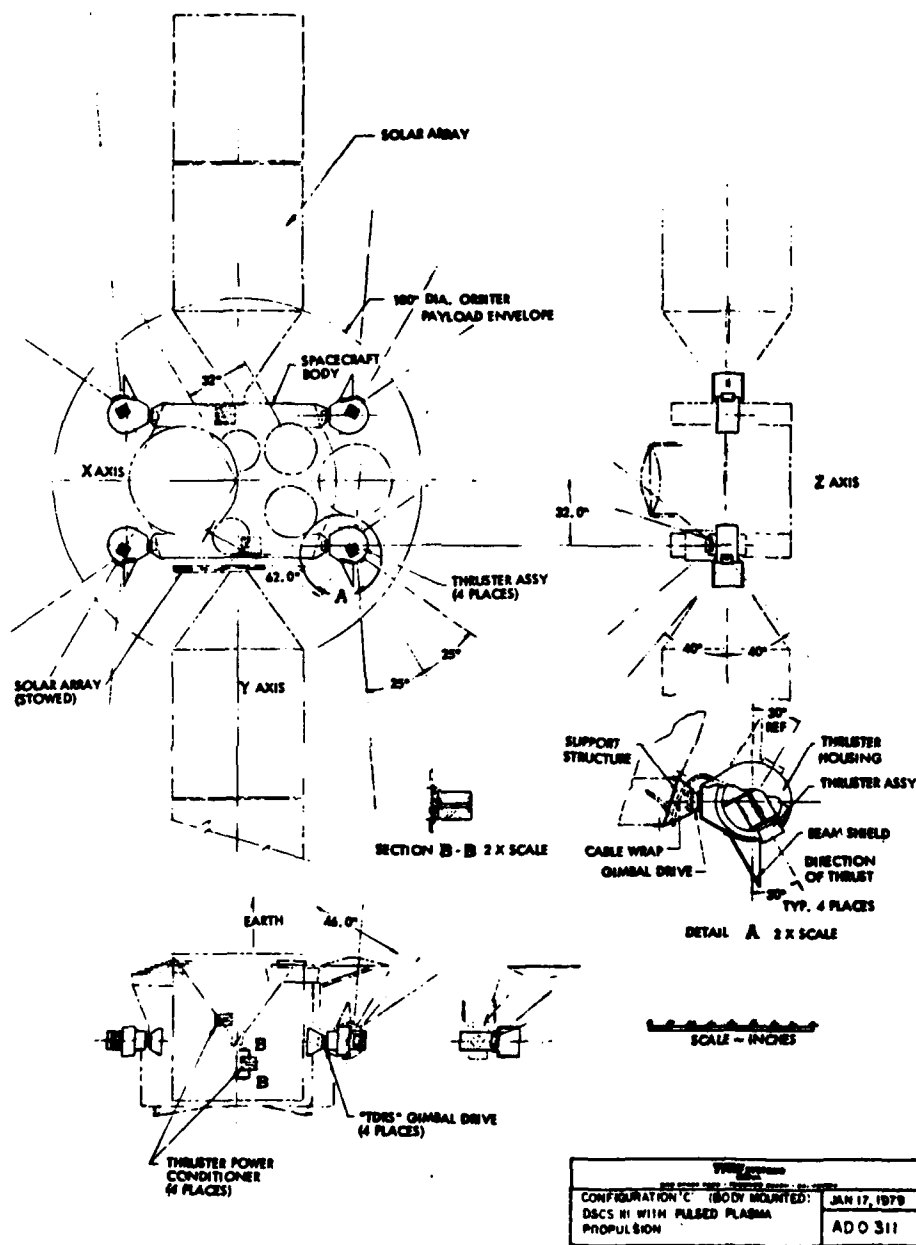


Figure 9. DSCS-III Configuration with Body Mounted Thrusters

are oriented with their minimum plume divergence angles in the X-Y plane and fitted with beam shields to further limit their plume divergence.

Each thruster is mounted on a TDRS (Tracking and Data Relay Satellite) gimbal drive to permit rotation about an axis parallel to, and displaced 23.5 inches from the east-west (X) axis. The thruster assemblies are attached to the power converters by flexible cable wraps which permit a 180-degree gimbal rotation.

The thruster support structures extend outward from the central spacecraft body to provide lateral separation of the thruster exhaust from nearby spacecraft surfaces. This lateral separation is constrained by the 180-inch diameter Shuttle orbiter payload envelope.

The power converters are mounted separately from the thruster assemblies to simplify propulsion subsystem thermal control. Two converters are mounted on the north equipment panel, and two on the south equipment panel of the central spacecraft body. One converter from each panel is energized when the thrusters operate in pairs. Thus, for example, the converters in the north equipment panel operate the thrusters mounted on the east face, while the converters in the south panel operate those on the west face. The thrusters are located on the east-west faces because the north-south faces are needed for thermal control and the earth pointing face is needed for mounting the antenna frame. The thrusters are gimbal mounted so that they may be reoriented to provide torque control, thrust vector control for specific ΔV maneuvers, or backup capability for other thrusters.

For normal mode operation, two thrusters are nominally pointed north (-Y) and two are nominally pointed south (+Y). The thrusters are operated in pairs at each nodal crossing for north-south satellite stationkeeping. This permits lateral separation of the thrusters from the solar array axis in order to further minimize plume impingement.

The baseline propulsion subsystem weight is summarized in Table 4. The propellant requirements were calculated on the basis of completely replacing the existing hydrazine subsystem. Radiation hardening will be required for protecting power converter electronics and the fuel rods.

Table 4. Baseline Propulsion Subsystem Weight for DSCS-III

Hardware	Unit Weight (lb)	No. Required	Weight (lb)
Thruster (anode, cathode, ignitor plug, exhaust cone)	2	4	8
Capacitor Set	23	4	92
Power Converter	8	4	32
Gimbal Assembly	4	4	16
Fuel Housing	7	4	28
Radiation Hardening	2	4	8
Structure and Thermal Control	-	As required	22
Propellant (7-year mission)	21	4	84
Cables	-	16	3
Total			293

Two pounds per thruster complement has been allocated for this purpose. Upon completion of the flight configuration design, a detailed spacecraft hardening analysis will be required to verify this allocation. Similar, albeit smaller, thrusters have been radiation hardened in the past for operational flight (Ref. 2).

Baseline analysis was restricted to operating a maximum of two thrusters simultaneously at 1 millipound each. For this case, the propulsion power requirement equals $(2 \text{ mlb}) (170 \text{ W/mlb}) = 340 \text{ watts}$ during normal mode thrusting. Thus, the propulsion subsystem electrical interface may be tabulated as shown in Table 5, where the power requirements for full thrust operation and gimbal actuation are identified. The total number of commands required are also listed, as are the number of signal channels needed for monitoring thruster status.

Results from the baseline thermal analysis indicated that each thruster assembly requires approximately 18 inches of second-surface mirror radiator

²W.J. Guman and S.J. Kowal, "Pulsed Plasma Propulsion System for TIP-II Satellite," JANNAF Propulsion Conference, 1975.

Table 5. Propulsion Subsystem Electrical Interface for DSCS-III

POWER	340 Watts at 28 VDC: Full Thrust 10 Watts at 28 VDC for Each Gimbal Motor Actuation		
COMMANDS	FUNCTION	TYPE	NO. REQUIRED
	Thrusting Pulse	Discrete	4
	Gimbal +	Discrete	4
	Gimbal -	Discrete	4
	Total		12
TELEMETRY	SIGNAL	TYPE	NO. REQUIRED
	Discharge Voltage	Analog	4
	Discharge Initiating Voltage	Analog	4
	Capacitor Temperature	Analog	4
	Total		12

area, and the power converters (mounted as shown in Section B-B on Figure 8) will require approximately 36 square inches each on the north and south equipment panels. These results were generated by a conservative transient thermal analysis which calculated radiator areas that can probably be reduced after detailed analysis is performed for flight hardware. The thermal analysis assumed that a pair of thrusters are operated daily for 2.5 hours at each nodal crossing. Three different power converter installations were considered as follows:

- (1) Each converter internally mounted within the thruster housing
- (2) Converter pairs mounted on the east and west faces
- (3) Converter pairs mounted on the north and south panels

Installation 3 was selected for this study. Installation 1 has the disadvantage of requiring a significant amount of heater power in the nonoperating mode. Installation 2 has the disadvantage of requiring additional radiator area and heater power for the converters mounted on the east and west panels. Installation 3 was selected because continuously operating electronic components are located on the north-south panels, hence the required radiator area could be achieved by simply opening up the existing radiator. A single node analysis was performed on a thruster for a worst case transient heatup of 2.5 hours with direct solar input into the radiators and a transient cool down to the minimum temperature limit of -50°C .

It is desirable to have the capability to operate thrusters continuously for several days during orbit maneuvers. The thermal impact for operating a thruster continuously is to increase the thruster assembly radiator area to approximately 120 square inches. In addition, each thruster assembly will require 8 watts of standby power to maintain capacitor temperatures above survival limits after the thruster has been off for approximately 8 hours.

Of the other basic configurations studies in addition to the configuration A baseline, configuration B differs only in the electrical interface, which requires 680 watts maximum to operate four thrusters simultaneously

(versus 340 watts and two thrusters simultaneously for the baseline). Configuration C is shown in the layout drawing of Figure 9. It provides for body mounting of the gimbal drive and thruster assemblies, thereby decreasing the lateral separation afforded by the baseline. Configuration C reduces the structural weight budget for the propulsion subsystem by approximately 10 pounds.

4.2 INTERACTIONS WITH ATTITUDE CONTROL SUBSYSTEM

The following discussion presents the attitude control subsystem (ACS) considerations which affected configuration, the propulsion functions performed, and performance estimates. An investigation was also conducted to show that the pulsed plasma thrusters can be used as the principal torquing devices of the ACS on orbit normal mode control. This allows elimination of the reaction wheels.

4.2.1 Baseline Configuration

The baseline thruster configuration is shown schematically in Figure 10. It consists of four, single-axis gimballed pulsed plasma thrusters positioned near the mid-points of the N/W, N/E, S/W and S/E edges of the spacecraft body. Each thruster is canted out from N/S at a 30-degree angle and gimballed so that it can rotate around an axis parallel to the E-W axis. The gimball freedom required is approximately 280 degrees (from -95 to +185 degrees).

In the nominal configuration (as shown in Figure 10, all gimbal angles at 0 degrees), the thrusters fire in pairs for orbit control. Thrusters 1 and 2 fire for south stationkeeping; thrusters 2 and 3 for east stationkeeping; similarly for north and west. The thrusters are gimballed to provide torque control either to reduce disturbances due to thruster activity during stationkeeping (caused by thrust impulse unbalance, thrust misalignment and CG uncertainty), or to exploit this thrust vectoring capability to reduce reaction wheel stored momentum. This gimbaling also permits total capability with the failure of any single thruster and also opens the option of replacing the reaction wheels with direct thruster activity. These functions are discussed in more detail later.

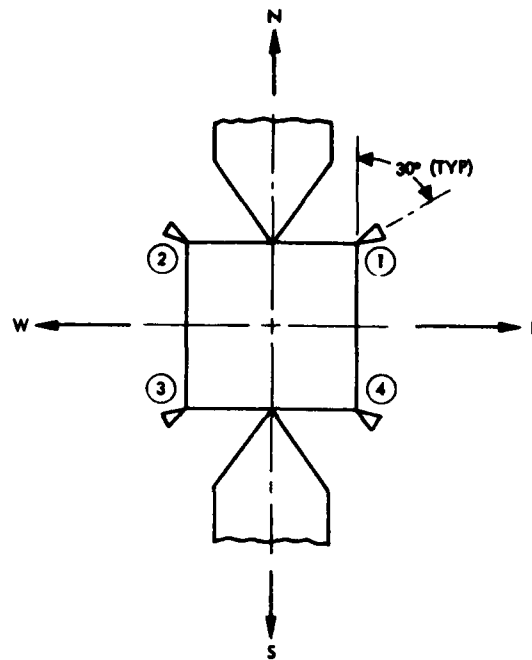


Figure 10. DSCS-III Thruster Configuration

The pulsed plasma thrusters are located on the same spacecraft faces as the hydrazine thrusters and can completely replace the hydrazine subsystem, with the only disadvantage being a relatively slow change of station capability. The PPT locations and selected cant angles reduce possible spacecraft contamination and are reasonably optimal in terms of propellant utilization.

The gimbal is normally operated at 0 ± 5 degrees with one thruster required for movement to the 180 ± 5 degree location in case of a single thruster failure. The control logic is assumed adaptable from the on-board ACS.

4.2.2 Functions Performed

The functions performed include initial stabilization, orbit trim and stationing, relocation, E-W stationkeeping, N-S stationkeeping, reaction wheel momentum unloading and torque control.

4.2.2.1 Initial Stabilization

It is assumed that large angle stabilization is achieved with sun sensors and a gyro(s) to create a semistabilized spacecraft, followed by a search for earth coverage with an earth sensor. Almost independently of the stabilization concept, the propulsion subsystem is required to reduce body spin rates from tip-off rates to an acceptable rate, and then three-axis pointing is acquired. The propulsion subsystem must provide three-axis torque control sufficient to reduce body rates. The low average thrust level of pulsed plasma thrusters is undesirable, but acceptable. The particular configuration selected does, indeed, provide three-axis torque control with any two thrusters operative with proportionately increased torque capabilities with three or four thrusters operative. The fact that two thrusters provide three axis control with this capability is illustrated in Figure 11. The torque is increased by increasing the angle the thrusters can be rotated. With this design, and the thrusters located as far from the CG as practical (i.e., maximum moment arms), best utilization is made of the low thrust levels.

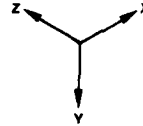
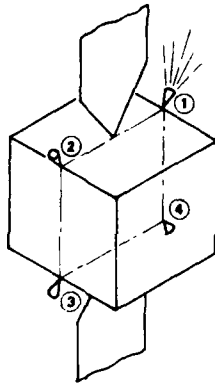
4.2.2.2 Orbit Trim and Stationing

This maneuver is achieved primarily with E-W thrusting to correct for booster velocity residuals and to allow the spacecraft to change from the inserted longitude (determined by launch efficiency demands) to the desired station. The launch vehicle is assumed to have imparted an initial drift rate and the spacecraft is required to make a predetermined east or west velocity change to reduce the drift to zero. This correction can be made by firing thrusters 1 and 4 or 2 and 3.

The 30-degree cant angle (from north) trades the efficiency of E-W maneuvers versus thrust efficiency for the much more used N-S stationkeeping. Because of this, the efficiency for orbit trim and stationing is only 50%. The maneuver can take a considerable length of time (38 days as shown in Section 4.2.3.2). If the time is critical, it can be shortened by a factor of 2.2 by rotating the spacecraft 90 degrees about the north-south axis and rotating the thrusters 90 degrees so that all four are vectored in the correct direction. When the spacecraft is rotated 90 degrees

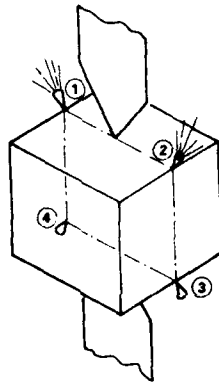
A) YAW CONTROL (TORQUE ABOUT Z AXIS)

FOR + YAW, FIRE 1
FOR - YAW, FIRE 2
GIMBAL ANGLE
FOR 1 AND 2 = 0 DEG



B) ROLL CONTROL (TORQUE ABOUT X AXIS)

FOR + ROLL, FIRE 1 AND 2, BUT
GIMBAL 1 AND 2 < 0 DEG ABOUT X AXIS
FOR - ROLL, FIRE 1 AND 2, BUT
GIMBAL 1 AND 2 > 0 DEG ABOUT X AXIS



C) PITCH CONTROL (TORQUE ABOUT Y AXIS)

FOR + PITCH, FIRE 1 AND 2, BUT
GIMBAL 1 < 0 DEG AND 2 > 0 DEG
FOR - PITCH, FIRE 1 AND 2, BUT
GIMBAL 1 > 0 DEG AND 2 < 0 DEG

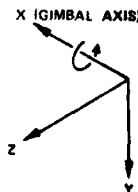
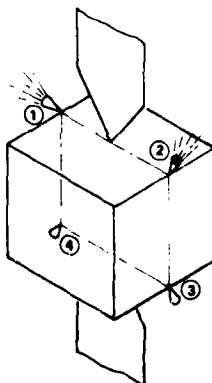


Figure 11. Three Axis Torque Control Capabilities Using Thrusters 1 and 2

about its Y axis to provide for in-track thrusting, it does not have use of its earth sensor. Thus, the sun sensor and rate gyro are employed for attitude control. This is only possible for approximately 12 hours daily because the sun vector must be nearly parallel to the earth vector and normal to the spacecraft yaw axis if the sun sensor is to be used.

4.2.2.3 Relocation

Relocation is an acceleration in an east or west direction followed by deceleration into the desired longitude station and stable orbital velocity. The maneuver is a two stage version of orbit trim and no further discussion is necessary.

4.2.2.4 E-W Stationkeeping

This is a periodic east or west thrusting required to prevent the spacecraft from drifting longitudinally off station. The basic approach is similar to 4.2.2.2 or 4.2.2.3 except the 90-degree rotation in this case is out of the question since payload operation is desired during this maneuver. Also, in order to minimize average power usage, the maneuvers may be performed at those times in orbit when N-S stationkeeping is undesirable.

4.2.2.5 N-S Stationkeeping

This is the predominant source of propulsion demands and justification of a high I_{sp} system. The requirement is due to lunar-solar perturbation upon the orbit. The most desirable times to perform the precession occur twice per orbit (once every 12 hours) at the nodes of the perturbed orbit plane and desired orbit plane. The nodes are inertially relatively fixed, and hence are crossed at different times of the day over a solar year. For example, the eclipse seasons require stationkeeping around 6 AM and 6 PM and do not increase the battery demands.

The thrusting efficiency falls as a cosine function of the orbital arc angle away from the nodes. For low level thrusting, the thrusting period is necessarily stretched out. In fact, since thruster power demands are directly proportioned to average thrust level, it is desirable to stretch the thrusting out until the incremental propellant weight of inefficient off-node firing offsets the incremental savings in the power subsystem.

4.2.2.6 Torque Control and Reaction Wheel Unloading

The reaction wheels are the primary attitude control torques for the spacecraft. They react to thruster torques as well as to other disturbances such as solar pressure induced torques. The wheels will store and not need assistance for periodic torques, but the inertially fixed components of torque cause the wheels to build up momentum.

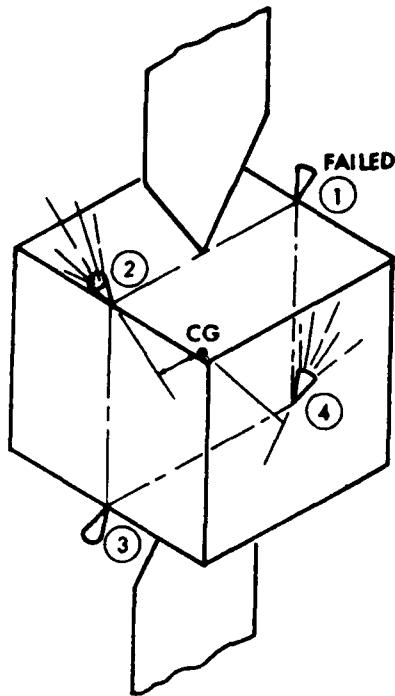
During an orbital correction, disturbance torques are generally produced from thrust misalignments and unbalances. This requires added thrusting to prevent these torques from overpowering the very small reaction wheels. In addition, even during periods of time when orbital stationkeeping is not required, propellant is required to unload the reaction wheels.

The gimballed pulsed plasma system is ideally suited for mating with a reaction wheel control system. Each thruster pulse is adequately small so that it does not overpower the reaction wheels. The relative duty cycle of the pair of thrusters required for stationkeeping plus small angle rotation of the thrusters can be scheduled so that the torques generated are of a polarity to reduce the momentum of the reaction wheels. In this manner, all reaction wheel unloading is done at insignificant propellant cost (since thrust efficiency falls off as the cosine of the gimbal angle and these angles are maintained at less than 5 degrees).

4.2.2.7 Single Point Failure Considerations

It has been shown that any pair of thrusters can provide three-axis torque control, hence be used for acquisition and reaction wheel unloading. A single thruster failure does not affect the ability to provide torque functions, merely the amount of torque available.

Stationkeeping is still possible with a single thruster failure as shown in Figure 12. If thruster 1 fails, east and north stationkeeping continue normally. For south stationkeeping, thruster 4 is rotated 180 degrees and fired in conjunction with 2. Since thruster 2 has a shorter moment arm, it will fire more frequently to maintain torque balance. For south stationkeeping then, it produces more of the impulse.



FOR SOUTH STATIONKEEPING, FIRE 2 AND 4 WITH 4 GIMBAL ANGLE = 180 DEGREES. IT CAN BE SEEN THAT MOMENT ARM 2 IS LESS THAN 4, HENCE MUST FIRE MORE FREQUENTLY TO MAINTAIN TORQUE BALANCE.

Figure 12. Single Point Failure Stationkeeping Strategy

Thus, the nonfailed thrusters need only be supplied with additional propellant to permit thrusting at both nodes. A net east component of velocity is also provided so that simultaneous east stationkeeping is provided. If east stationkeeping is not desired or is excessive, this is taken out by a west stationkeeping maneuver later in the day.

4.2.3 Performance Summary

The performance of this propulsion subsystem can be summarized in terms of time to perform certain functions, propellant, and electrical power requirements. These three parameters are considered below for the various functions. A total spacecraft weight of 2000 pounds was used in the calculations. Also, Teflon propellant consumption effects on weight were neglected.

4.2.3.1 Initial Stabilization

The tip off rates of the DSCS-III are not known, but a current propellant budget is provided calling for 229.2 lb-sec of propellant

(Ref. 3). The pulsed plasma thrusters are gimballed and located further from the spacecraft CG than the replaced hydrazine thrusters and therefore have longer moment arms. The assumption that pulsed plasma can acquire with no more than 229.2 lb-sec is then conservative. This maneuver would take 16 hours to complete and draws 680 watts of power during operation, necessitating sun oriented solar array panels during this time. While the presence of sun sensors plus the solar array drive would permit this operation, it is not known what detailed implementation problems this would entail. The propellant expended is a negligible 0.1 pound.

4.2.3.2 Orbit Trim and Stationing

Current estimates are that the initial orbit trim requires 52.3 ft/sec of ΔV (Ref. 3). Assuming the conservative earth oriented configurations, this requires 38 days, at 2.9 pounds of propellant and 340 watts average power. Should control revert to sun sensor and gyro and the spacecraft be rotated 90 degrees, the maneuver is reduced to 17 days, 2.0 pounds of propellant, and 680 watts average power.

4.2.3.3 Relocation

The propellant budget given for relocation is 9.3 ft/sec (Ref. 3) velocity increment (9.3 to accelerate and 9.3 to decelerate). This corresponds to approximately 0.5 deg/day. To achieve this velocity of station change requires approximately 13 days for the earth oriented configuration. This maneuver requires 1.0 pound of propellant and 340 watts average power during thrusting. The acceleration time can again be reduced to 6 days with the 90-degree spacecraft rotation.

4.2.3.4 East-West Stationkeeping

The budget given for this function is 85.0 ft/sec over 7 years (Ref 3). If a thrust segment is assumed twice per day (6 hours separated from the nodes of the N-S precession maneuver), the maneuver requires 17 minutes thrusting per segment with power requirements of 340 watts average or 94 watt-hours. The total propellant requirements are 4.8 pounds.

³"Mission Integration Study for Solid Teflon Pulsed Plasma Millipound Propulsion System," Appendix A, DSCS-III Data, TRW Report 33775-6002-RE-00, 5 October 1978.

4.2.3.5 North-South Stationkeeping

Considerable attention has been paid to north-south stationkeeping functioning for low level thrusters in previous studies (Ref. 4, 5, and 6). The yearly velocity increment required is about 150 ft/sec/yr. It is desirable to fire stationkeeping pulses at those two points in orbit which allow exact cancellation of the precession of the orbit plane. Making orbital corrections away from the desired nodes affects thrusting efficiency since the orbit axis is not being precessed exactly opposite to that of drift. The loss of efficiency is roughly proportional to $(1 - \cos \epsilon)$ where ϵ is the orbital angle between the node and the point where the thruster was fired. This translates directly into increased propellant consumption.

If the thrusting is distributed over a significant percentage of the orbit (> 10 degrees) as is certainly the case with 1 millipound thrusters, the integrated efficiency factor is $\sin \alpha / \alpha$ where α is the orbital half-angle over which thrusting takes place.

Thrusting inefficiency is also introduced when the thrusters are canted away from the north-south axis. When the thrusters are body mounted on three-axis stabilized spacecraft, canting is implemented to minimize effluent interaction with the solar arrays. For a cant angle ϕ with respect to the north-south axis, a cant angle efficiency factor, $\cos \phi$ is introduced.

Combining the above factors, the required number of thrusting hours per node, t , is given by:

$$t = \frac{24}{\pi} \sin^{-1} \left[\frac{\pi}{(24)(32.2)(3600)} \cdot \frac{1}{N_N N_D} \cdot \frac{M \Delta V}{F \cos \phi} \right]$$

⁴B.A. Free, W.J. Guman, B.G. Herron, and S. Zafran, "Electric Propulsion for Communications Satellites," AIAA Paper 78-537, April 1978.

⁵D.H. Mitchell and M.N. Huberman, "Ion Propulsion for Communications Satellites," Progress in Astronautics and Aeronautics, Vol. 55, 1977, pp 199-220.

⁶D.H. Mitchell and S. Zafran, "Ion Propulsion for Spacecraft Reaction Control," AIAA Paper 78-651, April 1978.

where

M = spacecraft weight, lb (assumed to be constant, i.e., neglecting cumulative propellant expulsion as the mission progresses)

ΔV = yearly mission velocity increment, ft/sec/yr

F = thrust, lb

N_N = number of nodal firings/day

N_D = number of days firing/year

These effects are shown graphically in Figure 13, where orbital efficiency and thrust are plotted versus thrusting time at each node for a spacecraft weight of 2000 pounds. North-south stationkeeping is performed daily to provide ΔV of 150 ft/sec/yr. Thrusting time requirements are shown for cant angles of 0 and 30 degrees. If stationkeeping is done at both nodes with a pair of millipound thrusters canted 30 degrees, then each thruster operates for about 2 hours a day. This equates to 33.4 pounds of propellant over 7 years. The average power during the 2-hour thrust periods is 340 watts.

4.2.3.6 Reaction Wheel Momentum Control and Torque Control

Since north and south and either east or west stationkeeping is performed every day, these periods of time can be used to unload the momentum of the reaction wheels via the gimbaling of the thrusters and uneven thruster duty cycles. All these effects can easily be controlled by gimbaling over ± 5 degrees and duty cycle unevenness of less than 10%. These small perturbations of the thrust vector are imperceptible in terms of propellant since the efficiency is proportional to the cosine of the gimbal angle.

4.2.3.7 Redundancy Considerations

It has been shown that the mission can be completed with any single thruster failed. In order to do so, sufficient propellant must be provided at nonfailed thruster locations to complete the mission. Assuming failure at launch, approximately 2 times the basic propellant is needed at each location.

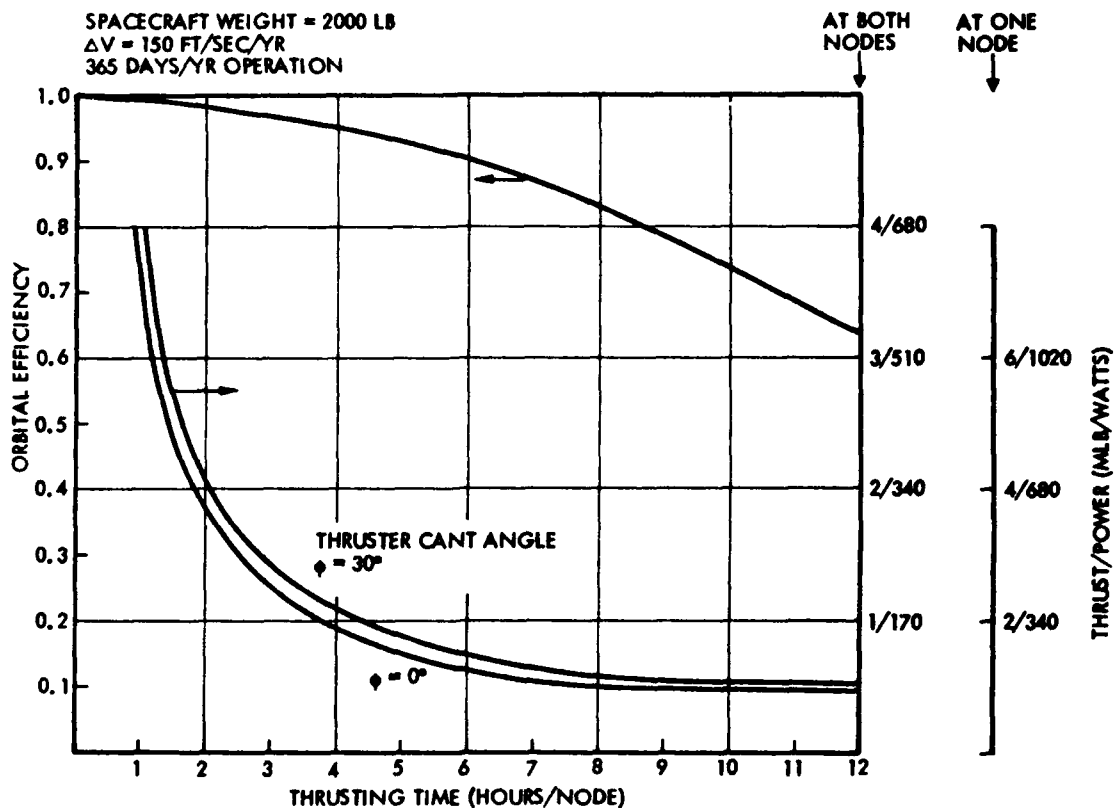


Figure 13. Orbital Efficiency and Thrusting Time for N-S Stationkeeping

4.2.3.8 Propellant Summary

Table 6 summarizes the propellant requirements for this baseline mission (7 years duration).

4.2.4 Attitude Control with Pulsed Plasma Thrusters

An investigation was conducted to see if the pulsed plasma thrusters can be used as the principal torquing devices of the attitude control subsystem on orbit normal mode control. This allows the elimination of the reaction wheels. The aspects investigated include accuracy, duty cycle requirements, impact on ACS, and gimbal duty cycling. In order to investigate these aspects, a disturbance torque model had to be developed. Since explicit disturbance calculations for DSCS-III were not known, a model developed for a more severe (higher disturbance torques due to antenna geometry) case of FltSatCom was used. The conclusions of the investigation

Table 6. Propellant Requirements for 7-Year* DSCS-III Mission

Function	Teflon Weight (lb)
Initial Stabilization	0.1
Orbit Trim	2.9**
Relocation	1.0**
E-W Stationkeeping	4.8
N-S Stationkeeping	33.4
Wheel Control	-
Torque Control	-
Redundancy Factor (X2)	42.2
Total	84.4

* Pulsed plasma propellant capability is for >10 years if no single point point failures occur.

** Weight estimate for the conservative earth pointing orientation.

are that the reaction wheels can be replaced, and this further step in integration of pulsed plasma thrusters onto DSCD-III shows the potential for added weight and cost savings. The one area of concern not addressed was flexible body bending effects. This is not considered a serious problem.

4.2.4.1 Current DSCS-III ACS Configuration

The equipment used to control the attitude of DSCS-III is summarized in Table 7. The earth sensor provides basic two-axis earth pointing information (pitch and roll data), while the sun sensors, some presumed estimation algorithm and, possibly, the rate gyro are used for yaw data. The basic yaw sensor is the sun sensor. However, near orbital noon and midnight, the sun vector is nearly collinear with the earth vector and cannot provide yaw information. It is presumed that ordinarily during this time, the disturbance torques are estimated and controlled out in an open loop fashion. The yaw gyro is available for high frequency yaw data should a change of station or stationkeeping thrusting be required at these inopportune times.

Three-axis torque control is provided by four reaction wheels (three active and one redundant) which store the angular momentum absorbed by reacting to disturbance torques. The reaction wheels reduce the number of

Table 7. DSCS-III ACS Components Physical Characteristics

Component	Total Number	Total Weight (lb)	Average Power (watts)	Heritage
Reaction Wheels	4	32.0	4.5	CTS, FltSatCom Model 35
Earth Sensor	1	8.5	2.7	Classified Programs LandSat, B-Sat
Sun Sensor Assembly	2	0.6	-	OA0 B-Sat Classified Programs
Attitude Control Electronics	1	27.4	26.0	B-Sat
Rate Gyro	1	1.4	*	B-Sat, Classified Programs
Total		69.9	33.2	
Solar Array Drive			0.9	
Total			34.1	

pulses required from hydrazine thrusters by permitting large impulse bits and averaging out periodic torques. When the momentum passes a preset threshold, the hydrazine thrusters are used to unload the momentum.

4.2.4.2 Proposed Changes to DSCS-III ACS Configuration

It is shown earlier that any pair of gimballed thrusters could provide three axes of torque control thus providing an opportunity for eliminating the reaction wheels. This is due to the possibility of arbitrarily small impulse bits (due to thruster gimbaling) and the inherently large number of pulses available. Technically, a pair of thrusters can provide a range of torques about any arbitrary axis (components of which can lie in all or any of the three spacecraft axes). Control is exerted to keep the attitude of the spacecraft within a tightly controlled dead zone. Each time the dead zone is exceeded (in any of the three axes), a thruster pulse must be fired to accelerate pointing toward the desired pointing attitude. The ACS would contain the same sensor set except the rate gyros and their

electronics would have to be modified to provide an integrated attitude sensing capability. The reaction wheel and hydrazine unloading functions would be served by the pulsed plasma thrusters. The control equations would need to be modified, dictating a microprocessor based controller (which appears to be the case anyway).

It is possible to design the control logic to minimize the frequency of thruster pulses with a simple disturbance torque estimation algorithm while the pointing drifts within the desired dead zone. This algorithm allows determination of the torque impulse bit which drives the spacecraft pointing back at a velocity which maximizes the time it drifts either across the dead zone or is driven back to the same dead zone.

The control law drives the gimbals to achieve this desired torque. Tight proportional torque is possible for roll and pitch torques since the thrusters are gimballed to produce these torques. These also happen to be the axes where tightest pointing is required (Table 8 reflects DSCS-III predicted pointing accuracies). Yaw torque is produced either from firing of a single thruster or the inadvertent impulse bit mismatch between thrusters. Since much less precise torque is required, this permits the reduced torque resolution of this axis. When a threshold is reached in one of the axes, the thrusters can be oriented in the other axes to anticipate pulse demands there and simultaneously control about all three axes.

4.2.4.3 Disturbance Torque Model

At synchronous orbit, the predominant disturbance torque source is the sun. Solar impingements on the spacecraft create forces about a center of mass and seldom along the vector from the sun to the center of mass. This factor plus the uneven re-radiation of photons creates torques. These torques vary with the shift in spacecraft surface facing the sun which occurs on a 24-hour basis. The fine grained detail of appendages creates changes in disturbance which shift at a higher rate than orbit rate. In addition, since the center of pressure is always forward of the center of mass, inertially constant torques exist. The reaction wheels are usually sized to exchange the higher frequency disturbance momentum and thruster unloading is required only for the inertially constant torques. These torques are modeled quite accurately via digital computer calculations. The solar

Table 8. DSCS-III Pointing Performance

	Operational Mode			Orbit Adjust Mode		
	Roll	Pitch	Yaw	Roll	Pitch	Yaw
Earth Sensor	.041	.043	-	.041	.043	-
Sun Sensor	-	-	<u>.34</u>	-	-	<u>.26</u>
Calibration Effect	-	-	.29	-	-	.14
Alignment Corrections	.005	.005	.02	.005	.005	.02
Dynamic Response	.030	.040	.45	.077	.05	.45
Total (RSS)	.051	.059	<u>.64</u>	.087	.066	<u>.54</u>

disturbance torque model used for DSCS-III was not available for this study, but the torques for FltSatCom are available. This is a very conservative model since the antennas on FltSatCom are much larger and less symmetric than DSCS-III, hence the periodic torques are greater. Since both spacecraft are approximately the same size, it is estimated that the inertially fixed torques are similar in magnitude.

The torques of the model are summarized in Table 9 and Figures 14 through 16. The figures provide typical roll, pitch, and yaw torques as a function of orbital time. The table is a Fourier series expansion of these disturbances giving the inertially fixed terms (a_0) (a , and b), and the new two harmonics. They are the first four terms of:

$$T_i = \frac{a_{i0}}{2} + \sum (a_{in} \cos n \omega_0 t + b_{in} \sin n \omega_0 t)$$

where T_i = torque of i = x (roll), y (pitch) and z (yaw) axes

and ω_0 = orbit rate ($\frac{2\pi}{24 \text{ hr}}$)

Table 9. Fourier Series Coefficients for Solar Torques

Case		Fourier Coefficients $\times 10^6$ (ft-lb)						
No.	T	a_0	a_1	b_1	a_2	b_2	a_3	b_3
1	T _x	-0.059	-2.514	0.241	0.033	-0.069	-0.517	-0.029
	T _y	-0.039	-19.378	-6.127	-0.09	0.308	-3.44	0.236
	T _z	0.138	0.	0.915	-0.069	0.01	0.	-0.002
2	T _x	0.182	-2.35	0.411	0.026	0.154	-0.665	0.108
	T _y	1.175	-18.28	-5.36	0.118	1.62	-4.075	1.174
	T _z	-0.077	-0.142	0.781	-0.069	-0.142	0.071	-0.041
3	T _x	0.185	-2.35	0.408	0.024	0.154	-0.665	0.108
	T _y	1.17	-17.98	-6.349	0.111	1.617	-4.068	1.189
	T _z	-0.078	-0.142	0.782	-0.068	-0.142	0.071	-0.041
4	T _x	0.182	-2.35	0.411	0.026	0.154	-0.665	0.108
	T _y	1.391	-24.21	-5.326	0.212	1.65	-4.287	1.204
	T _z	-0.057	-0.144	0.768	-0.082	-0.142	0.069	-0.04

where

$$T_x = \frac{a_{x0}}{2} + \sum_{n=1}^3 a_{xn} \cos n\omega_0 t + b_{xn} \sin n\omega_0 t$$

$$T_y = \frac{a_{y0}}{2} + \sum_{n=1}^3 a_{yn} \cos n\omega_0 t + b_{yn} \sin n\omega_0 t$$

$$T_z = \frac{a_{z0}}{2} + \sum_{n=1}^3 a_{zn} \cos n\omega_0 t + b_{zn} \sin n\omega_0 t$$

Case 1 = BOL, Equinox, unshaded

Case 2 = BOL, Equinox, shaded (by appendages)

Case 3 = BOL, Equinox, shaded

Case 4 = BOL, Equinox, shaded, -2 inch CG offset as worst case hydrazine imbalance

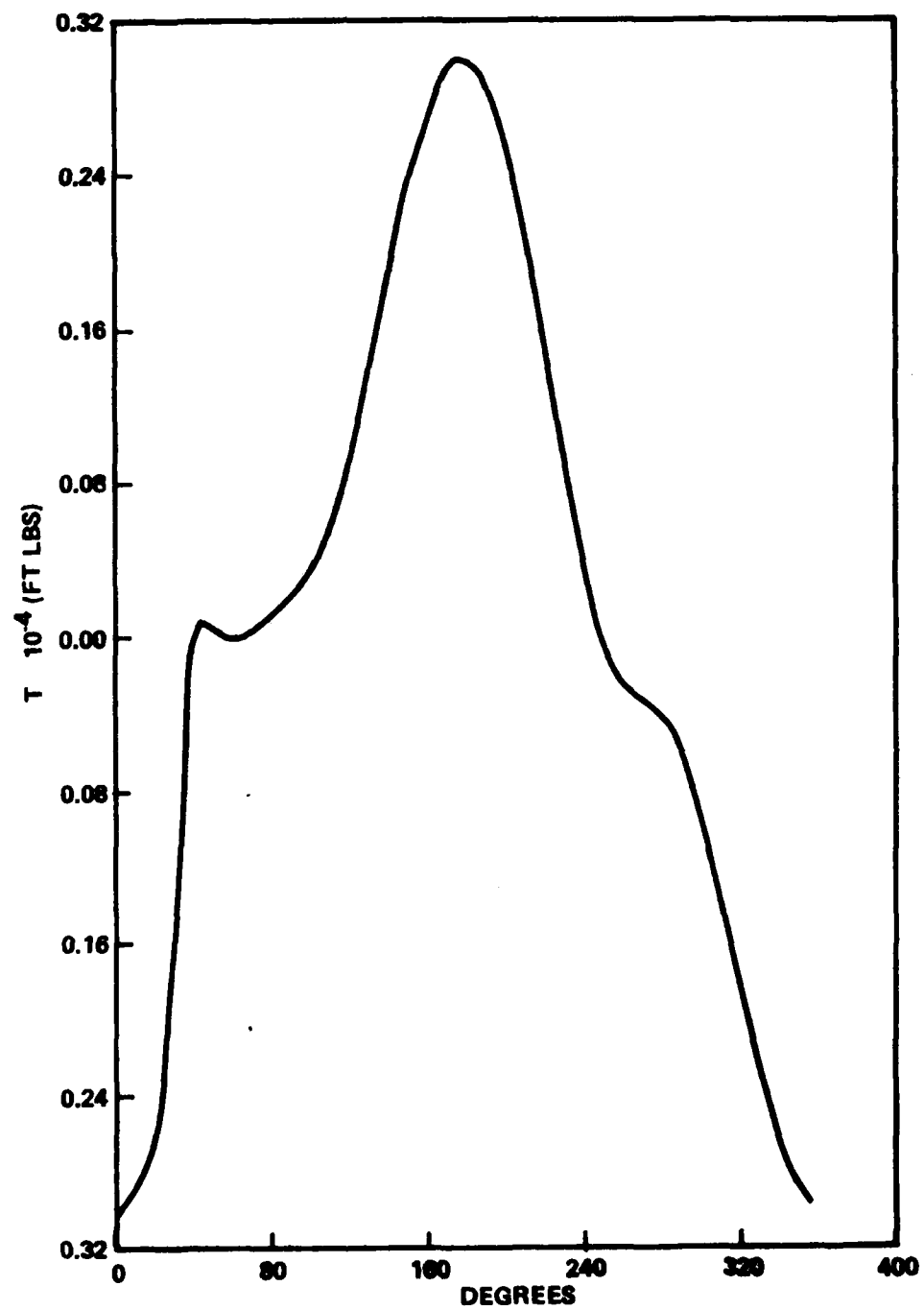


Figure 14. Roll Torque

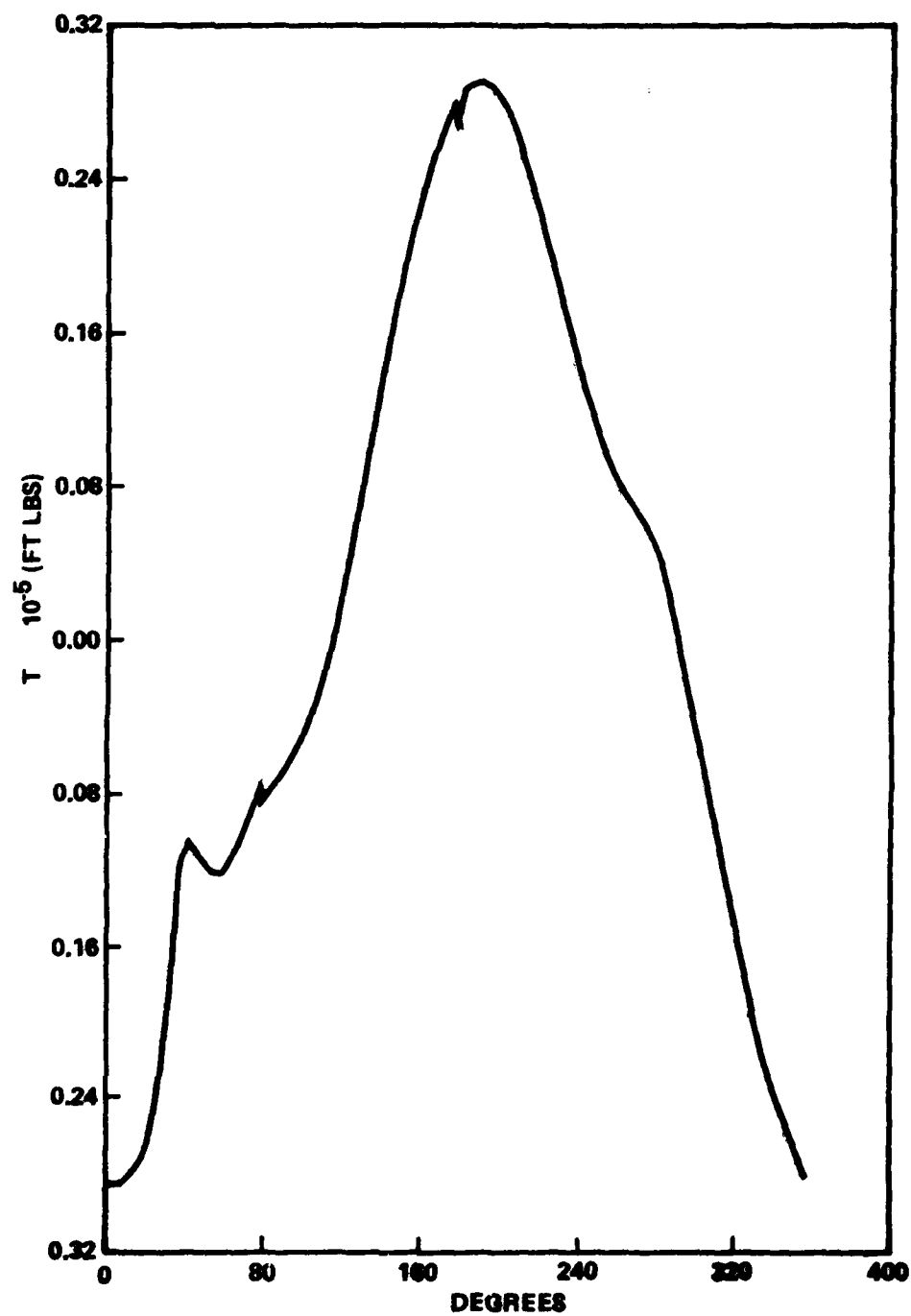


Figure 15. Pitch Torque

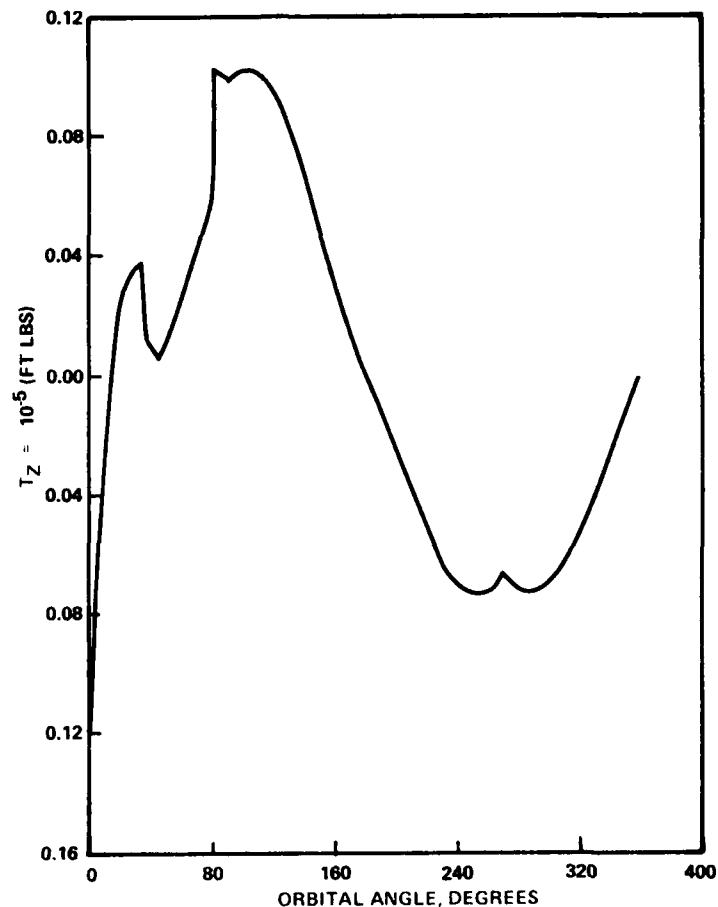


Figure 16. Yaw Torque

The significant factors which affect pulsed plasma effectiveness are: peak and average disturbances, monotonicity of disturbance over limited periods of time, and daily repeatability of the disturbances. The above model is quite attractive for use with a pulsed plasma system. Current spacecraft history suggests that all other and higher frequency disturbances are minimal and the above is a good first order approximation.

4.2.4.4 Pulsed Plasma Performance

The performance parameters of interest are pointing accuracy and number of pulses required to perform the mission. Accuracy is achieved by reducing the dead zone and precision in preprocessing sensor data while within

the dead zone. In order to achieve comparable pointing accuracy to the current system it is necessary to set the dead zone to fire at the + and - bounds of the dynamic response (see Table 8). Since sensor noise generally causes the thrusters to fire within the dead zone, the dead zone must be larger than this value, but the setting is dependent on sensor noise (unknown for the present study). However, if it is assumed the sensor processing algorithm and dead zones are set to maintain pointing within the dynamic response dead zone, the thrusters fire within roll, pitch, and yaw dead zones of 0.06, 0.08, and 0.90 degrees (distance from plus limit to minus limit).

The number of pulses is determined by (1) disturbance torque level, (2) size of dead zone, (3) torque impulse bit range of thrusters, (4) ability to estimate disturbance torques between pulses, and (5) ability to estimate and control thruster torque impulse bits. This interaction can be explained by the following brief mathematical derivation.

Look at the pitch axis pointing axis pointing error $\phi(t)$. The dead-zone is ϕ_{D+} or ϕ_{D-} and $\phi(t)$ moves within this range between thruster firings. Assume at $t = 0$, $\phi(t) = \phi_{D-}$ and a thruster pulse has been fired. The net result of this is to change the velocity $\dot{\phi}$ at $t = 0$ to a positive value so the pointing error will be diminished. At this time the pointing error has a negative ($\ddot{\phi}(0)$) due to disturbance torques. Since the largest disturbance torques are solar torques and these change slowly with time, disturbances can be assumed constant between thruster firings and likely to have a negative value since it was probably this disturbance that drove the pointing to ϕ_{D-} initially. The pointing error is then:

$$\phi(t) = \phi_{D-} + \dot{\phi}(0)t + \frac{1}{2}\ddot{\phi}(0)t^2$$

where $\ddot{\phi}(0)$ is negative and $\dot{\phi}(0)$ is positive.

Depending on the relative magnitude of $\dot{\phi}(0)$, and $\ddot{\phi}(0)$, the pointing error will either drift to ϕ_{D+} or slow, reverse direction and return to ϕ_{D-} . The time between pulses is maximized when the thruster pulses at $t = 0$ cause $\phi(0)$ to be such that the pointing vector drifts from ϕ_{D-} . The

ability to do this depends on the level of $\phi(0)$, the ability to estimate it, the control torque impulse bit flexibility and ability to estimate the impulse bit provided with the pulses.

It is assumed for this study that the disturbance torque can be estimated to within 10%, the torque impulse bit is controllable to within the tolerances of ± 1 degree thrust vector misalignment, the levels of torque were provided in Section 4.2.4.3 and control torque impulse bits are arbitrarily limited by vectoring capabilities of the thrusters to within ± 10 degrees of the nominal N-S pointing directions. With these very conservative assumptions, it can be calculated what the thrusting duty cycle is for relatively large disturbance torques and low torques in the transition regions. The dominant disturbance torque is $2.4 \times 10^{-5} \cos \omega_0 t$ ft-lb. The inertias for DSCS-III are not known, but for FltSatCom they are 450 slug-ft². Thruster moment arms are 32 inches.

The disturbance torque is then $\sim 3 \times 10^{-6} \text{ deg/sec}^2 \cos \omega_0 t$. The control impulse torque available from two north or south thrusters rotated to ± 10 degrees is $5 \times 10^{-4} \text{ deg/sec}$ with an uncertainty of $\pm 0.5 \times 10^{-4} \text{ deg/sec}$. For these levels, the control impulse bit is too small to drive the pointing vector across the 0.08-degree deadband and pulses are required every 167 seconds. As the disturbance torques decline from their peaks, the deadband excursion increases until the desired trend is achieved. This occurs when the disturbance has declined to $4.3 \times 10^{-7} \text{ deg/sec}^2$ and the time between thrust firings is 640 seconds. As can be seen from the disturbance torque model, this is the case for the majority of the time. When the disturbance torque gets smaller, the thrusters are vectored to reduce the control torque impulse bits. As the control torques get very small, the limiting factor in time between pulses becomes control torque repeatability. This has been assumed to be $\pm 0.5 \times 10^{-4} \text{ deg/sec}$, which in the worst case causes pulse firings on both sides of the dead zone with no disturbance torques and the time between firings becomes 160 seconds. It can be seen that the worst cases are 160 seconds between pulses and best is 640 seconds. A conservative average is 300 seconds between pulses.

The roll axis has a smaller deadzone (0.06 degree) but a much larger inertia (estimated at 2000 slug-ft²). The disturbance torques are also smaller by an order of magnitude. The larger inertia reduces the peak torque

impulse bit (in terms of pointing Δ velocity) to 1.12×10^{-4} deg/sec, hence uncertainty to 1.12×10^{-5} deg/sec. The worse case thruster duty cycle then becomes 540 seconds between pulses. These disturbances can easily be compensated for at each pitch firing by, at that time, also producing a roll component to drive the pointing vector away from the deadzone. This way a smaller number of total pulses is required and the roll pointing error seldom reaches a deadzone.

The yaw axis is controlled by occasionally firing just one thruster to keep the yaw pointing vector within the deadzone. This could be done simultaneously with a pitch/roll control or separately. One pulse by a single thruster is required approximately every 237 seconds.

Since the three axes do interact and cross-couple and simultaneous firings are not always possible, a conservative three-axis case would probably require, on the average, a pair of thrusters firing every 200 seconds. Over the 7-year mission, this reduces to 10,000 lb-sec of impulse required. Attitude control can be maintained with any thruster pair, so it is assumed the pair is selected which provides the appropriate north or south station-keeping component. In this case, the propellant used for attitude control contributes to N-S stationkeeping and reduces the amount of impulse budget for that function. Since thrusting is quasi-continuous for ACS, the N-S stationkeeping contribution is only 63% efficient. This means that in the worst case, only 3700 lb-sec of additional impulse must be provided by pulsed plasma thrusters to provide continuous attitude control in addition to the normal stationkeeping functions. This adds 1.7 pounds of propellant weight.

It is of interest to also investigate the amount of gimbal motion to evaluate the reliability impact on the gimbal drives. If the disturbance torques are as modeled in Section 4.2.4.3, they are essentially orbit rate sinusoids. In this case, the thrusters would move from 10 degrees in one direction to 10 degrees in the opposite direction. When the disturbance torques transition in polarities, there may be some +, - deadband limit cycling. Assuming 20 two-degree oscillations per day, a total gimbal travel of 60 degrees is provided. This is 1/6 the travel required of the solar array drive which uses a similar drive mechanism, hence, gimbal wearout is not a pressing concern.

4.3 ELECTRIC POWER

The following discussion summarizes the impact on the present DSCS-III electric power subsystem resulting from the integration and operation of the pulsed plasma millipound propulsion subsystem.

4.3.1 Electric Power Subsystem Description

The subsystem, shown in block diagram form in Figure 17, is a direct energy transfer system that provides a regulated bus voltage of $28 \pm 1\%$ Vdc for distribution to user loads. The subsystem operates in three distinct operating modes: battery discharge with the battery voltage boosted to the regulated bus; battery charge from the regulated bus; and shunt regulation of the solar array when its output exceeds the total power demand of the loads and the batteries. Transition from one mode to the next is smooth and continuous.

The capability of the DSCS-III solar array is shown in Figure 18 with beginning and end of mission (10-year) values obtained from Reference 3.

Three 16-cell 32-Ah (rated capacity) sealed nickel-cadmium batteries provide power during prelaunch, launch, ascent, and on-orbit service periods and provide energy to clear faults if they develop. The maximum depth-of-discharge for the batteries under normal operation with maximum eclipse discharge is 65.1%.

4.3.2 Propulsion Power Requirements

Table 10 summarizes the power requirements of the DSCS-III spacecraft, by subsystem and by mission phase, as given in Reference 3. Battery charge power requirements, not shown in the table, are 118 watts for full charge at equinox and 45 watts for trickle charge during the solstice seasons.

Table 11 provides the derivation of the total load requirement at the power regulation unit (PRU) after the electric power demands of the chemical propulsion subsystem have been removed.

Table 12 summarizes the revised load requirements that result with the addition of the pulsed plasma thruster propulsion subsystem to the DSCS-III spacecraft. The table delineates the requirements for thruster configurations A and B — 340 and 680 watts of thruster load, respectively, during the initial mission phase — and the associated heater power demands.

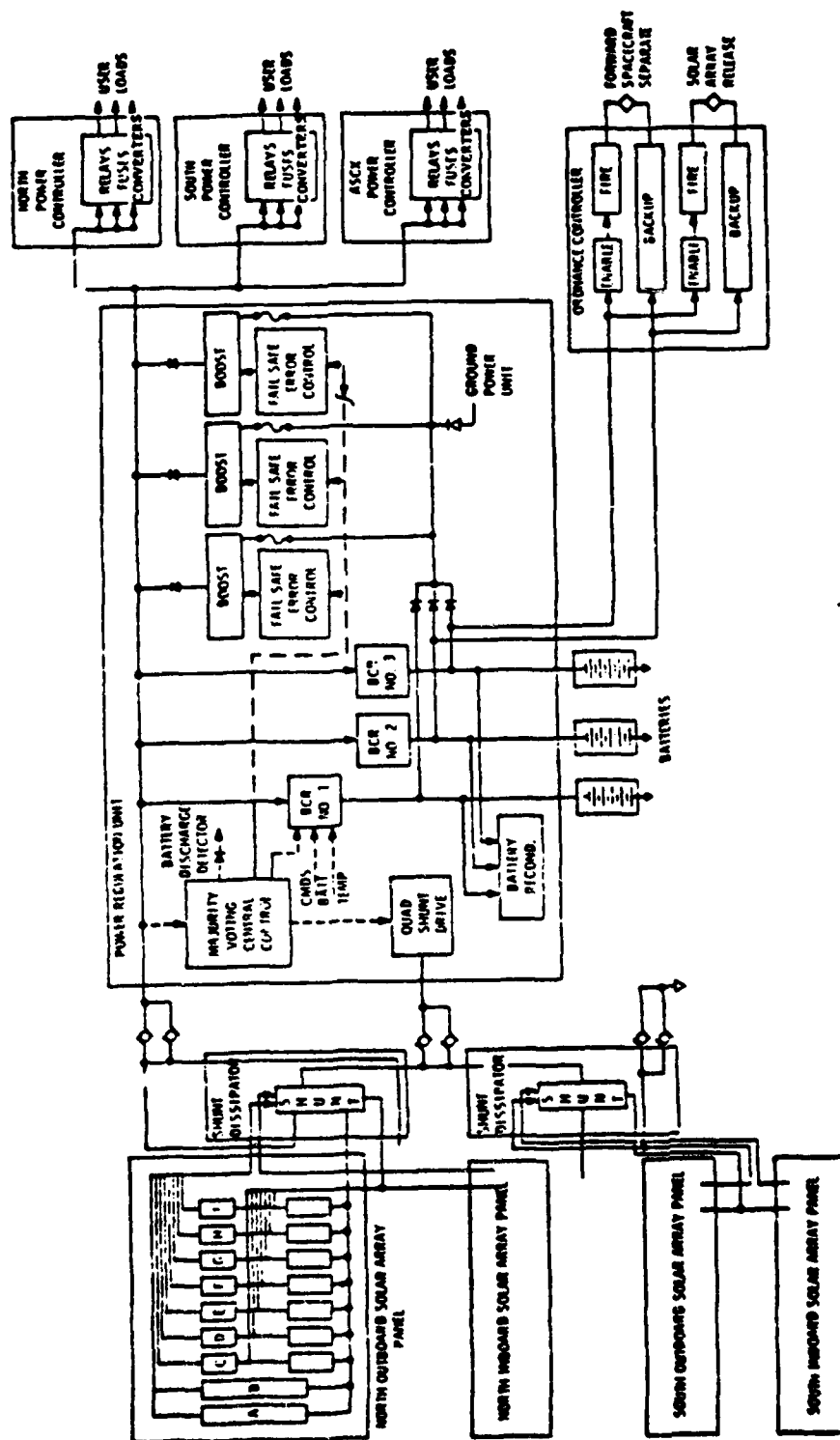


Figure 17. DSCS-III Electric Power Subsystem

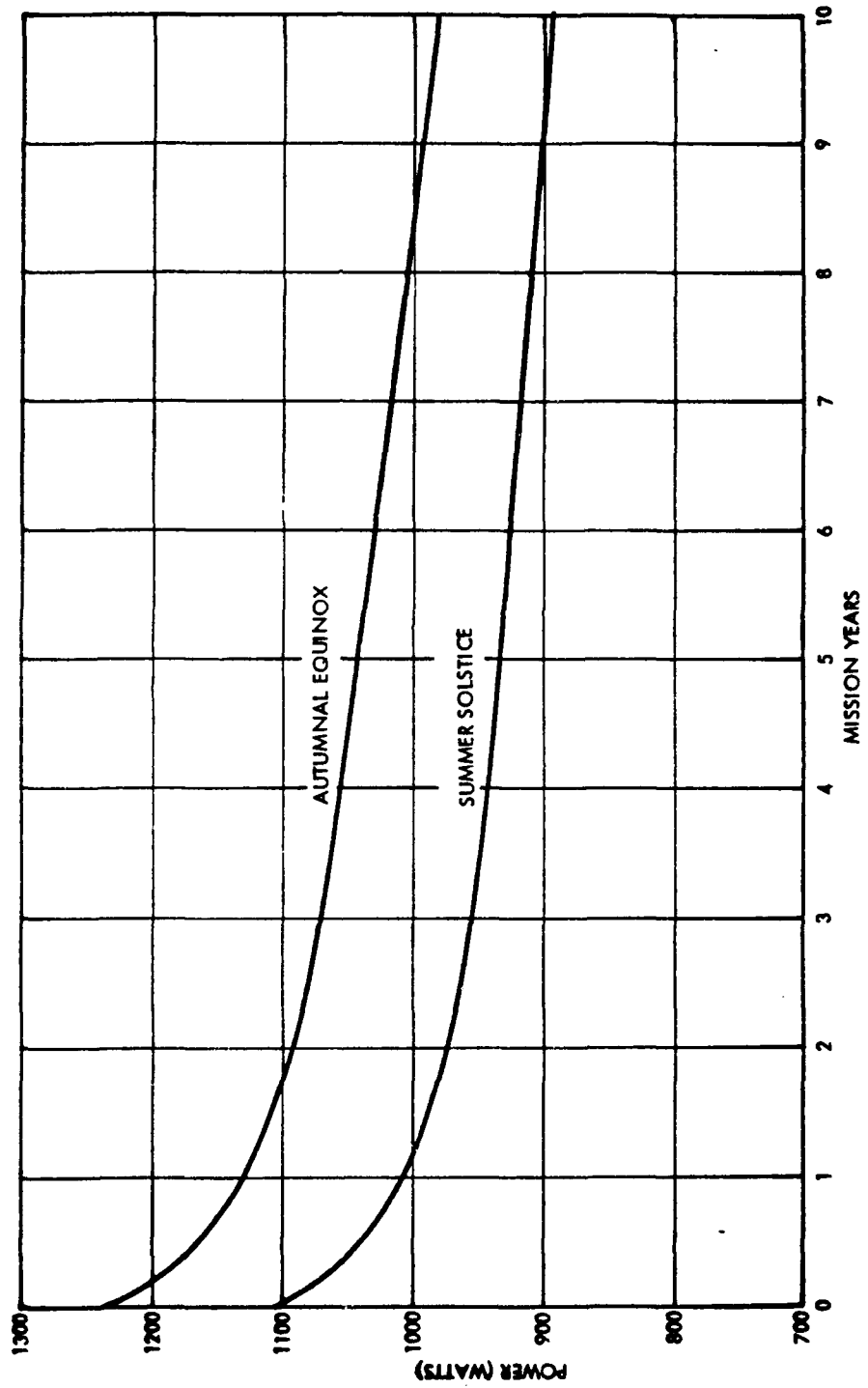


Figure 18. Solar Array Power Timelines (at PRU at 28 Vdc)

Table 10. DSCS-III Load Power Requirements

Power Requirement	Initial Stabilization	Orbit Trim and Stationing	Relocation	E-W Station-keeping	N-S Station-keeping	Summer Solstice	Winter Solstice	Sun-light	Equinox Eclipse
Attitude Control	58.3	50.4	50.4	50.5	50.5	50.5	50.5	50.5	50.5
Propulsion	18.0	23.3	23.3	39.6	39.6	1.8	1.8	1.8	-0-
TT&C	42.3	42.3	42.3	115.9	115.9	115.9	115.9	115.9	135.3
Communications	-0-	-0-	-0-	460.7	460.7	460.7	460.7	460.7	460.7
Electric Power	4.0	10.0	10.0	10.0	10.0	10.0	10.0	10.0	10.0
Gimbal Antenna	-0-	3.2	3.2	3.2	3.2	3.2	3.2	3.2	3.2
SCT	-0-	57.6	57.6	57.6	57.6	57.6	57.6	57.6	179.6
Thermal	437.3	437.3	437.3	63.8	63.8	54.3	48.7	89.2	64.2
Subtotal	559.9	624.1	624.1	801.3	801.3	754.0	748.4	788.9	903.5
Distribution Loss	11.2	12.5	12.5	16.0	16.0	15.0	15.1	15.8	18.1
PRU Standby	10.0	10.0	10.0	10.0	10.0	10.0	10.0	10.0	10.0
Total Load at PRU	581.1	646.6	646.6	827.3	827.3	779.0	773.5	814.7	921.6

Table 11. Load Requirements with the Chemical Propulsion Subsystem Removed

Power Requirement	Initial Stabilization	Orbit Trim and Stationing	Relocation	E-W Station-keeping	N-S Station-keeping	Summer Solstice	Winter Solstice	Equinox	
								Sun-light	Eclipse
Subtotal from Table 1	559.9	624.1	624.1	801.3	801.3	754.0	748.4	788.9	903.5
Less Propulsion Load	(18.0)	(23.3)	(23.3)	(39.6)	(39.6)	(1.8)	(1.8)	(1.8)	-0-
New Subtotal	541.9	600.8	600.8	761.7	761.7	752.2	746.6	787.1	903.5
Distribution Loss	10.8	12.0	12.0	15.2	15.2	15.0	14.9	15.7	18.1
PRU Standby	10.0	10.0	10.0	10.0	10.0	10.0	10.0	10.0	10.0
Total Load at PRU Less Propulsion	562.7	622.8	622.8	786.9	786.9	777.2	771.5	812.8	921.6

Table 12. Load Power Requirements with Pulsed Plasma Thruster Subsystem

Power Requirement	Initial Stabilization	Orbit Trim and Stationing	Relocation	E-W Station-keeping	N-S Station-keeping	Summer Solstice	Winter Solstice	Equinox	
								Sun-light	Eclipse
Total Load at PRU Less Propulsion	562.7	622.8	622.8	786.9	786.9	777.2	771.5	812.8	921.6
Pulsed Plasma Thrusters Duration (h)									
32/16	340.0/680.0	340.0/680.0	340.0/680.0	340.0	340.0				
902/404									
321/144									
0.283, twice/day									
2.0, twice/day									
Thrusters Heaters Duration (h/day)									
14	16.0/0.0	16.0/0.0	16.0/0.0	16.0	16.0	16.0	16.0	32.0	32.0
24									
Thruster Power Distribution Loss	7.1/13.6	7.1/13.6	7.1/13.6	7.1	7.1	0.3	0.3	0.6	0.6
Revised Total Load at PRU	925.8/1256.3	985.9/1316.4	985.9/1316.4	1150.0	1150.0	793.5	787.8	845.4	954.2

4.3.3 Subsystem Impact Assessment

The basic design approach is to utilize the existing batteries for support of daily thruster firing that cannot otherwise be accommodated by the solar array power available in excess of spacecraft load power demands. The solar array is not increased in size except by the amount that may be necessary to control the depth-of-discharge of other batteries or to provide required additional battery charge power.

Thruster configurations A and B were analyzed to determine the impact on existing electric power system energy source components and to identify necessary increases in component size. The design drivers for each configuration are quite different. For configuration A, each period of thrusting is well within the capability of the solar array at beginning-of-mission (BOM). At end-of-mission (EOM), the batteries support the E-W and N-S stationkeeping maneuvers with no effect on their size. The solar array must, however, be increased in size by 63.4 watts (7.1%) at EOM (10-year summer solstice) to provide full battery recharge capability of 118.0 watts. The design point for the solar array is thus

793.5 W	Summer solstice load
118.0	Battery charge power
<u>49.2</u>	6.2% power margin
960.7 W	10-year summer solstice array power requirement at 28 Vdc

The power margin is assumed based upon the minimum power margin of the existing subsystem design (50.5 watts referenced against an 814.7 watt total load at equinox). The performance characteristics of the power source components required by configuration A are summarized in Table 13.

Configuration B requires that thrusting during initial mission phases be accomplished at higher power levels in order that the propulsion intervals be reduced in time span. This impacts the solar array by requiring that it be increased in size by 210.1 watts (19.0%) at BOM summer solstice to 1316.4 watts. This BOM solar array requirement is equivalent to the total load requirement during trim orbit, stationing, and relocation

Table 13. Power Source Performance Characteristics for Thruster Configuration A

Mission Year	Season	Thruster Load (W)	Mission Phase	Required Array Power at 28 Vdc (W)	Revised Total Load Power at PRU (W)	Battery Discharge Per Thrusting Interval (Wh)	Battery Depth-of-Discharge (%)
0	Summer Solstice	340	Initial Stabilization	1184.8	925.8	0	0
			Orbital Trim and Stationing	1184.8	985.9	0	0
			Relocation	1184.8	985.9	0	0
			E-W Stationkeeping	960.7	1150.0	58.2	3.2
10			N-S Stationkeeping	960.7	1150.0	411.5	22.3
0	Autumnal Equinox		Initial Stabilization	1326.2	925.8	0	0
			Orbit Trim and Stationing	1326.2	985.9	0	0
			Relocation	1326.2	985.9	0	0
			E-W Stationkeeping	1053.0	1150.0	29.8	1.6
10			N-S Stationkeeping	1053.0	1150.0	210.9	11.4

*Per thrusting interval

maneuvers. The sensitivity of the batteries to the long duration of these thrusting intervals if the array is insufficient is illustrated as follows:

- 67.5% depth-of-discharge corresponds to 1266.4 Wh removed from three batteries
- For the orbit trim and stationing phase

$$\frac{1244.6 \text{ Wh}}{404 \text{ h}} \times 0.92 = 2.8 \text{ W at the battery.}$$

Thus, an error greater than 2.8 watts on array capability at BOM will cause the depth-of-discharge limit, which has been recomputed for the new equinox discharge load (was 65.1 %), to be exceeded. The 0.92 factor above accounts for power subsystem converter efficiency.

With the array increased in size by 19%, there is only battery discharge during the stationkeeping maneuvers that occur during the solstice seasons as EOM is approached. Otherwise, the available power margins at EOM are 19.7 and 24.4% of the load at summer solstice and autumnal equinox conditions, respectively (throughout these analyses, a load power margin is assumed to exist only during periods of nonthrusting). The performance characteristics of the power supply components required by configuration B are summarized in Table 14.

Table 15 defines the appropriate array weight and area increments required as a result of increasing the array capability to meet the requirements of configurations A and B.

The impact of superimposing battery discharge cycles on the normal eclipse season discharge profile has not been assessed. Prior studies indicate, however, that the battery utilization levels reported in Tables 13 and 14 are within the capabilities of the nickel-cadmium batteries being used.

Table 14. Power Source Performance Characteristics
for Thruster Configuration B

Mission year	Season	Thruster Load (W)	Mission Phase	Required Array Power at 28 Vdc (W)	Revised Total Load Power at PRU (W)	Battery Discharge Per Thrusting Interval (Wh)	Battery Depth-of- Discharge*
0	Summer Solstice	680	Initial Stabilization	1316.4	1256.3	0	0
			Orbit Trim and Stationing	1316.4	1316.4	0	0
			Relocation	1316.4	1316.4	0	0
10			E-W Stationkeeping	1067.8	1150.0	25.3	1.4
			N-S Stationkeeping	1067.8	1150.0	178.7	9.7
0	Autumnal Equinox		Initial Stabilization	1473.8	1256.3	0	0
			Orbit Trim and Stationing	1473.8	1316.4	0	0
			Relocation	1473.8	1316.4	0	0
			E-W Stationkeeping	1170.0	1150.0	0	0
			N-S Stationkeeping	1170.0	1150.0	0	0

*Per thrusting interval

Table 15. Weight and Area Impact on Solar Array Size

Thruster Configuration	Array Power Increment at BOM Summer Solstice (w)	Array Weight Increment (lb)	Array Area Increment (ft ²)
A	78.5	9.5	8.9
B	210.1	25.4	23.9

4.4 INTERACTIVE EFFECTS

Analysis of potential interactive effects between the pulsed plasma thruster and the DSCS-III spacecraft is principally concerned with material transport effects, electromagnetic compatibility, impact on communications, and spacecraft charging. These topics are addressed separately below.

4.4.1 Material Deposition on Spacecraft Surfaces

A review was made of the presently available body of plume data for the pulsed plasma thruster. These measurements divide into two forms: (1) measurements of ion density within the thruster plume (within a comparatively narrow range of directions), and (2) attempts at deposition measurements in the side flow (high divergence angle) and back flow (divergence angle in excess of 90 degrees) regions. In both instances the present data base does not extend into sufficiently high divergence angle regimes and into sufficiently dilute flow portions of the plume to allow the usual (and required) form of an interactive effects analysis.

Measurements of ion density in the thruster plume have been carried to approximately 45-degrees from the thruster axis. The measurements reveal the typical "parabolic core/exponential wing" form of ion density dependence with a dropoff of approximately two orders of magnitude in moving from the beam axis to one 45-degree divergence angle point. While these measurements are sufficient to determine the thrusting characteristics of the plume (which has been the intent of the studies to this point), the interactive effects analysis demand the knowledge of flux density to at least the 90-degree divergence angle point for an unshielded thruster and, if the thruster is shielded, will demand the measurements of all material transport into the penumbra and umbra regions created by the beam shield.

The second body of work on plume properties that has been examined describes measurements of material accumulation from the thruster using either deposition plates or quartz crystal microbalances (QCMs). Those reports have acknowledged the very serious effects of facility presence and have determined that facility effects are increasingly of dominant concern in the high divergence angle regimes which must ultimately be examined in these plume flows. In recognition of these difficulties, the AFRPL has initiated a plume measurements program in special test facilities at the Arnold Engineering Development Center (AEDC) in order to obtain the necessary data.

In the DSCS-III configurations, it is possible for plume products from the pulsed plasma thrusters to deposit on solar array surfaces and to alter the optical transmittals of the solar cell covers, and the solar absorptivity of both front and rear array faces. In the absence of definitive plume measurements in the high divergence angle regime ($\theta \geq 45^\circ$) during the time framework of this present study, the approach taken advocated use of a beam shield in the northerly direction for north firing thrusters and in the southerly direction for the south firing thrusters. The beam shield shape selected for the thrusters was, as an initial working choice, the configuration used earlier for beam shields on north-south stationkeeping 8-cm mercury thrusters. The combined thruster integration actions of lateral displacement, canting, and beam shielding have been found to be sufficiently protective of solar array surfaces on the (narrow) north-south oriented solar arrays of Intelsat V in a previous ion thruster study (Ref. 7). If the pulsed plasma thruster is, thus, no more divergent than the 8-cm mercury ion thruster, these integration design actions should prevent contamination of the DSCS-III solar array. It should be emphasized, however, that no actual data are presently available in the high divergence angle regime and no data are available over the extent of the thruster plume refraction into the umbra regions of a beam shield. Both of these should be carried out in a suitably large testing chamber, preferably using

⁷S. Zafran, ed., "Ion Engine Auxiliary Propulsion Applications and Integration Study," NASA CR-13512, July 7, 1977.

time-of-flight plume measurement techniques to eliminate the effects of facility presence.

As a final note for material deposition on DSCS-III surfaces, there is some concern relative to the optical solar reflectors (OSRs, very low second surface mirrors) on the north and south faces. These surfaces could be contaminated if the thruster plume has excessive refractibility over the beam shield edges and over the spacecraft edge. Secondary material transport processes (for example, from the pulsed plasma thruster to some other surface like the solar array and then to the OSRs) are also of concern for possible contamination of these north and south facing radiative surfaces. The above will provide interactive effects data relative to both the solar array and the OSR surfaces.

4.4.2 Electromagnetic Compatibility

The approach to be taken in assuring electromagnetic compatibility in the pulsed plasma thruster with DSCS-III is similar to that required for DSP. The discussion describing the approach for DSP is given in Section 5.4.2.

4.4.3 Impact on Communications

The earth facing side of DSCS-III contains a family of antennae for up-link and down-link radio frequency (RF) signals. Under typical operating conditions the RF lines-of-sight are approximately perpendicular to the pulse plasma thruster axes and, hence, the RF signals are not required to traverse the comparatively dense plasma regions of the plasma plume. It should be noted, however, that S-band signals will be completely absorbed for a distance of ~20 meters along the thruster axis during the period of the plasma burst (ρ_+ diminishes to levels of ~ 10 ions/cm³ at ~20 meters from the thruster) and that appreciable RF refraction effects of S-band signals will exist for distances of almost 100 meters.

Several factors combine to diminish the RF refraction effects of the plume. The first of these is the use of X-band frequencies on DSCS-III. At these higher frequencies the plume is more transparent to the RF and both the critical absorption zone and the critical refraction zones in the plumes shrink significantly. The second factor is the wide angular separation between the RF lines-of-sight and the thruster axes, so that

only the widely divergent portions of the plasma plume will move in the direction of the RF transmission path. A third factor is the shielding effect of the spacecraft edges on the east and west faces of the spacecraft. This shielding acts to further diminish the plume density along the RF lines-of-sight.

In spite of the actions cited above, it is recommended that a series of tests be undertaken to determine if significant levels of RF refraction and signal loss occur during the thrust burst. These tests include the previously discussed plasma flow measurements in the high divergence angle regime and in the umbra regions of various shielding structures, and, in addition, should include the live linkage of a representative DSCS-III antenna to a transmitting and/or receiving antennae to observe possible RF signal dropout during the burst period. These tests would also answer possible microwave breakdown problems resulting from electrons in the plasma plume in regions from the antennae. The principal concern here is that electrons may be present at sufficiently high levels to initiate microwave breakdown.

Communication services are provided on DSCS-III at UHF, X and S bands. The impact of a 30-microsecond pulse from the plasma thrusters on these RF services cannot be realistically assessed at this time because of a lack of experimental data on the plume and because the refraction analysis has not been done. Analyses of practical interactions (absorption and reflection) between a plasma and antenna beams have been done where the beam tries to penetrate the plasma (e.g., during a reentry), but these are of little use here. In order to bound the problem, then, some worst case assumptions are made and some system suggestions are developed that may make the impact tolerable. It is anticipated that actual impact will be much less because of the large angular separation between the thruster and antenna axes, because of physical shielding and because the actual services will be less demanding. Thus, other methods of making the propulsion and RF services compatible will emerge as more data are obtained, but the current "worst case" suggestions will still be useful.

The X-band repeater (transponder) services are provided by six channels, four of which are 60 MHz wide; the other channels are 50 and 85 MHz wide. These channels are each wide enough to accommodate a number of FDMA

(frequency diversity multiple access) links, each with moderate capacity, or one very high data rate TDMA (time diversity multiple access) link. It can be assumed that these links carry all types and priorities of military traffic, from narrow band voice and low bit rate teletype data, through medium band width television, video data and secure voice, to state-of-the-art wide bandwidth single signal links. Many links have algebraic and other codes with error detection and correction capability to obtain improved BER (bit error rate) characteristics. Some links operate in a duplex mode where an indistinguishable message can be identified by the receiver who can request total or partial retransmission. A few high priority messages require essentially complete assurance of error-free completion with a minimum time delay.

The potential impact and mechanisms for avoiding the problems depend strongly on the nature of the link, the service and the ground stations (i.e., are they field services with little sophistication or a large control site). Under a worst case assumption that each thruster firing causes a 30 μ sec blackout or destruction of the link, a number of problems can be identified. One concern is for the integrity of the basic message; at data rates of kilobits per second or less a 30 μ sec outage would not materially affect the transmission; at 100 kilobits per second (10 μ sec per bit), several bits would be affected but the common types of convolutional coding would be effective; at megabit rates, too many bits would be affected to be corrected by codes intended to protect against random errors. A second concern is for the integrity of the link itself. With spread-spectrum links, for example, the receiver and transmitter must acquire a synchronism that might be lost before the message rate is reached and appreciable time might be required to reestablish synchronism. Another concern relates to the protection against jammers provided by the link design. The DSCS-III multiple access antennas form beam patterns which put jamming sources in gain nulls and which can shift with beam refraction.

The above discussion primarily relates to the X-band repeater channels used for the majority of DSCS-III capacity. The plasma becomes less transparent as the RF frequency decreases, and the RF beamwidths tend to be larger at lower frequencies. Thus, while the likelihood of interference from the plasma is still low, it is higher than for X band. The DSCS-III

uses S-band (and X-band) for TT&C service and UHF (and X-band) for the so-called single channel transponder. Plasma firings might impair S-band commands slightly under worst case assumptions, but typically such links have large margins, low bit rates and good protection from encryption and command procedure. The UHF links, on the other hand, are more affected by plasma, are planned for use with smaller stations, and handle high priority messages; the beam widths are relatively large, however, so that both the likelihood of and the tolerance for a refraction disturbance increase. The UHF situation needs more study than has been possible to date.

The X-band impact can be serious under worst case assumptions if no remedial action is taken. Recognizing that the "cost" of a solution should not outweigh the improvement obtained by the thrusters, primarily relatively simple changes have been examined here. Possible methods of avoiding serious effects include modifying network procedures, ground station hardware, spacecraft hardware, and spacecraft software. The thruster firings typically are not extremely time sensitive because a three-axis control system is used (i.e., the satellite is not spinning). They will not occur closer together than about 5 seconds apart. Each firing presumably affects all X-band channels simultaneously, but because the nature of the traffic through each channel will help establish the impact, some channels may be able to work right through a firing while others must be shut down. This argument suggests that decisions be made at ground stations rather than automatically at the satellite.

Some suggested methods are:

- (1) Let the attitude control subsystem determine firing times; notify ground stations of an impending firing by modulating the X-band beacons either (a) 250 ms before a firing, or (b) during a firing. With (a) ground stations will receive the beacon message before it transmits a message that would arrive during the firing; with (b) the ground station will know that a specific, already transmitted message may have been interfered with.
- (2) Use (1), but plan periodic firings so that the ground station can predict firings. With the millipound thruster, large numbers of firings will be the rule and assuring accurate periodicity will be a help.

- (3) Let the firing times be defined by a specified ground station; it will cause a firing either by a TT&C command (X or S band) or by dropping the carrier momentarily on its channel (such a power transient, detected by a satellite receive label monitor, would act as an enable signal and would permit a firing, not cause one). The specified ground station would either be the source of priority messages or a network control station.
- (4) Let the firing times be defined by the attitude control subsystem, but allow a specified ground station the ability (as in 3) to inhibit firings temporarily for critical periods.

The last approach seems most appealing since it requires little more than procedural changes, and it provides a level of protection consistent with the limited state of knowledge about the threat.

In summary, the UHF threat needs more study and the X-band situation is such that if testing should show a significant refraction threat exists, there is a DSCS-III service capability that could be adversely affected if no action is taken. If the thruster firings do impact the X-band links, the severe problem is that of maintaining synchronism on secure links. A burst of more than 5 or 10 chip errors would make normal coding ineffective on all high rate links. A recommended precautionary step would be to consider a means of inhibiting thruster firings via X (and S) band commands from ground communication stations, a means of detecting communication channel commands and a means of modulating the beacon transmissions with thruster firing data.

4.4.4 Spacecraft Charging

During the past decade a significant body of information has been generated on the charge-up of spacecraft during geomagnetic substorms when such storms penetrate the region of geosynchronous orbits. In some instances it is believed that total spacecraft failures have resulted from the discharges that followed the differential charge-ups on the vehicle. The concern of the interactive effects analysis in this area is the possibility of the pulsed plasma thruster acting as a "trigger" for differentially charged spacecraft surfaces. The experience on ATS-6 and with a continuously operated plasma source (the 8-cm cesium ion thruster) is that the plasma source presence and operation generally quench both charge-up and differential charge-up of the spacecraft and result in a very quiescent spacecraft electrical equilibration, even in the midst of comparatively

severe charge-up environmental conditions. It should be noted, however, that these data were obtained with a continuously operating plasma source. The pulsed plasma thruster, on the other hand, has a pulse-to-pulse separation time which is approximately the period of time required to attain complete steady-state charge-up on the host spacecraft if geomagnetic substorm conditions were to be present. The thruster firing, thus, could act as a trigger to the differentially charged spacecraft with all of the attendant problems which the spacecraft discharges can create.

It is not readily apparent that an appropriate test can be devised in this area. As a suggestion, however, an electron swarm tunnel illumination test of a spacecraft dielectric coating could be carried out with a specified pulsed plasma thruster orientation relative to this surface. If the thruster firing caused the dielectric surface to "clean off" in the usual propagating discharge wave manner, then the concerns of the thruster as a trigger for spacecraft discharging would appear to be valid and a series of protective measures to prevent spacecraft upsets or damage would have to be devised.

4.5 RELIABILITY ANALYSIS

A reliability assessment was conducted to determine the millipound propulsion subsystem reliability as a function of operational lifetime. The baseline DSCS-III thruster configuration is represented by the block diagram presented in Figure 19. It consists of four, single axis gimballed, pulsed plasma thrusters located two each on the east and west faces of the spacecraft. Orbit control is achieved by firing the thrusters in pairs. Thruster gimbal operation permits total subsystem capability with the failure of any single thruster and provides dual thruster failure tolerant performance with the exception of the failure of the east or west pair.

A solid propellant pulsed plasma thruster complement consists of a power converter, discharge initiating circuit, thruster gimbal mechanism, and propellant-discharge assembly including energy storage capacitors. The power converter transforms input dc power typically found on spacecraft into energy to be stored in the capacitor bank. The capacitor bank

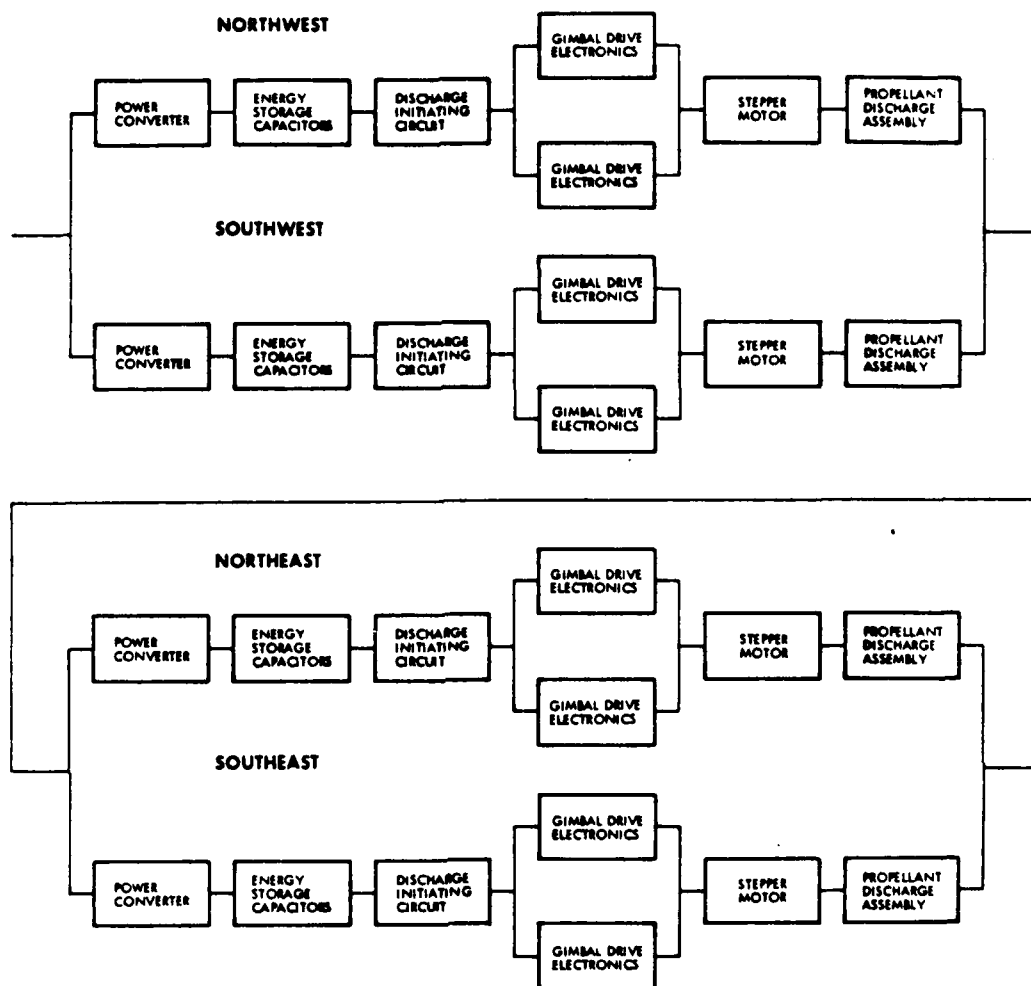


Figure 19. Reliability Block Diagram

consists of four energy storage capacitors connected in parallel. This energy is periodically discharged across the thruster electrodes depolymerizing surface layers of Teflon which become energized and ejected as a plasma through the thruster nozzle.

An absolute assessment of subsystem reliability was not possible because of a lack of accurate failure rate data for some of these components. In order to facilitate as accurate an assessment as possible, actual failure rates, where they were well defined, were utilized in conjunction with a parameterization of failure rates for those components

lacking a well defined and accepted failure rate history. Failure rates for the components in the block diagram are contained in Table 16. Individual failure rates for the power converter and discharge initiating circuitry were determined by analyzing their respective circuit diagrams (Ref. 8) with anticipated flight quality components in accordance with Section 3, MIL-HDBK-217B, Notice 2. This resulted in a projected total electronic component failure rate, less energy storage capacitors, of 990 bits, which is in good agreement with previously demonstrated data as reported in References 9 and 10. The thruster gimbal mechanism utilized is the TDRS (Tracking and Data Relay Satellite) gimbal system and the failure rate data for its components are consistent with the current design experience. The energy storage capacitors represent the area of greatest uncertainty in the present reliability assessment. These devices represent a significant percentage of the total subsystem failure rate and thereby are a primary contributor to the ultimate subsystem reliability. High reliability capacitors of the appropriate size for the millipound system are presently under development, but definitive failure rate data are currently unavailable. Additionally, prior reliability evaluations of pulsed plasma thrusters have either assumed a thruster reliability of unity or have addressed only the electronic components. Therefore, little if any failure rate data presently exist for the thruster and propellant feed system.

To accomplish the present reliability assessment, an effort was undertaken to define the anticipated range of failure rates for the energy storage capacitors, propellant feed system, and thruster. Once established,

⁸D.J. Palumbo, W.J. Guman, and M. Begun, "Pulsed Plasma Propulsion Technology," AFRPL-TR-74-50, July 1974.

⁹W.J. Guman, "Task 1 - Design Analysis Report, Pulsed Plasma Solid Propellant Microthruster for the Synchronous Meteorological Satellite," NASA-CR-122358, December 1971.

¹⁰"Reliability Estimating Procedures for Electric and Thermochemical Propulsion Systems," Booz Allen Applied Research, AFRPL-TR-76-99, February 1977.

Table 16. Solid Propellant Pulsed Plasma Thruster System Failure Rate Data

	Bit Rate*	Remarks
Power Converter	863	MIL-HDBK-217B Analysis
Discharge Initiating Circuitry	<u>127</u>	MIL-HDBK-217B Analysis
Total Thruster Electronics Less Main Energy Storage Capacitors	990	1006 (Ref. 9) 466-2850 (Ref. 10)
Thruster Gimbal Drive Electronics	684	TDRS
Gimbal Drive Stepper Motor	143	TDRS
Propellant-Discharge Assembly	500-3500	Anticipated Range of Applicability

* 1 bit = 10^{-9} failures/hour

these data were combined into a representative failure rate for the propellant discharge assembly. The reliability evaluation was then performed by parameterizing the propellant discharge assembly failure rates over the range presented in Table 16.

A representative range of failure rates for the energy storage capacitors was determined by evaluating MIL-HDBK-217B data for similar devices. This evaluation resulted in an anticipated failure rate range of 150 to 250 bits per capacitor. The propellant feed system representative failure rate range was determined through the summation of typical failure rate data for the individual components. When possible, component failure rates were based upon in-space performance of similar components as reported in Reference 11. However, no generic failure rate data exist for the propellant retainer or negator spring. These components were

11 "Generic Failure Rates for Spacecraft Applications," TRW IOC No. 74-2288-051, July 1974.

evaluated in accordance with guidelines established for military aircraft (Ref. 12) and ratioed by means of a common item to spacecraft loads. This evaluation indicated that the anticipated failure rate for the propellant feed system might be as high as 2500 bits.

It is assumed that only random failures are addressed in this evaluation as sufficient screening and component "burn-in" was performed to eliminate infant mortality failures and all components are utilized within their demonstrated lifetime thereby eliminating wearout failures.

The actual failure rate of each box in Figure 19 is a function of the duty cycle at which it operates. For any given duty cycle, D (where $0 < D < 1.0$), the box failure rate was calculated as a weighted average of the active and standby failure rates:

$$\lambda(D) = D \lambda_a + (1-D) \lambda_s$$

Failure rates for components in a standby mode, λ_s , were assessed fractional values of their active failure rates, λ_a , as follows:

For all electronic components	$\lambda_s = 0.1 \lambda_a$
For the gimbal mechanisms	$\lambda_s = 0.1 \lambda_a$
For the propellant discharge assembly	$\lambda_s = 0.1 \lambda_a$
	$\lambda_s = 0.5 \lambda_a$
	$\lambda_s = 1.0 \lambda_a$

The parameterization of standby failure rates for the propellant discharge assembly was performed to evaluate the influence of the propellant feed system standby stress levels on the overall subsystem reliability.

As implied by Figure 19 for the baseline four-thruster subsystem, a failure of any single thruster is noncatastrophic, as is the failure of any pair of thrusters, with the exception of the east or west pair. Any

¹²"Standardized Failure Rate Data," Bureau of Naval Weapons, April 1970.

failure of three thrusters will be catastrophic to the subsystem. In calculating the reliability of the subsystem, it is not computationally valid to apply simple reliability models to each box and then multiply the box reliabilities across the block diagram in the usual manner. The difficulties arise from the fact that the duty cycle at which each box operates (and therefore its failure rate) is dependent upon the good/failed status of other boxes in the system. This implies that box failure occurrences within the subsystem are not statistically independent, the essential condition which makes multiplying box reliabilities across the diagram a valid procedure.

In order to accurately take into account the significant duty cycle and failure rate perturbations which result from failure occurrences, a previously developed Markov process model was utilized to evaluate each of the candidate designs. The Markov model is of the discrete state, continuous time variety, sometimes referred to as continuous time Markov chains. Models of this type provide a means of analyzing the behavior of systems which can be regarded as always existing in one of several discrete states, and which are subject to random disturbances or hazards which cause the system to change states at unpredictable times. In Markov reliability models the states correspond to various numbers and kinds of failures, and the state transition probabilities are determined by the failure rates of the various parts of the system.

The Markov model which was used for the baseline evaluation is shown in the state transition diagram of Figure 20. As the figure shows, each Markov state is a specific combination of thruster complement good/failed states, each thruster complement consisting of one thruster with its associated gimbal mechanism and electronic components. As suggested by Figure 20, the system begins the mission in state 1, remains there for some random amount of time, then makes a transition into one of the single failure states (2, 3, 4, or 5), remains there for some random amount of time, then makes another transition, and so on. The reliability of the system at any given time is the probability that the system has not entered state 10 by that time. Failure rate data for the various boxes of the system enter into the Markov model in the form of transition rates,

G = GOOD THRUSTER COMPLEMENT
F = FAILED THRUSTER COMPLEMENT

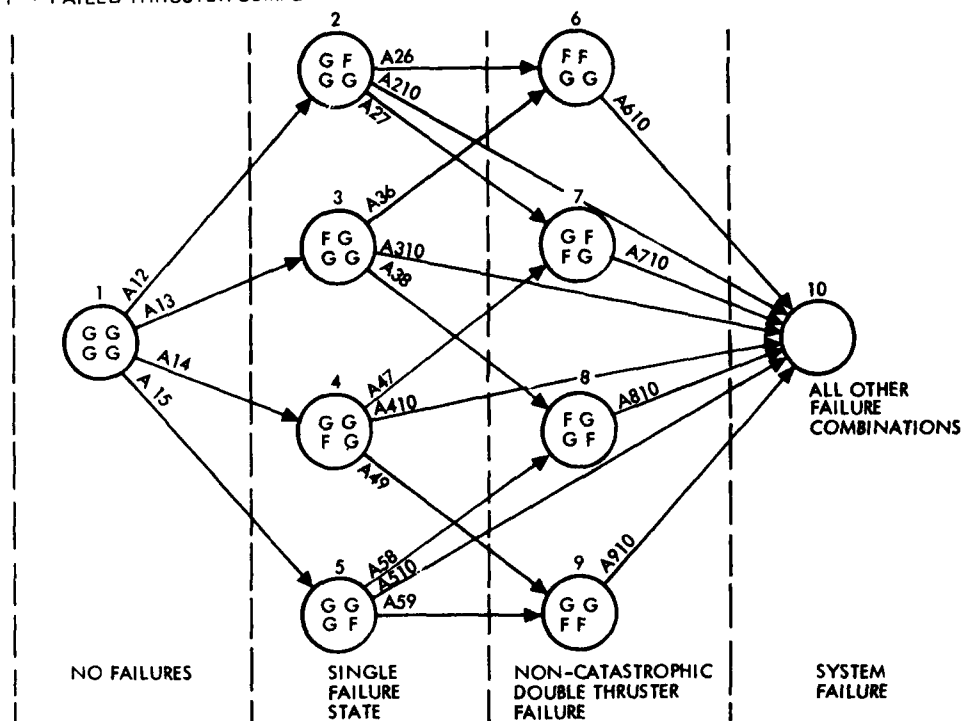


Figure 20. Markov State Transition Diagram

denoted A₁₂, A₁₃,, in Figure 20. The magnitudes of these transition rates define the state transition probabilities, as well as the probability distribution of the amount of time spent in each state. Since the transition rate between each pair of states may be specified independently, the dependency of box failure rates upon the good/failed status of other boxes is easily incorporated. Thus, the transition rates out of each state are calculated based upon the specific duty cycle associated with the thrusting requirements.

Table 17 shows the daily hours of on-orbit thruster operation required of each thruster for the DSCS-III mission. These data are tabulated for each Markov state and represent the thruster and electronic box operating time interactions resulting from failure occurrences.

Thruster operation during initial stabilization and orbit trim was evaluated in a classical manner externally from the Markov model with the resultant thruster reliability applied to the Markov model at the begin-

Table 17. Solid Propellant Pulsed Plasma Subsystem
Thruster Duty Cycle

System Markov State	Thruster Hours per Day			
	North- East	North- West	South- West	South- East
1	2.39	1.82	1.82	2.39
2	Failed	1.82	1.82	4.77
3	2.39	Failed	3.63	2.39
4	2.39	3.63	Failed	2.39
5	4.77	1.82	1.82	Failed
6	Failed	Failed	3.63	4.77
7	Failed	3.63	Failed	4.77
8	4.77	Failed	3.63	Failed
9	4.77	3.63	Failed	Failed
10	Failed	Failed	Failed	Failed

ning of state 1. The resultant propulsion subsystem reliability predictions for this baseline configuration are presented in Table 18. For example, the baseline subsystem reliability for a 7-year DSCS-III mission is 0.98 for an assumed propellant-discharge assembly failure rate of 2500 bits at $\lambda_s/\lambda_a = 0.5$.

4.6 CONFIGURATIONS COMPARISON

Weights of various DSCS-III tradeoff configurations were computed and compared in order to establish the margin available for added payload when implementing pulsed plasma propulsion. Table 19 summarizes the results of the tradeoff comparison for the configuration identified in Table 20. The configurations listed are those of most interest because they illustrate the impact of configurational differences.

Table 18. Parametric Reliability Assessment, DSCS-III Baseline Configuration

$(\lambda_{PDA})_A$ $(\lambda_{PDA})_s$ (bits) $(\lambda_{PDA})_A$		Reliability (Years On-Orbit)									
		1	2	3	4	5	6	7	8	9	10
500	0.1	.99990	.99979	.99964	.99946	.99923	.99897	.99867	.99834	.99797	.99756
1500	0.1	.99984	.99961	.99928	.99886	.99834	.99773	.99703	.99624	.99536	.99439
2500	0.1	.99976	.99937	.99880	.99805	.99713	.99603	.99477	.99335	.99177	.99002
3500	0.1	.99968	.99908	.99820	.99704	.99559	.99389	.99192	.98970	.98723	.98453
500	0.5	.99984	.99962	.99932	.99894	.99847	.99793	.99730	.99660	.99581	.99496
1500	0.5	.99962	.99891	.94785	.99646	.99474	.99270	.99036	.99772	.98480	.98161
2500	0.5	.99930	.99782	.99558	.99260	.98892	.98458	.97961	.97405	.96792	.96127
3500	0.5	.99889	.99639	.99255	.98746	.98120	.97386	.96551	.95624	.94611	.93520
500	1.0	.99972	.99932	.99875	.99803	.99714	.99610	.99491	.99357	.99209	.99046
1500	1.0	.99917	.99749	.99498	.99165	.99757	.98277	.97729	.97117	.96444	.95715
2500	1.0	.99832	.99457	.98885	.98133	.97216	.96149	.94946	.93622	.92189	.90660
3500	1.0	.99720	.99061	.98059	.96753	.95181	.93378	.91378	.89211	.86906	.84489

$(\lambda_{PDA})_A$ = Active failure rate, propellant-discharge assembly

$(\lambda_{PDA})_S$ = Standby failure rate, propellant discharge assembly

Table 19. DSCS-III Tradeoff Comparisons, 7-Year Mission

Configuration	A	A-2	B-2	C-2	C-3	C-4	C-5*	C-6
Maneuver Times, Days (a)								
• Initial Stabilization	1.3	1.3	0.7	1.3	1.3	1.3	1.3	1.3
• Orbit Trim	38	28	17	28	<0.1	28	28	<0.1
• Relocation (b)	13	10	6	10	<0.1	10	10	<0.1
Propulsion Subsystem (Dry) Weight, 1b								
• Pulsed Plasma Subsystem	209	208	208	197	195	199	199	197
• Hydrazine Subsystem	---	---	---	---	27	---	---	27
Propellant Weight, 1b								
• Teflon (c)	84	82	82	82	76	86	86	80
• Hydrazine	---	---	---	---	25	---	---	25
Attitude Control Subsystem Weight Impact, 1b								
• Reaction Wheels	---	---	---	---	---	(22)	(22)	(22)
Power Subsystem Weight Impact, 1b								
• Additional Solar Array	10	10	25	10	10	10	---	---
Net Weight for Propulsion, 1b	303	300	315	289	333	273	263	307

(a) Assumes average spacecraft weight = 2000 1b

(b) At rate of 0.5 deg/day after full acceleration; maneuver time is for acceleration and deceleration.

(c) Meets 7-year life requirement with any single point failure. Carries > 10 years of propellant with no failures in first 3 years.

* Preferred configuration

Table 20. Candidate DSCS-III Configurations

Identification	Layout Drawing	Maximum Number of Thrusters Operating Simultaneously	S/C Rotated 90 degrees for Orbit Trim and Relocation	N ₂ H ₄ for Orbit Trim and Relocation	ACS Reaction Wheels Deleted	245 Days/yr Station-keeping
* A	AD0310, Figure 8	2	-	-	-	-
A-2	AD0310, Figure 8	2	X	-	-	-
B-2	AD0310, Figure 8	4	X	-	-	-
C-2	AD0311, Figure 9	2	X	-	-	-
C-3	AD0311, Figure 9	2	-	X	-	-
C-4	AD0311, Figure 9	2	X	-	X	-
C-5	AD0311, Figure 9	2	X	-	X	X
C-6	AD0311, Figure 9	2	-	X	X	X

* Baseline

The baseline configuration, A, is described in Section 4.1. Its propellant weight requirements include a redundancy factor of 2.0 at each thruster location so that the subsystem can tolerate any single point failure. The power subsystem weight includes an additional 10 pounds of solar array for full battery recharge capability during summer solstice. Table 19, therefore, shows a net weight of 303 pounds for propulsion on DSCS-III with configuration A, including propellant redundancy and impacts on attitude control subsystem and power subsystem weight allocations. Also shown for comparison on Table 19 are the times required for several propulsive maneuvers including initial stabilization, orbit trim, and relocation. Other maneuver times are not significantly affected by configurational differences.

Configuration A-2 is identical to the baseline except that the spacecraft is rotated 90 degrees for orbit trim and relocation maneuvers. (This is discussed more fully in Section 4.4.2.2.) In this manner, the maneuver time for orbit trim is reduced to 28 days from the baseline time of 38 days.

Configuration B-2 increases the power available to the propulsion subsystem to enable simultaneous operation of four thrusters instead of two. Thus, the maneuver time for orbit trim is reduced to 17 days. The power subsystem impact, however, is 25 pounds of added solar array (see Section 4.3) to support the increased load at beginning of mission.

Configuration C-2 is identical to A-2 except that the thrusters are body mounted instead of boom mounted (baseline mounting). Configuration C mounting is described in Section 4.1 and illustrated in Figure 10. Body mounting of the propulsion subsystem reduces the structural weight requirements by 11 pounds.

Configuration C-3 is a combined hydrazine/pulsed plasma propulsion subsystem. Hydrazine is used for orbit trim and relocation, reducing these maneuvers to less than an hour each. The hydrazine subsystem consists of a single propellant tank, four hydrazine thruster assemblies oriented for in-track thrusting, and associated hardware. The pulsed plasma subsystem is used for the remainder of the propulsive requirements: initial stabilization, stationkeeping, and momentum wheel unloading.

Configurations C-4, C-5, and C-6 eliminate the attitude control subsystem reaction wheels and use pulsed plasma propulsion directly for attitude control. This approach was described in Section 4.2.4. In this manner, 32 pounds of reaction wheel weight is deleted from the attitude control subsystem. Thus, there is a reduction in the net weight impact for propulsion.

Configuration C-4 is the same as C-2 except for attitude control implementation. C-2 implements reaction wheels; C-4 does not.

Configuration C-5 is identical to C-4 except that stationkeeping is restricted to 245 days/year. In this manner stationkeeping is not performed during solstice seasons, yet inclination control is maintained within ± 0.1 degree. Additional solar array is not required for battery recharging, and there is no weight impact on the existing power subsystem.

Configuration C-6 is also a combination hydrazine/pulsed plasma propulsion subsystem. Maneuver times for orbit trim and relocation are minimized, and stationkeeping is performed for 245 days annually to avoid power subsystem impact for battery recharge during the solstice seasons.

As indicated in Table 19, configuration C-5 is the preferred configuration. Its maneuver times appear to be of acceptable duration (less than 30 days) and it exhibits the lowest net weight for propulsion. The existing hydrazine propulsion subsystem on DSCS-III requires 358 pounds of propellant to accomplish the baseline 7-year mission. Its dry weight is 77 pounds (Ref. 3), thereby yielding a total weight for propulsion of 435 pounds. Table 21 compares the existing hydrazine subsystem with the pulsed plasma subsystems discussed above. It also compares a combination hydrazine/ion propulsion subsystem. Table 21 identifies the additional weight margin afforded by the various tradeoff configurations when compared with the existing hydrazine subsystem. This margin may be put to use in the form of additional spacecraft component redundancy, payload capability, etc. C-5, the preferred configuration, shows an additional weight margin of 172 pounds for implementing pulsed plasma propulsion on DSCS-III.

The approach taken for calculating combination hydrazine/ion subsystem weights was as follows: the hydrazine subsystem was the same as

Table 21. Weight Margin Comparison (7-Year Mission)

Configuration	Net Weight for Propulsion* (lb)	Additional Weight Margin Available (lb)
Hydrazine Propulsion (existing subsystem)	435	0
A	303	132
A-2	300	135
B-2	315	120
C-2	289	146
C-3	333	102
C-4	273**	162
C-5 (preferred configuration)	263**	172
C-6	307**	128
Hydrazine/ion propulsion	281	154

*Includes power subsystem impact

**Includes 22-pound weight savings due to elimination of reaction wheels.

that used for combination hydrazine/pulsed plasma subsystems; the mercury ion subsystem was similar to the one analyzed in Reference 8 for an advanced communications satellite.

A mercury ion propulsion subsystem similar to the one described in Reference 7 for an advanced communications satellites, was compared with the pulsed plasma configurations studied for DSCS-III. The ion subsystem exhibits long, and probably unacceptable, maneuver times for orbit trim and relocation. It may require additional thruster redundancy to achieve acceptable reliability. The ion subsystem that is being compared has four thruster complements (thruster, gimbal assembly, propellant reservoir, and power processor per complement). In the event of single thruster failure, north-south stationkeeping is performed at one node only.

Table 22. Weight Margin Comparison (10-year mission)

Configuration	Net Weight for Propulsion* (lb)	Additional Weight Margin Available (lb)	Total Impulse Required per Teflon Thruster (lb-sec)
Hydrazine Propulsion (existing subsystem)	577	0	--
A	340	237	66,400
A-2	337	240	65,500
B-2	351	226	65,100
C-2	326	251	65,500
C-3	370	207	62,200
C-4	311**	256	68,100
C-5 (preferred configuration)	301**	276	68,100
C-6	345**	232	64,800
Hydrazine/Ion Propulsion	304	273	--

* Includes power subsystem impact

** Includes 22 pounds weight savings due to elimination of reaction wheels

The ion subsystem will require 340 watts from a 70 ± 20 Vdc bus, 14 watts from a 28 ± 1 Vdc bus, and 7 watts at 28 Vdc for each gimbal actuation. This is similar to the 1-millipound pulsed plasma propulsion subsystem electrical interface. Therefore, it was assumed that the impact on the DSCS-III electrical power subsystem would be the same. It was further assumed that there was no thermal impact (active heater power required) for integrating the mercury propulsion subsystem. Thus, there is no additional solar array or battery required for the ion propulsion subsystem provided that north-south stationkeeping is restricted to about 245 days annually.

The all mercury ion propulsion subsystem described above weighs about 229 pounds, including 40 pounds of propellant. When compared with the existing hydrazine propulsion subsystem on DSCS-III, it provides an additional 206 pounds of weight margin.

Table 22 presents the weight margin comparison for a 10-year mission together with the total impulse capability requirements for each thruster in order to satisfy a 10-year life requirement with any single point failure. From this table, it may be seen that the preferred configuration, C-5, yields 276 pounds of additional weight margin compared with the existing hydrazine propulsion subsystem. In order to provide enough Teflon at each thruster location for 10 years with any single point failure at launch, the total impulse requirement is 68,100 lb-sec for each thruster, 36% more than the presently specified 50,000 lb-sec. The added weight margin for a dual launch where configuration C-5 is implemented is then $2 \times 276 = 552$ pounds.

If the pulsed plasma propulsion system is constrained to its present 50,000 lb-sec/thruster specification, the additional weight margin increases to 314 pounds for a single launch (628 pounds per dual launch). However, its 10-year duration can be achieved only if there is no single point failure in the first 3 years.

4.7 COST ANALYSIS

Cost estimates were generated for comparing propulsion subsystems which are totally pulsed plasma or hydrazine, combination hydrazine/pulsed plasma, and combination hydrazine/mercury ion propulsion. All estimates are presented in 1979 dollars. Costs are accumulated to the level of integrating contractor's cost. Contractor's fee has been

excluded from the estimates shown. It is assumed that similar hardware will be in production at the time the subsystem is needed for application.

Recurring costs for various DSCS-III tradeoff configurations are presented in Tables 23 through 26. Table 23 presents the estimates for the existing hydrazine propulsion subsystem on DSCS-III. Table 24 presents the estimates for a pulsed plasma propulsion subsystem containing four 1-millipound thrusters. Table 25 shows estimates for a combined hydrazine/pulsed plasma propulsion subsystem, and Table 26 contains estimates for a combined hydrazine/ion propulsion subsystem. All four of these subsystems are intended to perform the basic 7-year DSCS-III mission.

Nonrecurring cost estimates for implementing pulsed plasma propulsion on DSCS-III are shown in Table 27.

Cost estimates for the 1-millipound pulsed plasma thruster, fuel supply, energy storage capacitors, and power converter were obtained from Fairchild-Republic. Estimates for the gimbal assembly, drive electronics, structure and thermal control were based on spacecraft experience with similar hardware. Hydrazine propulsion costs were based on the assessment made for NASA's Multimission Modular Spacecraft (MMS) by Battelle and Rockwell International (Ref. 13 and 14). Ion propulsion costs were based on the cost effectivity study performed for NASA-GSFC (Ref. 15). In all cases, programmatic costs were arbitrarily allocated according to the MMS assessment cited above. These allocations vary from contractor to contractor, depending on accounting practices employed.

¹³N.H. Fischer and A.E. Tischer, "Study of Multimission Modular Spacecraft (MMS) Propulsion Requirements," NASA-CR-159919, August 8, 1977.

¹⁴F. Etheridge, W. Cooper, and J. Mansfield, "Landsat/MMS Propulsion Module Design," Rockwell International Space Division, Report SD 76-SA-0095-3, September 24, 1976.

¹⁵S. Zafran and J.J. Biess, "Ion Propulsion Cost Effectivity," NASA-CR-159902, December 1978.

Table 23. Recurring Cost Breakdown, Hydrazine Propulsion Subsystem for DSCS-III

Item	Unit Cost (\$ Thousands)	Quantity	Total (\$ Thousands)
HARDWARE			
Thruster Assembly	18	16	280
Propellant Tanks	44	4	176
Valves	--	(a)	47
Valve Driver Electronics	3	32	106
Other Fluid Components	--	As Req'd	34
Structure	--	As Req'd	37
Thermal Control	--	As Req'd	30
Integration & Assembly	--	As Req'd	295
PROGRAMMATIC			
Subsystem Engineering			165
Reliability & Quality Assurance			115
Project Management			115
TOTAL			1400

(a) 6 latching valves, 8 fill and drain valves

Table 24. Recurring Cost Breakdown, Pulsed Plasma Propulsion Subsystem for DSCS-III

Item	Unit Cost (\$ Thousands)	Quantity	Total (\$ Thousands)
HARDWARE			
Thruster & Fuel Supply	36	4	144
Capacitors	60	4	240
Power Converter	149	4	596
Gimbal Assembly	25	4	100
Gimbal Drive Electronics	16	8	128
Structure	--	As Req'd	5
Thermal Control	--	As Req'd	15
Integration & Assembly	--	As Req'd	30
PROGRAMMATIC			
Subsystem Engineering			207
Reliability & Quality Assurance			144
Project Management			144
TOTAL			1753

Table 25. Recurring Cost Breakdown, Pulsed Plasma/Hydrazine Propulsion Subsystem for DSCS-III

Item	Unit Cost (\$ Thousands)	Quantity	Total (\$ Thousands)
PULSED PLASMA PROPULSION HARDWARE			
Thruster & Fuel Supply	36	4	144
Capacitors	60	4	240
Power Converter	149	4	596
Gimbal Assembly	25	4	100
Gimbal Drive Electronics	16	8	128
Structure	--	As Req'd	5
Thermal Control	--	As Req'd	15
Integration & Assembly	--	As Req'd	30
HYDRAZINE PROPULSION HARDWARE			
Thruster Assembly	18	4	70
Propellant Tank	31	1	31
Valves	--	(a)	15
Valve Driver Electronics	3	8	26
Other Fluid Components	--	As Req'd	9
Structure	--	As Req'd	21
Thermal Control	--	As Req'd	12
Integration & Assembly	--	As Req'd	77
PROGRAMMATIC			
Subsystem Engineering			250
Reliability & Quality Assurance			173
Project Management			173
TOTAL			2115

(a) 2 latching valves, 2 fill and drain valves

Table 26. Recurring Cost Breakdown, Ion/Hydrazine Propulsion Subsystem for DSCS-III

Item	Unit Cost (\$ Thousands)	Quantity	Total (\$ Thousands)
ION PROPULSION HARDWARE			
Thruster & Gimbal Assembly	122	4	487
Propellant Storage & Distribution	---	1 set	89
Power Electronics Unit	132	4	530
Digital Controller & Interface Unit	83	4	330
Structure & Thermal Control	---	As Req'd	73
Integration & Assembly	---	As Req'd	222
Boost Regulator	26	4	104
DC-DC Converter	20	2	39
HYDRAZINE PROPULSION HARDWARE			
Thruster Assembly	18	4	70
Propellant Tank	31	1	31
Valves	--	(a)	15
Valve Driver Electronics	3	8	26
Other Fluid Components	--	As Req'd	9
Structure	--	As Req'd	21
Thermal Control	--	As Req'd	12
Integration & Assembly	--	As Req'd	77
PROGRAMMATIC			
Subsystem Engineering			351
Reliability & Quality Assurance			244
Project Management			244
TOTAL			2974

(a) 2 latching valves, 2 fill and drain valves

AD-A090 514

TRW DEFENSE AND SPACE SYSTEMS GROUP REDONDO BEACH CA F/G 21/3
MISSION INTEGRATION STUDY FOR SOLID TEFLON PULSED PLASMA MILLIP--ETC(U)
SEP 80 M N HUBERMAN, S ZAFRAN, M H GRAN F04611-78-C-0064

AFRPL-TR-80-37

NL

UNCLASSIFIED

2 11 2

ALL

ADP/AF/DTIC

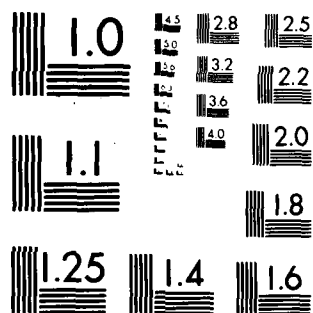
END

DATE

FILMED

11 80

DTIC



MICROCOPY RESOLUTION TEST CHART
NATIONAL BUREAU OF STANDARDS 1963 A

Table 27. Nonrecurring Cost Breakdown, Pulsed Plasma Propulsion Subsystem for DSCS-III

ITEM	\$ THOUSANDS
PULSED PLASMA PROPULSION SUBSYSTEM	
Thruster Development	2500
Subcontract Control	200
Subsystem Qualification	840
Design of Gimbal Drives & Drive Electronics	<u>175</u>
Subtotal	3715
SYSTEM INTEGRATION RETROFIT	
Control Subsystem Analysis	950
Structural Design	100
Thermal Design	80
Electrical Design Integration	100
Ground Segment	120
System Test & Evaluation	<u>275</u>
Subtotal	1625
RELIABILITY & QUALITY ASSURANCE	120
PROJECT MANAGEMENT	740
TOTAL	6200

The nonrecurring thruster development estimates were obtained from Fairchild-Republic. Qualification testing assumed two thrusters subjected to vibration, mission duty cycle, and thermal-vacuum tests. Several major assumptions were made in preparing the nonrecurring estimates:

- It was assumed that DSCS-III has a programmable processor, and that its attitude control subsystem implements the control laws and associated thruster commands through this processor. If the programmable processor is not available, then additional development is needed for redesign of control electronics.
- It was assumed that interactive effects data resulting from thruster plume and electromagnetic compatibility testing would only result in minor spacecraft design impact.

From the cost comparison (Table 28), it is readily seen that the existing hydrazine subsystems exhibit the lowest recurring costs, followed by pulsed plasma propulsion, combination hydrazine/pulsed plasma, and finally, combination hydrazine/mercury ion propulsion.

Table 28. Recurring Cost Comparison (DSCS-II)

Subsystem	Cost (\$ thousand)
Hydrazine	1400
Hydrazine/Pulsed Plasma	2115
Pulsed Plasma	1753
Hydrazine/Ion	2974

V. DSP MISSION

The DSP Satellite is shown schematically in Figure 21. The satellite is positioned in an earth synchronous equatorial orbit and spins at 6 rpm around its earth pointing (+Z) axis. In order to precess the spin axis around in orbit without excessive propellant demands, a retrograde momentum wheel is added to give the satellite zero momentum. Electric power is provided at all times of the day by a distributed solar cell system consisting of a conical segment, cylindrical segment, and four two-way solar paddles. Batteries provide power during eclipses.

Table 29 lists the major design characteristics assumed for the pulsed plasma study. These are based on a future version of DSP. Because of the special characteristics of DSP, three areas of concern have been identified to be of special interest for pulsed plasma propulsion: (1) EMC/EMI, (2) particulate contamination, and (3) optical radiation.

Currently, a hydrazine propulsion system provides orbital correction and attitude control functions. In order to get the small impulses required for precise attitude control and permit the millions of pulses required, the propulsion system has a plenum which decomposes the hydrazine and stores the pressurized, warm gas until ejected through the proper thruster valve.

The candidate pulsed plasma system can replace many of the functions of this hydrazine system. However, two functions would be difficult—rapid change of longitudinal station and earth acquisition. These two functions require a much higher average thrust level than pulsed plasma permits. Because of these requirements, a hybrid propulsion system is required with retention of a simplified 3.5 pound hydrazine thruster capability to achieve repositioning and high level attitude control.

5.1 PULSED PLASMA PROPULSION SYSTEM

The hydrazine subsystem is comprised of a central tank and four relatively high level thrusters to provide lateral ΔV and torque capability.

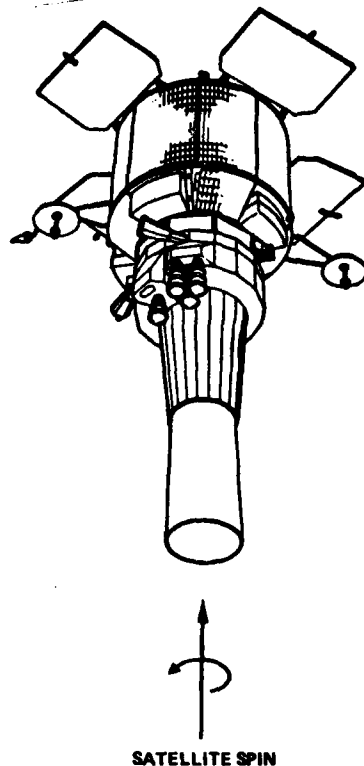


Figure 21
Schematic Diagram of DSP

Table 29. DSP Design Data Assumed for Study

DESIGN LIFE	7 Years
SPACECRAFT WEIGHT (DRY)	3200 lbs (352 lbs hydrazine capacity)
STABILIZATION	Tight Pointing Accuracy for Spin Axis 2° Orbit Positioning Accuracy BOL 1° Orbit Positioning Accuracy EOL
ATTITUDE CONTROL SUBSYSTEM	Zero Total Angular Momentum Satellite; Main Body Spin Rate 6 ± 0.225 rpm Around Yaw Axis
ELECTRICAL POWER SUBSYSTEM	750 watts BOL 23 watts Margin 31.8 ± 0.2 volts Noneclipse 24.5 to 32.0 volts Eclipse Season
EXISTING HYDRAZINE PROPULSION SUBSYSTEM	Thrust Levels - 3.5 lbf High Level Attitude Control and ΔV 0.039 lbf Low Level Attitude Control

Figure 22 illustrates the basic layout of the hybrid propulsion system. The pulsed plasma sybssystem consists of three thruster systems placed in line on the outer shell of the spacecraft. Figures 23 and 24 show the detailed installation concept and Figure 25 shows the installation concept for the hydrazine subsystem.

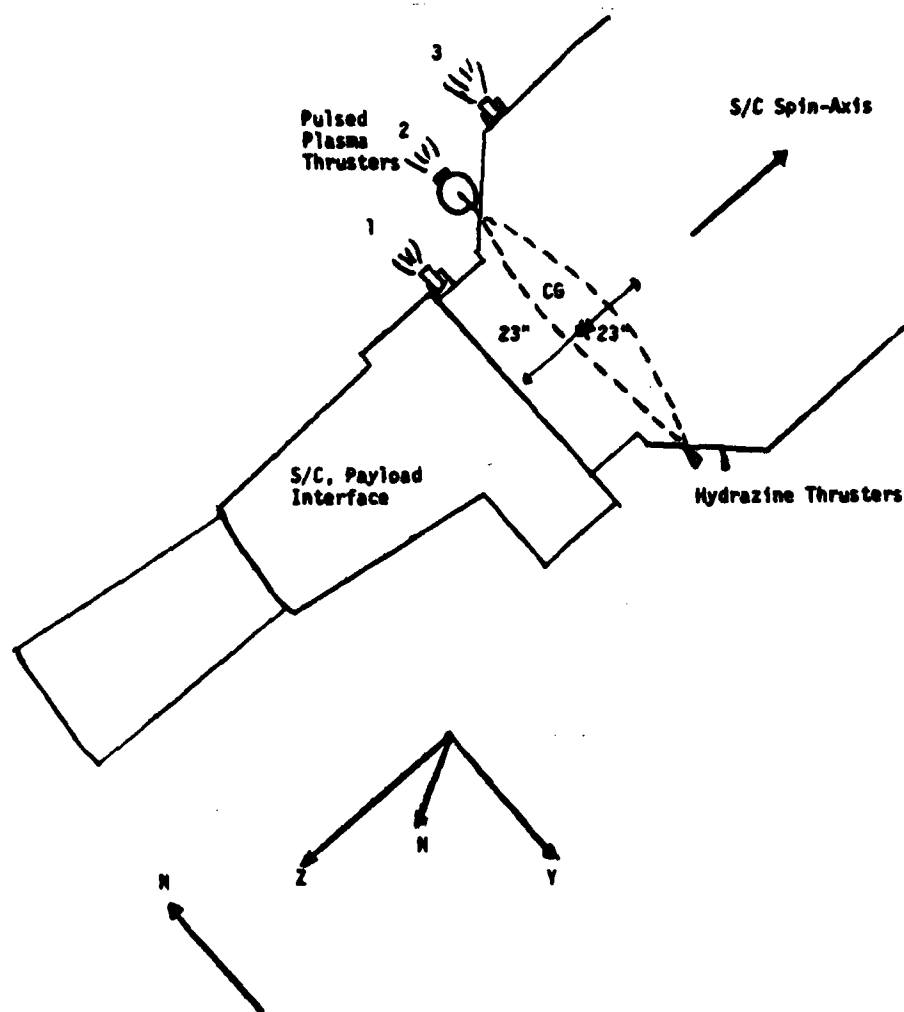
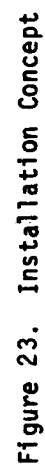


Figure 22. Thruster Configuration



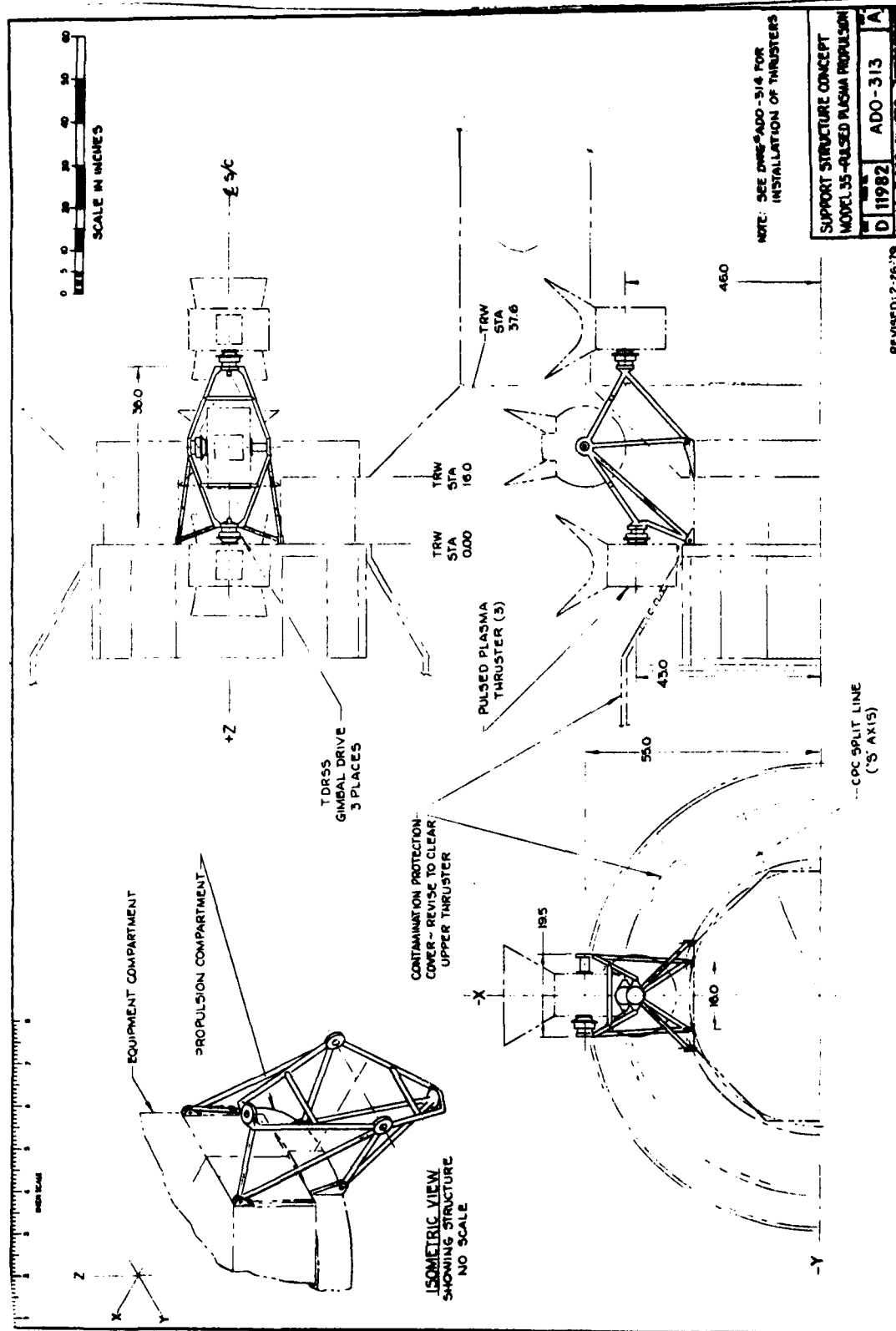


Figure 24. Support Structure Concept

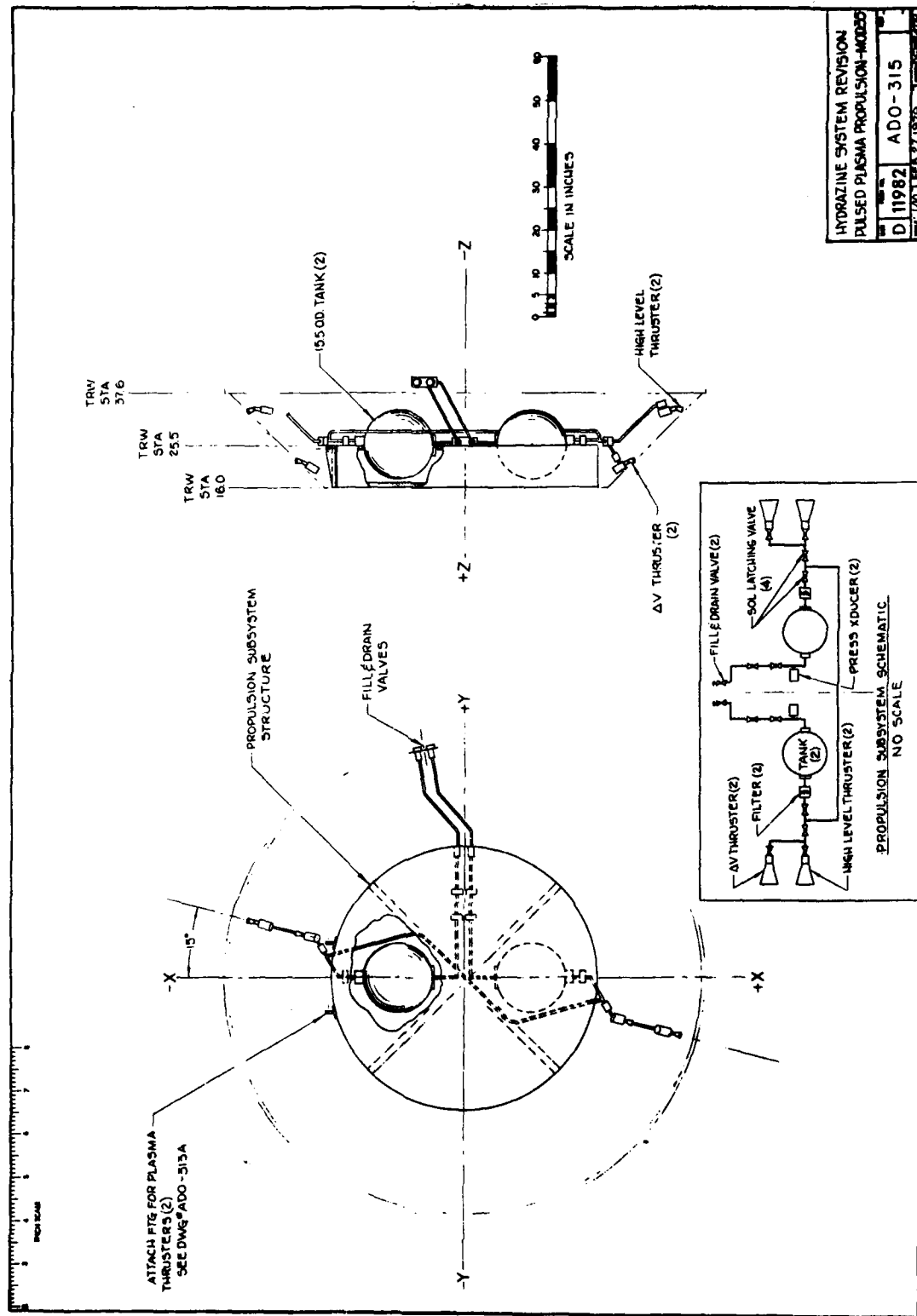


Figure 25. Hydrazine System Revision - Pulsed Plasma Propulsion

The outermost (primary) pulsed plasma thrusters (1 and 3 in Figure 22) provide the required propulsive capability. The middle thruster (2 in Figure 22) is included for redundancy. The primary thrusters are displaced 27.8 inches to either side of the plane through the spacecraft center of mass. They can be fired in tandem to provide a horizontal ΔV in any desired direction. Roll/pitch torque control can be provided by either commanding a phased delay between the two thrusters or firing only one of the two primary thrusters. The primary thrusters are gimballed about axes parallel to the spin axis to provide yaw (spin) control. The gimbal axis for the redundant thruster is parallel to the Y axis in order to allow a choice of roll/pitch polarity, depending on which thruster is being replaced. When all three thrusters are operational the spare thruster can be used to enhance system flexibility.

A simple thermal model was made of each of the three pulsed plasma thrusters and the power converter compartment based on the worst case orbit environment during north-south stationkeeping. During this period two thrusters are operated quasi-continuously. North-south stationkeeping is performed twice daily.

Calculations of the transient heat-up and cool-down behavior for the active thruster external to the spacecraft body indicate that the thruster will require approximately 120 square inches of second-surface mirror radiator area. This area is somewhat oversized in order to account for spacecraft blockage of the radiator and radiation heat inputs from the spacecraft structure. During the periods when north-south stationkeeping is not being performed, 8 watts will be required to maintain the thruster's minimum survival temperature.

The analysis for the redundant thruster was based on a steady-state thermal condition. The radiator area is set at 120 square inches since this thruster is exposed to the same thermal environment as the previous thruster. Continuous heater power on the order of 8 watts will be required.

The analysis for the active thruster recessed into the solar array was based on a steady-state thermal analysis which indicates that the thruster will require approximately 57 square inches of black paint for thermal coupling to the spacecraft interior. Heater power on the order of 7.2 watts will be required during equinox operation in eclipse. During non-north-south stationkeeping in winter and summer solstice, and the remainder of equinox operation, on the order of 4.2 watts will be required to maintain the thruster's minimum survival temperature.

The analysis for the power converter compartment was based on a steady-state thermal analysis which indicates that the compartment will require about 138 square inches of second-surface mirror radiator area. The compartment has a similar thermal environment as the recessed thruster. Hence, during equinox operation in eclipse, the converters will require approximately 27.5 watts for survival. For all other environments when the thrusters are not operating in the north-south stationkeeping mode, the compartment will require 6.6 watts.

Equinox eclipse does not necessarily represent the design point for thermal control impact on electrical power subsystem design. During eclipse, noncritical equipment may be turned off for purposes of remaining within the total power budget allocation.

5.2 PROPULSION CONSIDERATIONS

The auxiliary propulsion considerations which affected the configuration, propulsion functions performed, and the performance estimates are discussed in this section.

5.2.1 Propulsion Functions

The functions performed include initial stabilization, orbit trim and stationing, relocation, E-W stationkeeping, N-S stationkeeping, and attitude control.

5.2.1.1 Initial Stabilization

After tip-off, the satellite goes through a conventional acquisition in that it uses wide field-of-view sun sensors to partially stabilize the satellite. It rotates about the sun vector to find the earth and is then

three-axis stabilized. The satellite is spun up and orbit trim is performed. Though undesirable, the low torque of the pulsed plasma thrusters is acceptable for sun acquisition. Any two thrusters (with their gimbaling capability) provide three axes of torque control. The earth acquisition requires a higher level thruster since the earth search mode is made at a reasonably high search rate so that the earth can positively be acquired during a limited search window in orbit. The high level thrusters are required to acquire the earth within the limited field of view of the earth sensor (~18 deg arc). Other earth acquisition schemes could be employed that would permit the low level pulsed plasma thrusters if hydrazine were not required for change of station. Since hydrazine would be available, it is a small cost and weight penalty to use and retain a proven acquisition technique.

5.2.1.2 Orbit Trim and Stationing

After attitude stabilization has been achieved, a longitudinal correction capability must exist to move the satellite from the injection station to its desired station and correct out any residual drifts. The total velocity correction is estimated to be 28 ft/sec. This correction can be performed either by the pulsed plasma or hydrazine system. Each thruster produces a pulse each rotation when the thruster is parallel to the desired thrust direction. It is likely that a pulsed plasma system would require 14 days to complete, firing all three thrusters once per rotation, and would require 300 watts of average power. The pulsed plasma thrusters would be used to maintain attitude control during the maneuver.

5.2.1.3 Relocation

There is a requirement to change the satellite station once in orbit. If required, the change of station could be as much as 180 degrees and must be completed within 14 days. This would require 120 ft/sec ΔV capability (240 ft/sec for distributed low level thrusting) and the pulsed plasma system could only provide 28 ft/sec within this time frame. This is the predominant requirement for a hydrazine capability.

5.2.1.4 Combined E/W, N/S Stationkeeping and Attitude Control

These are the primary propulsive functions, for which the pulsed plasma thrusters are well suited. In the interests of minimizing propellant and average power requirements, a strategy has been developed which simultaneously performs each of these thrust functions. The algorithm employed is discussed below, followed by requirements for each function and then a summary of the joint propulsive needs.

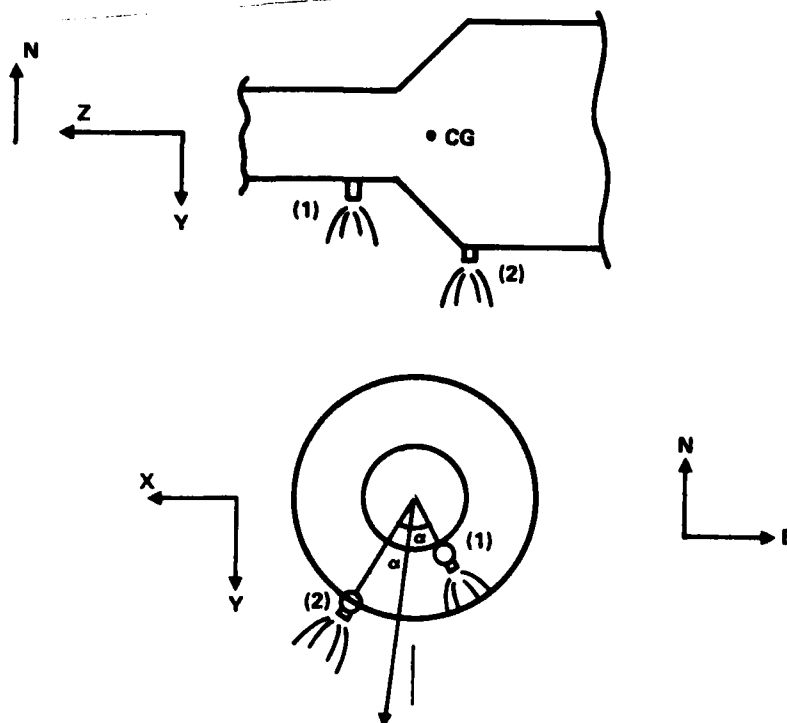
5.2.1.5 Firing Algorithm

N/S ΔV , E/W ΔV , and any desired combination of three axes of torque control can be provided with a timed pair of thruster pulses. Although use of thruster 3 increases the flexibility, the following discussion assumes use of thrusters 1 and 2. Similar arguments can be made with use of 1 and 3 or 2 and 3.

The major propellant consumption is due to N-S stationkeeping. To achieve a north increment, thrusters 1 and/or 2 are fired while their thrust vectors are in the southern half of the satellite rotation (Figure 26). Peak efficiency is achieved at the south pointing direction and the efficiency degrades as a cosine function of the angle away from the location. By symmetry, the opposite angles are used for south stationkeeping.

To combine one east component with the north stationkeeping, the pulse pair is delayed the appropriate amount to allow the satellite to produce an east component of velocity. Conversely, a west component is generated by early firing of the pulse pair.

A torque about the spin axis (Z or yaw) is created by gimbaling the thrusters. A torque about the other two axes is produced by either firing just one thruster when its thrust vector is normal to the desired inertial torque axis; or the two thrusters are staggered in time, producing a torque about the axis bisecting the two firings. These are idealized situations, assuming each thruster pulse is identical in terms of Δ angular momentum. Actual misalignments create second order disturbances which must be controlled out at some future time.



NET STATIONKEEPING VECTOR DIRECTION AND TORQUE AXIS

Figure 26. Example of Combined North and East Stationkeeping Plus Yaw Attitude Control Pulse

The control algorithm to create these composite maneuvers consists of simple and logical decisions. When a pulse is commanded for either stationkeeping or attitude control, the timing is selected to contribute towards the other factor. For example, if a Y (pitch) torque is required to correct for solar disturbance torques, a rapid scan is made to see whether north or south and east or west stationkeeping is called for. The satellite is allowed to rotate to the point where both a pitch torque and appropriate stationkeeping are provided. If south stationkeeping is called for, thruster 1 is fired when it points north.

The implementation of this logic in the current analog control electronics would be difficult, but a current product improvement in changing over to a very high speed microprocessor is being made and such logical firings can easily be made.

5.2.2 DSP Attitude Control and Stationkeeping

This section describes detailed attitude control and stationkeeping considerations. The major conclusions are:

- The baseline pulsed plasma thrusters can provide the required attitude control capability
- Stationkeeping can be performed with a 45-watt average increase in electrical power (of which 15 watts is required just to upgrade DSP to a 7-year mission)
- Current stationkeeping requirements of an initial +2 degree offset drifting to -1 degree at end of life (EOL) are improved to an initial +1 degree offset drifting to -0.13 degree at EOL with no thruster failed for the first 6 months, and -0.60 degree at EOL with a thruster failure at launch.

These conclusions are based on the previously discussed hybrid hydrazine/pulsed plasma propulsion subsystem with hydrazine providing high thrust requirements (initial pointing acquisition, initial positioning and change of station), and pulsed plasma providing the main line normal mode attitude control and stationkeeping functions. The mass properties assume a gross satellite mass, with the propulsion subsystem included, of 100 slugs (3220 lbm). The electrical power subsystem (before any growth due to pulsed plasma or 7-year requirements) has the seasonal and yearly capability and demand shown in Figure 27. Thruster moment arms are assumed to be 20 inches.

5.2.2.1 Attitude Control of DSP with Pulsed Plasma Thrusters

The purpose of this particular study was to verify that the pulsed plasma thrusters can adequately replace the current low level hydrazine thrusters on DSP, and to calculate the demand placed on the thrusters (in terms of total pulses, impulse, and average pulse repetition rate). A summary of the results are that:

- The pointing accuracy is unchanged since the pulsed plasma thrusters are a virtual replacement of the existing system. They provide 8.33 mft-lb-sec torque impulses while the low level hydrazine thrusters provide 7.815 mft-lb-sec torque impulses

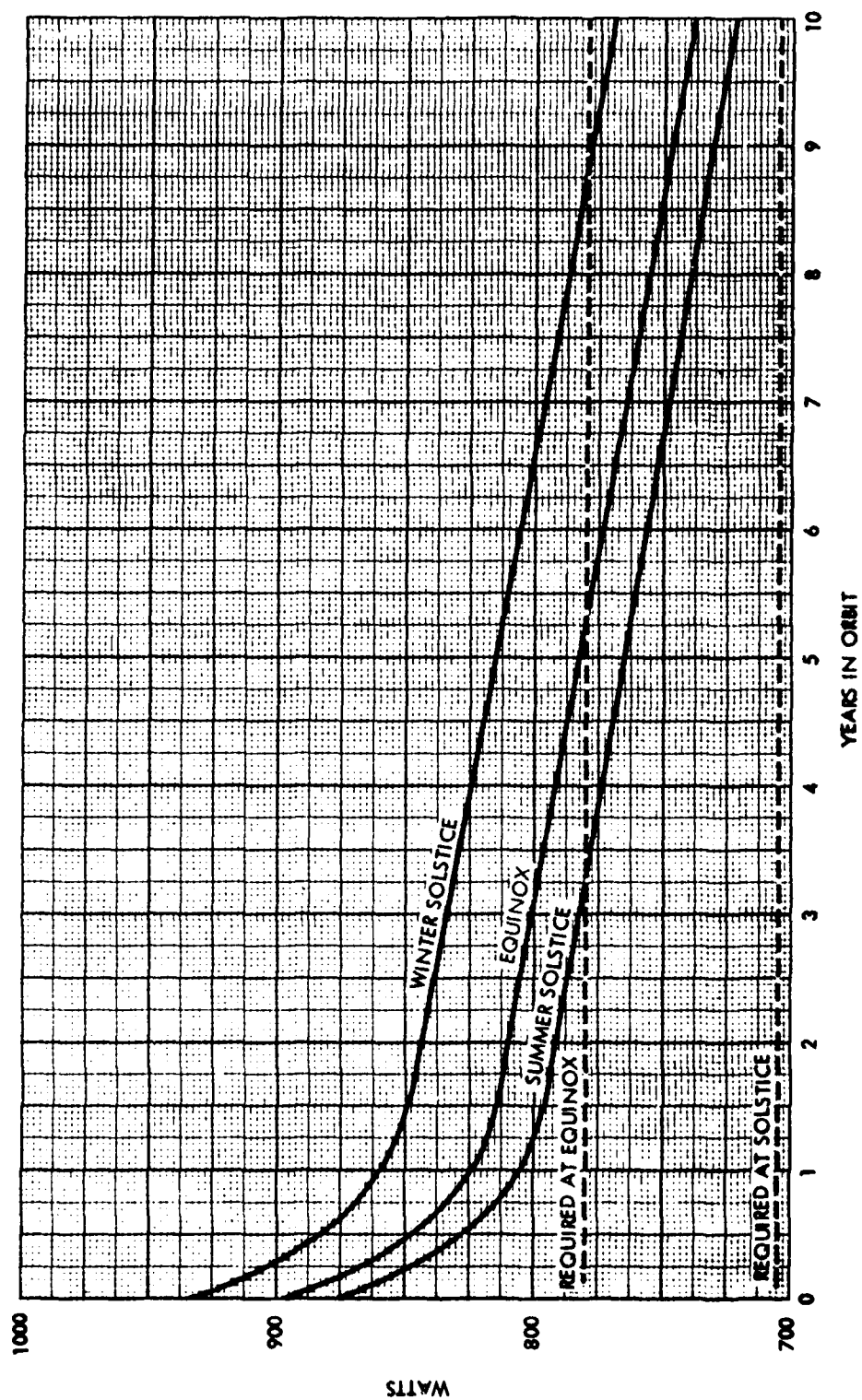


Figure 27. Average Electrical Power Availability and Requirement for DSP as a Function of Life and Season

- Total 7-year thruster demand for attitude control is 29,540 ft-lb-sec, equally divided between single thruster pulses from each thruster and pulse pairs from both.
- When combined with N-S stationkeeping this requirement consumes 22,380 lb-sec of additional impulse and adds 133.3 ft/sec of N-S stationkeeping control as well as providing in excess of the 24 ft/sec required for E-W stationkeeping.

Current DSP Attitude Control Subsystem (ACS) Design

The current ACS design is a digital implementation of a control loop whose original design was analog. It consists of an earth sensor with smoothing and a derived rate pulse width modulator. This pulse width modulator provides identical minimum pulse widths for normal mode control with the stretched pulse widths being used only during acquisitions. A block diagram of a single axis of the design is shown in Figure 28. The control loop parameters have been studied to determine optimal values. A summary of these studies is presented in Table 30 which plots various "goodness" values as variation in control torque (T_c) and a derived rate modulator parameter γ . These studies have indicated a composite favoring of $T_c = 0.3$ ft-lb. For a minimum pulse width of 25 msec, this translates to a 7.5 mft-lb-sec thruster impulse. These studies helped configure the hydrazine system which has a 35 mlb thrust level and approximately 4.5 ft moment arm (thrusters are fired in pairs). These parameters give control loop pointing accuracy as shown in the histograms of Figures 29 through 31 which are plots for various disturbances.

The levels of disturbances ultimately determine the total normal mode thruster impulse requirements. Disturbances primarily occur from the solar torques, precession of the satellite about the orbit plane and thruster cross coupling due to slight unpredictability in thrust level and vector direction of pulses. The solar torques arise from the impingement of photons from the sun on a spacecraft that is not perfectly symmetric with respect to its center of mass. Since the satellite is spinning, torques about the spin axis (\bar{Z}) tend to balance out over a 10-second rotation removing the need for the ACS to control this axis except for the very gradual change of satellite spin speed. The solar torques tend to have greatest effect about the axis normal to both \bar{Z} and the sun vector, i.e.,

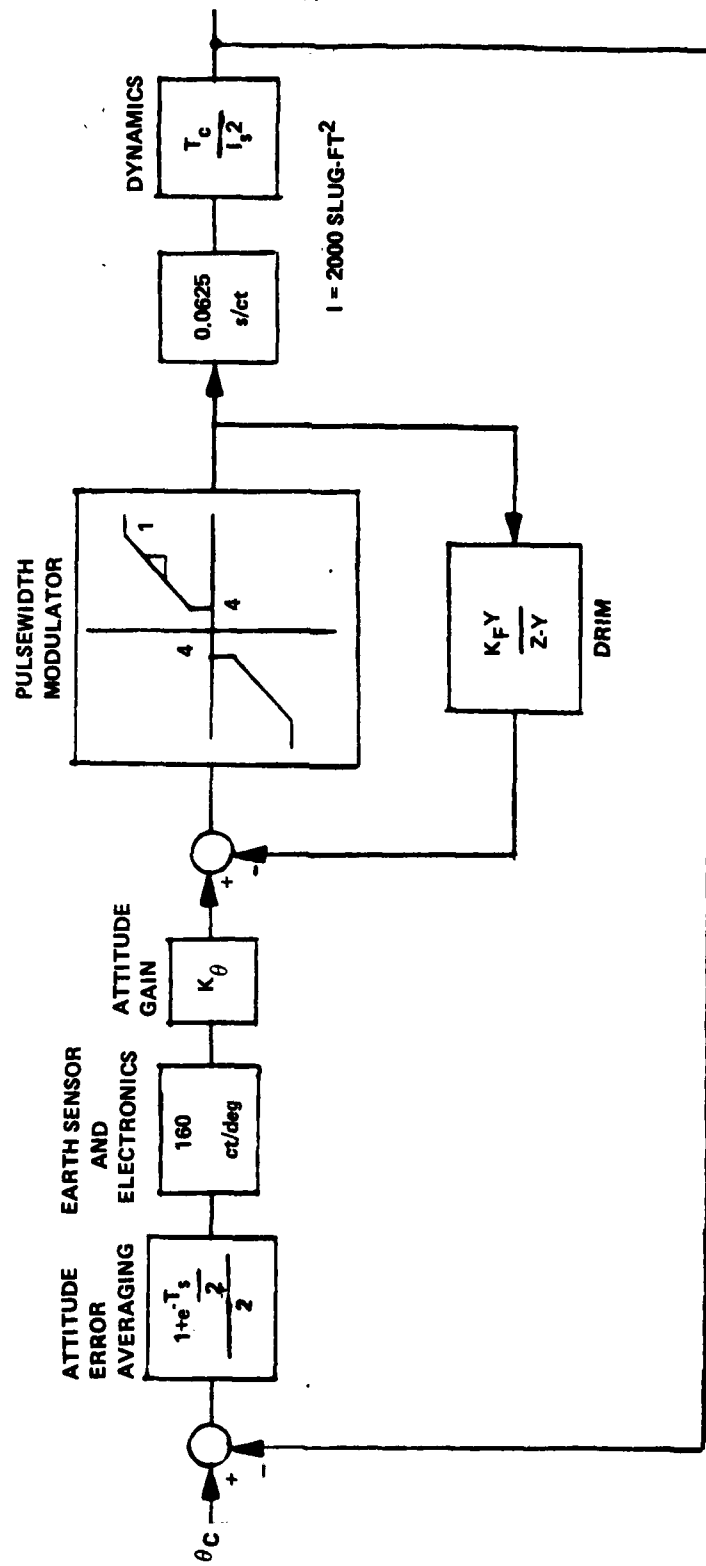


Figure 28. Single Axis Model of DSP Normal Mode Attitude Control Subsystem

Table 30. Performance Criteria vs Control Torque (T_c) and DRIM Relay (γ)

E/S Noise = 0

(a) Max Attitude Error ($^\circ$)

$\gamma \backslash T_c$.1	.3	.5
.5	.033	.036	.039
.7	.032	.034	.036
.9	.030	.035	.035

(b) % of Time $\theta_e > .025$

$\gamma \backslash T_c$.1	.3	.5
.5	25.7	11.1	12.0
.7	25.9	10.6	10.9
.9	29.7	10.7	9.9

(c) Control Impulse (ft-lb-sec)

$\gamma \backslash T_c$.1	.3	.5
.5	1.04	1.46	2.74
.7	1.05	1.42	2.49
.9	1.05	1.15	2.05

(d) No of Valve Firings

$\gamma \backslash T_c$.1	.3	.5
.5	416	193	222
.7	420	188	198
.9	418	151	163

E/S Noise = .04 deg (1 σ)

Max Attitude Error ($^\circ$)

$\gamma \backslash T_c$.1	.3	.5
.5	.056	.058	.054
.7	.053	.043	.048
.9	.046	.046	.046

% of Time $\theta_e > .025$

$\gamma \backslash T_c$.1	.3	.5
.5	26.6	34.3	30.4
.7	16.3	15.6	21.0
.9	28.1	13.6	16.4

Control Impulse (ft-lb-sec)

$\gamma \backslash T_c$.1	.3	.5
.5	1.84	6.97	10.94
.7	1.24	3.33	6.64
.9	1.27	2.53	4.89

No of Valve Firings

$\gamma \backslash T_c$.1	.3	.5
.5	650	802	751
.7	449	405	477
.9	456	327	247

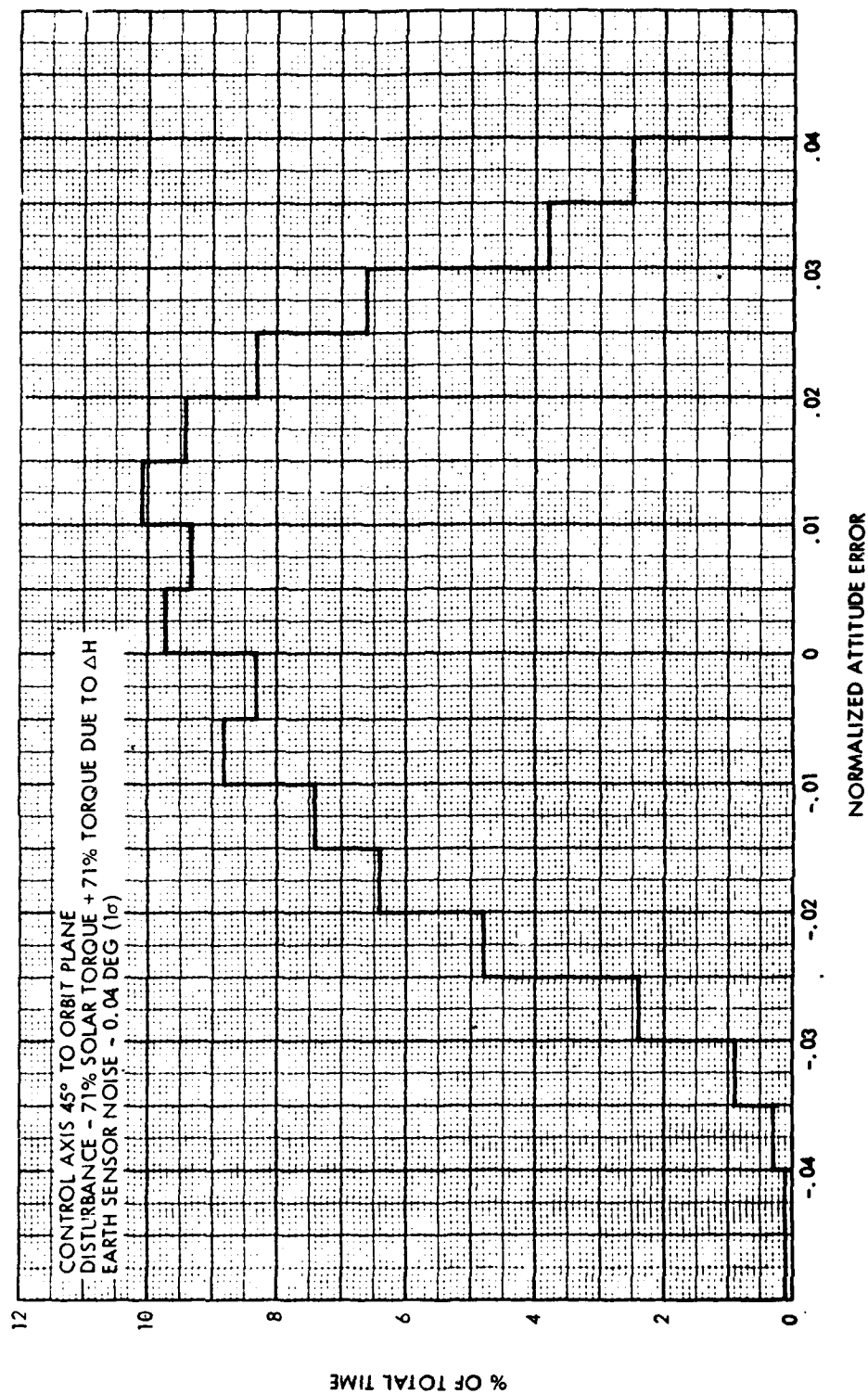


Figure 29. Histogram of Attitude Error, Control Axis in Orbit Plane

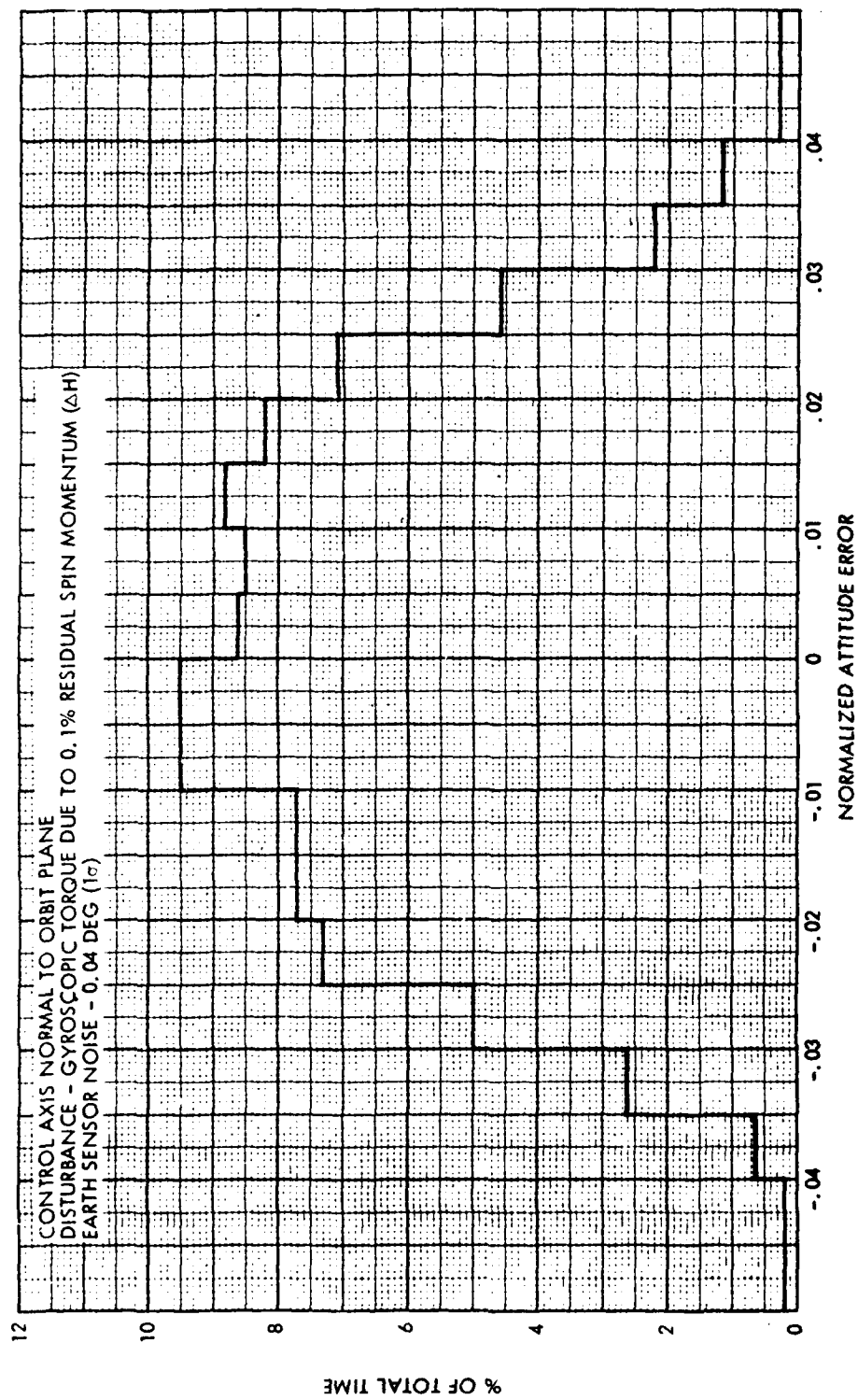


Figure 30. Histogram of Attitude Error, Control Axis Normal to Orbit Plane

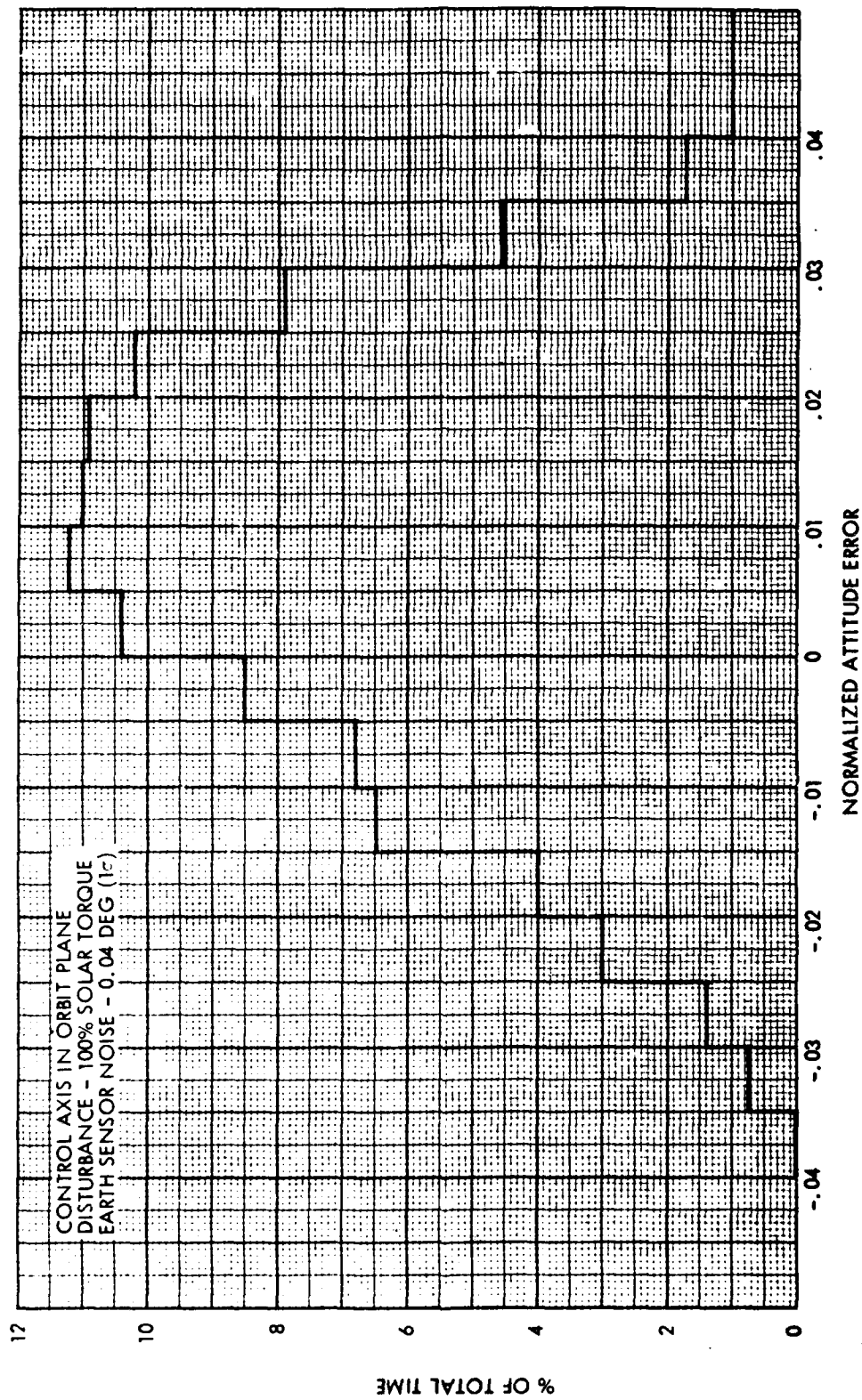


Figure 31. Histogram of Attitude Error, Control Axis 45 Degrees to Orbit Plan

mostly about the \bar{Y} axis. An elaborate computer model has been built modeling the solar torques. An example of the results is shown in Figure 32 which plots torque as a function of position in orbit for a typical equinox condition.

The second principal disturbance is due to precession of residual angular momentum about the orbit plane. The satellite is theoretically a zero momentum vehicle. It spins at $2\pi/10$ rad/sec causing a 1084 ft-lb-sec momentum. This is removed by counter rotating a momentum wheel on the satellite at sufficient speed to exactly balance this momentum. However, over the course of time, the spin speed of the satellite will gradually change due to thruster misalignments and solar torque residuals. The current approach is to infrequently adjust the spin speed, leaving a small residual momentum on the satellite most of the time. If the satellite has a residual momentum, it must be precessed about the orbit plane so that the \bar{Z} axis remains earth centered. This torque is primarily about the satellite X axis and is comparable in magnitude to solar torques (on the average). Examples of thruster activity for various combinations of solar torque and residual momentum is shown in Table 31.

These studies determined average thruster requirements. The requirements are for 4220 ft-lb-sec per year and do not change dramatically based on time of day or season. Since the impulse per pulse is 7.5 mft-lb-sec, this translates into the requirement of 564,000 pulse pairs/year.

Pulsed Plasma Attitude Control Subsystem

The overall ACS requirements that the pulsed plasma subsystem must satisfy are: 29,540 ft-lb-sec of total torque impulse with average impulse bits of 7.5 mft-lb-sec. These pulses are at best guess, reasonably uniformly distributed over the time of day and between \bar{X} and \bar{Y} torque axes. The thrusters have nominal 20-inch moment arms which can be adjusted $\pm 15\%$ to match torques. The thrusters deliver 5 mlb-sec impulse bits. Firing either thruster at the appropriate phase in its rotation about the \bar{Z} axis will cause a torque pulse of approximately the correct magnitude, axis, and polarity. An alternate means of achieving the same torque is to fire one thruster when its vector direction is ± 30 degrees from the torque axis. This is inefficient from a torque standpoint since pulses are required to

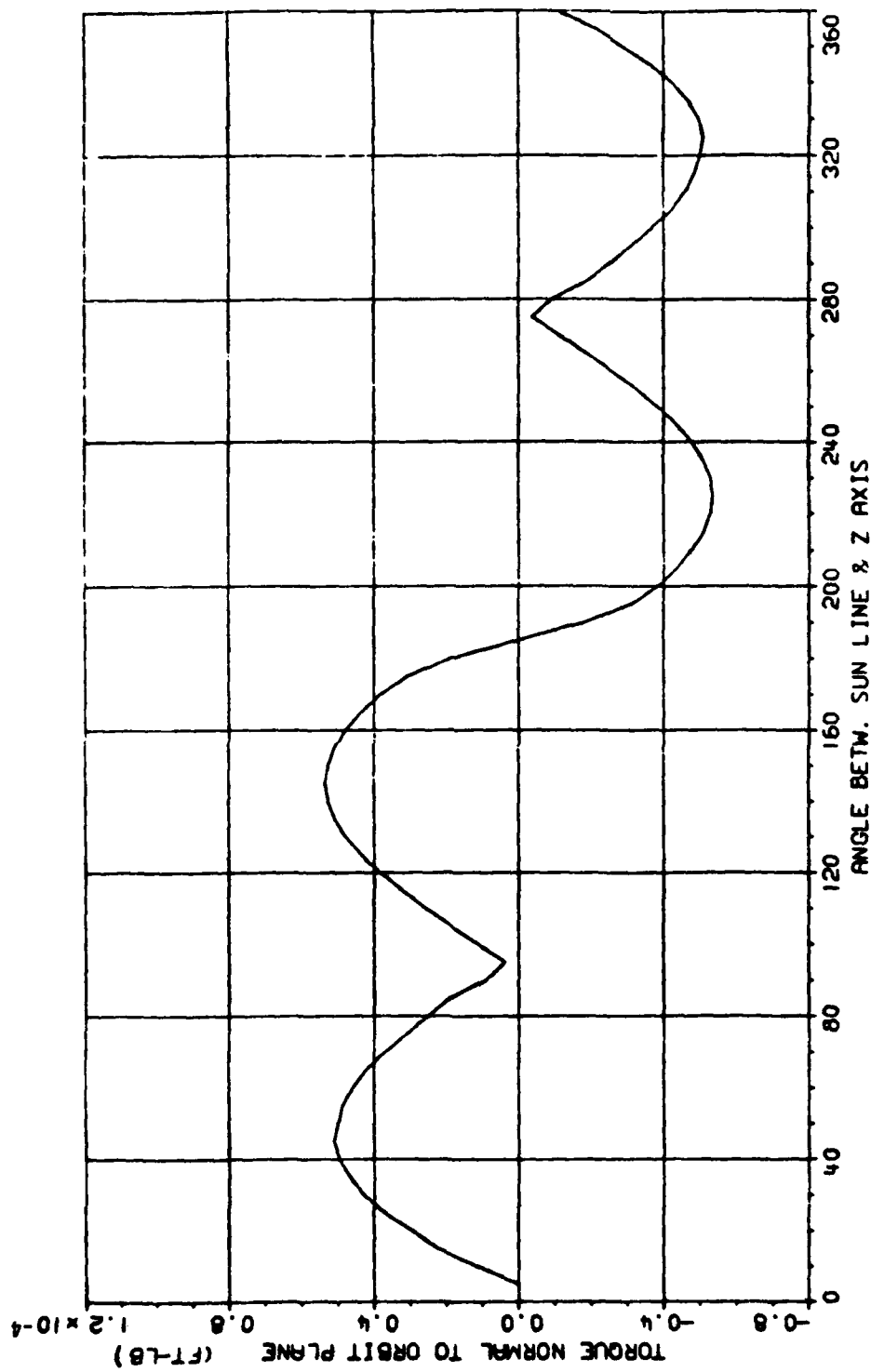


Figure 32. Solar Disturbance Torque at Equinox

Table 31. Thruster Activity (Equinox Solar Torques: 0.1% Residual Momentum; E/S Noise = 4 deg)

Case	Max. Attitude Error (deg)	Max. Attitude Rate (deg/sec)	Control Impulse* Used (ft-lb-sec)	No. of Firings**	Histogram Figure
(a) Control axis in orbit plane (solar torque only)	0.052	6.36×10^{-4}	5.68	686	29
(b) Control axis normal to orbit plane (residual momentum only)	0.047	6.28×10^{-4}	5.68	685	30
(c) Control axis 45 deg from orbit plane (both torques)	0.051	5.64×10^{-4}	5.78	696	31

* The specified value for control is 26,000 ft-lb-sec, or a daily average of 23.74 ft-lb-sec.

** The specified maximum number of firings is 2.5×10^6 per valve, or a daily average of 2283.

develop an equivalent amount of torque. However, as it will be seen, there are times when this is desired.

Since the attitude control requirements consume a considerable portion of the total thruster impulse, it is desired to utilize this impulse to simultaneously accomplish N-S, E-W stationkeeping in the most efficient manner possible. For the 16 hours a day when N-S stationkeeping is performed (8 hours around each nodal crossing), a single thruster is fired along the N-S direction for \bar{X} axis torque and a pair of thrusters centered along the same direction for \bar{Y} axis torque. For \bar{X} axis torque, 100% of impulse contributes toward N-S stationkeeping and for \bar{Y} axis torque, 87% of impulse contributes toward N-S stationkeeping. Therefore, even though inefficient for torque control, it is nearly as efficient for N-S stationkeeping as normal thrusting.

For the two 4-hour segments each day when N-S stationkeeping is not performed, a single thruster is fired at all times in either N-S direction for \bar{X} axis control or E-W direction for \bar{Y} axis control. This limited E-W time is adequate for satisfying E-W stationkeeping requirements and the N-S pulses, though inefficient (since they are fired far away from orbital nodes), do help somewhat.

Table 32 summarizes the net impact of attitude control functions on thruster impulses required, pulses, and ΔV available for stationkeeping.

5.2.2.2 Stationkeeping

East-West Stationkeeping

The basic E-W stationkeeping accuracy is required to be ≤ 1.0 degree. The resulting impulse requirement depends on the spacecraft longitude (Figure 33). Average DSP requirements indicate that 24 ft/sec over the 7-year period is satisfactory. It has been shown that ACS functions provide 26.5 ft/sec capability, so that no added thrusting need be provided.

North-South Stationkeeping

N-S stationkeeping also has a basic accuracy requirement of ≤ 1.0 degree. However, for an all hydrazine system, in the interests of reducing propellant weight, the basic DSP N-S stationkeeping strategy is to initially incline

Table 32. Summary of ACS Functions on Thruster Impulse and ΔV Augmentation

	No. of Torque Pulses	Avg. Time Between Pulses (sec)	Impulse Used (lb-sec)	ΔV for N-S Stationkeeping (ft/sec)	ΔV for E-W Stationkeeping (ft/sec)
N-S Stationkeeping Period	\bar{X} Torque	124.6	5,595	46.4	-
	\bar{Y} Torque	124.6	11,190	80.4	-
	Total	62.3	16,785	126.2	-
E-W Stationkeeping Period	\bar{X} Torque	124.6	2,792	7.1	-
	\bar{Y} Torque	124.6	2,792	-	26.5
	Total	62.3	5,595	7.1	26.5
Totals	3,545,000	62.3	22,380	133.3	26.5

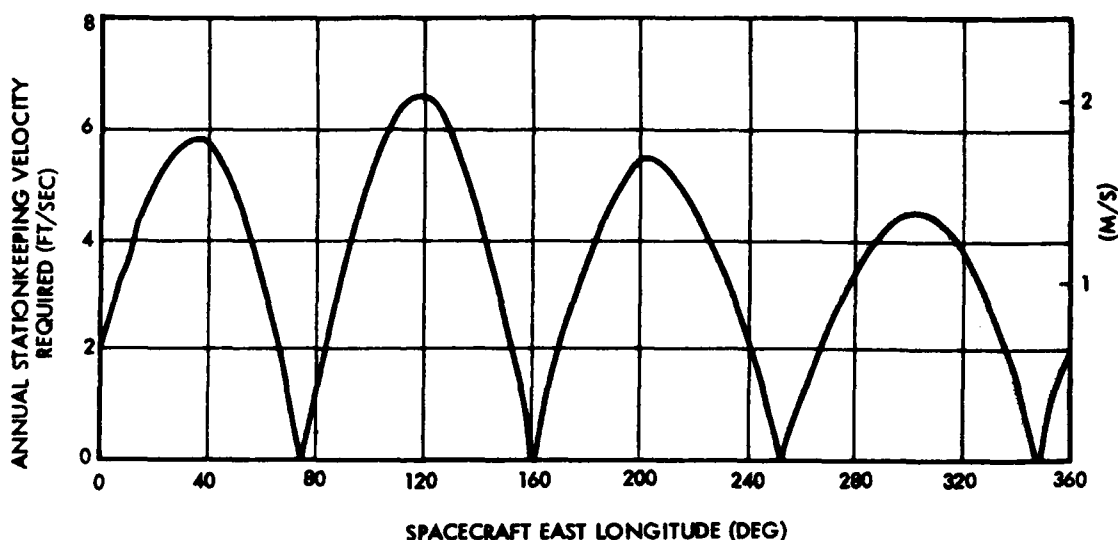


Figure 33. Annual Longitude Stationkeeping Velocity Increment

the orbit with a 2-degree bias relative to the plane of the equator. The orbital plane is then allowed to freely rotate for approximately 2 years, without N-S stationkeeping, until the orbit plane is nearly geosynchronous. At this time stationkeeping is employed until all the fuel is expended (approximately 1 year before end of mission). The orbit plane is then allowed to incline 1 degree during the last year of the mission. The end-of-life (EOL) criteria is tighter than beginning-of-life (BOL) since the sensor will then be degraded. The degradation is partially compensated by tighter stationkeeping. This particular strategy would not be optimum for pulsed plasma thrusters since thrusting is eliminated at the beginning of the mission, a time when excess power is readily available. A more optimum strategy is to use the early surplus power to maintain an off-geosynchronous bias and allow gradual drifting as less power becomes available. This maintains tight pointing at EOL and minimizes added power demands.

Thus, basic strategy is to thrust as close to the orbital nodes as possible and exploit as much early life excess power as possible to minimize both propellant and electrical power consumption. These two goals are somewhat contradictory since concentrating thrusting at the nodes requires a high average electrical power and spreading the thrust cycling about the

entire day causes inefficient propellant utilization. In addition to this basic incompatibility, there are other constraints to consider. The basic redundancy approach has been to use two thrusters, holding the third in reserve until a failure occurs. This way, only two are available for firing at any time. Since the satellite rotates at 1 revolution/10 seconds, two thruster pulses/10 seconds is the highest average stationkeeping thrust available. When the preempting of these thrusters on the average of once every 62.3 seconds for ACS is factored in, the average stationkeeping thrust level becomes 0.84 mlb when 170 watts of power are available for stationkeeping and ACS. Another problem arises in attempting to make full use of the thrusters at the very beginning-of-life since at that time sufficient power exists to over-correct and actually precess the orbit plane away from geosynchronous orbit. Finally, the average electrical power available fluctuates seasonally as well as with orbit life. Figure 27 shows these fluctuations. Peak excess power exists at the equinoxes since power is required to charge the batteries in preparation for solar eclipses.

In developing a thruster strategy, the following factors were considered:

- Launch was assumed at winter (worst case)
- Power excess dictated average thrust level available per season
- A nominal thrust schedule of two 8-hour segments each day was assumed (where possible)
- Added lifetime average power requirements were calculated to achieve ~ 880 ft/sec ΔV over a 7-year period
- Existing batteries can be used to augment array power provided depth-of-discharge/cycle life is not exceeded

With this strategy, only 45 watts of additional array power capability is required for pulsed plasma application. It should be noted that this is possible because thrusting is greatest when excess power is greatest. At end-of-life eclipse periods, in order to put minimum strain on the electrical system, pulsed plasma thrusting levels are low. Note also that 15 of the 45 watt increase is required in any case just to bring the

current DSP 5-year lifetime up to the new 7-year mission duration. The data are summarized in Table 33. With 45 watts added power, the desired 880 ft/sec was not achieved. However, the delivered 856.4 ft/sec permitted end-of-life inclination of -0.13 degrees which is certainly satisfactory. With a thruster failed at launch, the inclination at EOL is -0.6 degree. A later analysis (Section 5.3) indicated that the total 880 ft/sec can be achieved if the added power is increased to 53 watts.

The total impulse required from the pulsed plasma thrusters for N-S stationkeeping, taking orbital inefficiencies into account for thrusting ~8 hours at each node, equals 87,100 lb-sec. To this is added 22,380 lb-sec required for ACS (see Table 32). Thus, the total impulse required for ACS and stationkeeping equals 109,480 lb-sec. To satisfy this requirement, the thruster provided for redundancy at BOL is employed near EOL to furnish 9480 lb-sec for achieving inclination of -0.13 degree at EOL in absence of any primary thruster failures. Thus, the two primary thrusters are fueled to provide 50,000 lb-sec each.

5.2.3 Weight Summary for DSP

Table 34 presents the DSP propulsion subsystem comparison resulting from the configuration studies. The combination pulsed plasma/hydrazine subsystem provides for beginning-of-life satellite inclination error of 1 degree and end-of-life inclination of 0.13 degree. When compared with the basic hydrazine subsystem, which provides for 2 degrees BOL and 1 degree EOL, the combination pulsed plasma/hydrazine subsystem exhibits a weight advantage of 131 pounds. When compared with a hydrazine subsystem having equal capability, it exhibits a weight advantage of 340 pounds. Increased accuracy for inclination control at EOL is desirable to accommodate sensor degradation. As indicated in Table 34, 1 degree EOL is acceptable for the basic mission.

Table 33. N-S Stationkeeping Impulse Summary (with 45 W addition to electric power subsystem)

YEAR	SEASON	POWER AVAILABLE FOR ACS & N-S ΔV (w)	AVERAGE THRUST AVAILABLE FOR N-S ΔV (m)b	N-S ΔV FROM ACS FIRING (ft/sec)	N-S ΔV AT NODAL FIRINGS (ft/sec)	TOTAL N-S ΔV	CUMULATIVE ΔV (ft/sec)
1	WINTER	275	.84	7.2	49.7	56.9	56.9
	SPRING	130	.64	2.3	13.7	16.0	72.9
	SUMMER	170	.84	7.2	52.3	59.5	132.4
	FALL	100	.47	2.3	10.1	12.4	144.8
2	WINTER	200	.84	7.2	55.9	63.1	207.9
	SPRING	80	.35	2.3	7.5	9.8	217.7
	SUMMER	135	.67	7.2	44.0	51.2	268.9
	FALL	75	.32	2.3	6.9	9.2	278.1
3	WINTER	185	.84	7.2	57.8	65.0	343.1
	SPRING	70	.29	2.3	6.2	8.5	351.6
	SUMMER	120	.59	7.2	38.8	46.0	397.6
	FALL	70	.29	2.3	6.2	8.5	406.1
4	WINTER	175	.84	7.2	57.8	65.0	471.1
	SPRING	65	.26	2.3	5.6	7.9	479.0
	SUMMER	120	.59	7.2	38.8	46.0	525.0
	FALL	60	.23	2.3	4.9	7.2	532.2
5	WINTER	165	.84	7.2	55.9	63.1	595.3
	SPRING	55	.20	2.3	4.3	6.6	601.9
	SUMMER	110	.53	7.2	34.8	42.0	643.9
	FALL	50	.17	2.3	3.7	6.0	649.9
6	WINTER	155	.79	7.2	51.9	59.1	709.0
	SPRING	45	.14	2.3	3.0	5.3	714.3
	SUMMER	100	.47	7.2	30.4	38.1	752.4
	FALL	40	.11	2.3	2.4	4.7	757.1
7	WINTER	145	.73	7.2	49.0	55.2	812.3
	SPRING	35	.09	2.3	2.0	4.3	816.6
	SUMMER	95	.44	7.2	28.9	36.1	852.7
	FALL	30	.06	2.3	1.4	3.7	856.4

Table 34. DSP Propulsion Subsystem Comparison, 7-Year Mission

Configuration	Hydrazine (Basic Mission)	Combination Pulsed Plasma- Hydrazine	Hydrazine (Expanded mission)
Orbit Inclination Error, Degrees			
BOL	2	1	1
EOL	1	0.1 ^a	0.1
Dry Weight, Pounds			
Hydrazine Subsystem	99	30	127
Pulsed Plasma Subsystem	--	155 ^b	---
Propellant Weight, Pounds			
Hydrazine	353	68	534
Teflon	---	68	---
Total Subsystem Weight, Pounds	452	321	661
Δ Weight, Pounds	131		340

^a With no single point failure in first 5 months. With a failure at launch, EOL inclination error = 0.6 degree.

^b Assumes additional 53 watts are made available by using high efficiency hybrid BRS solar cells.

5.3 DSP ELECTRIC POWER SUBSYSTEM ANALYSIS

The following sections summarize the analysis of the impact on the DSP satellite electric power subsystem due to the integration and operation of the pulsed plasma millipound propulsion system. The results obtained reflect the status of the most recent design.

5.3.1 Electric Power Subsystem Description

The subsystem, shown in block diagram form in Figure 34, is a bus voltage limited direct energy transfer system that provides power to user loads at voltages between 24.5 and 32.0 Vdc. The main bus voltage is limited to 31.8 ± 0.2 Vdc by shunt element assemblies tapped into the solar array at its electrical midpoint. The capability of the solar array shown in Figure 27 is extrapolated from the available 5-year mission predictions to the desired 7-year operating point.

Three 22-cell 24-Ah (rated capacity) sealed nickel-cadmium batteries provide power during prelaunch, launch, ascent, and on-orbit service periods, and provide energy to clear faults if they develop. The maximum depth-of-discharge for the three batteries under normal operation with a 705-watt, 72-minute eclipse load is 43%.

5.3.2 Propulsion Power Requirements

Section 5.2 provided a description of the requirements for E-W and N-S stationkeeping and attitude control using electric propulsion. Approximately two 8-hour thrusting intervals each day in addition to a low level continuous thrusting are used. The average thrust level varies during the 7-year mission to take advantage of the excess power capability early in the mission. The thrusting strategy employed results in an average power increase of 45 watts from that already available.

The input voltage requirement to the pulsed plasma thrusters is 28 ± 2 Vdc. A buck/boost converter/regulator will be required to match the main bus voltage to the thrusters or the thrusters could be redesigned to operate at the bus voltage. For this analysis, it was assumed that the pulsed plasma power converter operates at DSP bus voltage.

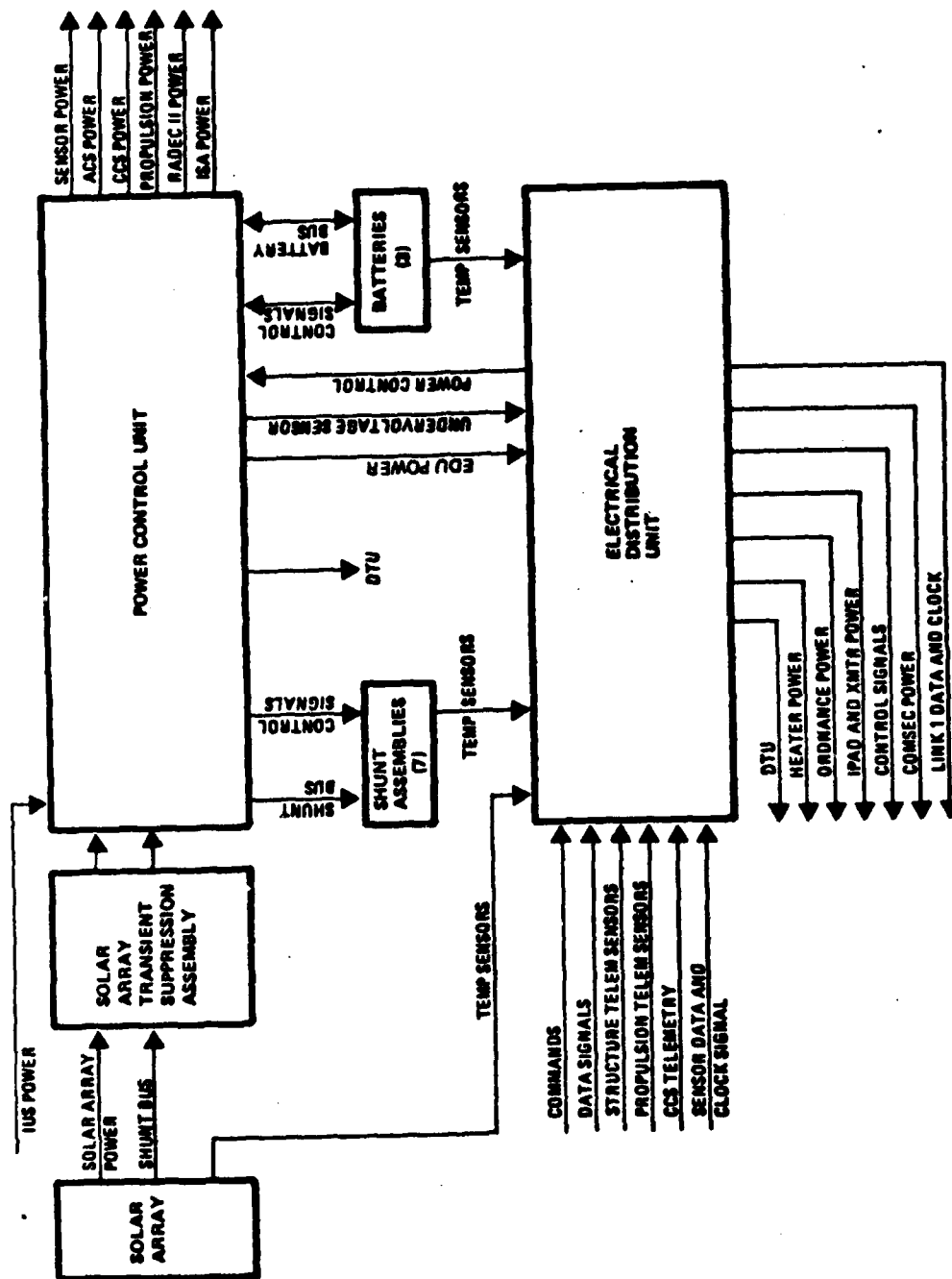


Figure 34. Electric Power and Distribution Subsystem Block Diagram

In addition to providing additional power for thrusting, thermal integration requirements indicate that 8 watts are needed for maintaining the redundant thruster above its survival temperature limit. Thermal control power is provided by heat dissipation from the thrusters and power converters during attitude control firings, and by heaters on the equipment.

5.3.3 Subsystem Impact Assessment

The basic design approach is to utilize the existing batteries to support daily thruster firings that cannot otherwise be accommodated by the solar array power available in excess of spacecraft load power demands. The solar array is not increased in size except by the amount that may be necessary to control the depth-of-discharge of the batteries or to provide required additional battery charge power.

The DSP solar array is composed of 16 body-mounted and 4 deployed panels. Of the body-mounted panels, 4 are flat quadrantal base panels, 4 are wide cylindrical panels, 4 are narrow cylindrical panels, and 4 are conical panels. The 4 deployed panels are covered on both sides by solar cells.

The satellite spins at 6 rpm with the spin axis earth oriented. Because of this controlled attitude, the solar array exhibits a variable output as shown in Figure 35 in the equinox season. Also, as a result of the array and orbit geometry, the seasonal variation in average array output does not follow a conventional pattern and equinox, rather than summer solstice, becomes the design point due to the battery charge power requirements. The total power requirement for the solar array is thus:

705 watts	Equinox Load
75 watts	Battery Charge Power
30 watts	Active Thrusters*
8 watts	Redundant Thruster
<hr/>	
818 watts	7-year Equinox Array Power Requirement at 31 Vdc

* 15 watts additional power would be required for a 7-year mission in absence of electric propulsion; thus, the active thrusters power requirement at the design point equals $45 - 15 = 30$ watts.

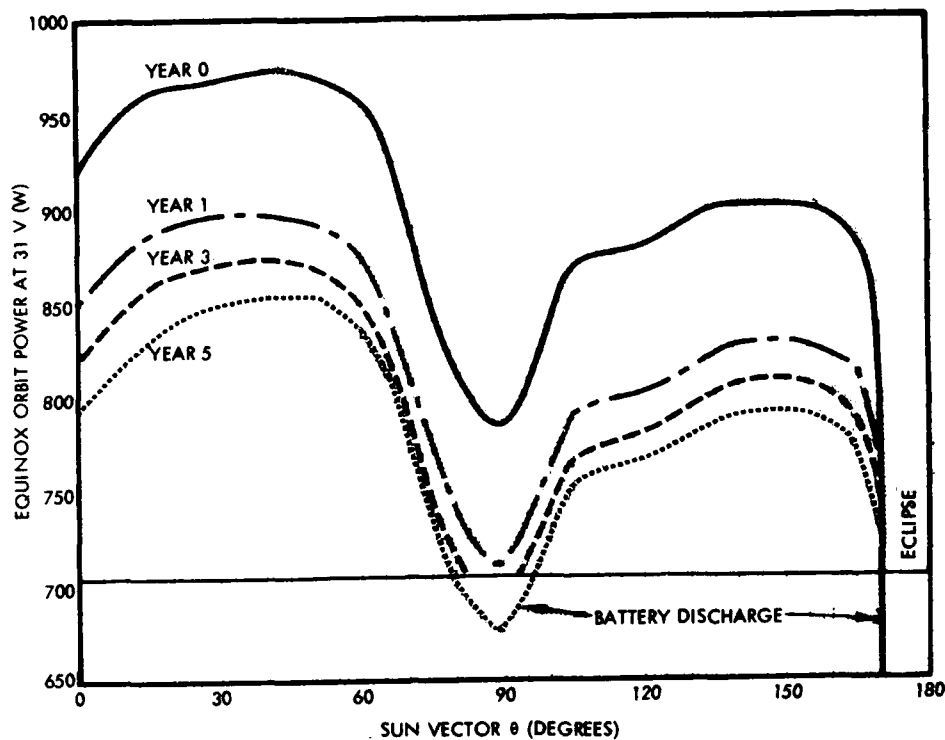


Figure 35. Solar Array Output per Half-Orbit, Equinox

The present design has a predicted year 7 capability of 765 watts. Thus the array must be upgraded to provide an additional 53 watts at year 7. This can be done without a weight impact by replacing the existing cylindrical panels with new panels assembled with the high efficiency (hybrid-BSR) solar cells already being used on the upgraded paddle and base panels. Such a configuration change would yield a 55-watt average power increase over the current design, just offsetting the 53 watts required for the implementation of a 7-year electric propulsion design.

5.4 INTERACTIVE EFFECTS

The potential DSP/pulsed plasma interactive effects that were studied include material transport effects (with particular emphasis on potential contamination of thermal control and solar array surfaces), electromagnetic compatibility, and impact on communications.

5.4.1 Material Deposition Requirements for Pulsed Plasma Thruster on DSP Spacecraft

The various factors contributing to material deposition requirements for pulsed plasma thrusters (PPT) to be placed on the DSP spacecraft are discussed below. The specific areas of concern for material deposition on spacecraft surfaces are discussed. The accretion and alteration processes for spacecraft surface contaminant films and present estimated levels of surface film buildup on DSP Flight 4 are reviewed, and recommendations are made for a material deposition requirement for the pulsed plasma thruster and for placement of these thrusters on the DSP spacecraft.

5.4.1.1 Areas of Concern for Material Deposition on Spacecraft Surfaces

The DSP spacecraft employs a body mounted solar array with additional fold-out panels. All elements of spacecraft are a single spin state, that is, there are no despun portions. The payload sensors and their thermal control materials will have the proposed configuration of Flight 6.

For the overall DSP satellite, the principal areas of concern for material deposition are the solar array cover glasses and the sensor payload thermal control surfaces. For the solar cell cover glasses, the accretion and alteration of contaminants can lead to two effects. The first of these is a loss of transmittivity (T_r) of solar radiation to the underlying solar cells as the result of contaminant film presence and a resultant loss of power in the solar array. The second effect for the solar cell cover glasses is a rise in the solar absorptivity (α) by the contaminant film with a consequent rise in the surface temperature. Of the two effects, the principal concern is for a loss in cover glass transmittivity and the consequent diminution in solar array output.

For the DSP sensor payload thermal control surfaces, the concern for contaminant films is that the accretion and alteration of such films will lead to a rise in the solar absorptivity which will, in turn, cause the sensor temperature to increase. Because low sensor temperatures are required and because low solar absorptivity surfaces are employed, the requirements on allowable surface film buildups are very stringent.

In developing requirements for PPT material deposition on spacecraft surfaces, the recommended approach is to establish a single criterion

which satisfies the most stringent of requirements for all spacecraft surfaces. For the DSP spacecraft, the most stringent requirements are those which are to maintain the low solar absorptivity of the sensor thermal control surfaces. The material deposition requirements of the PPT thruster, and its placement and beam shielding on the DSP spacecraft will, thus, be derived to satisfy a "sensor generated" contaminant requirement. These recommended PPT integration procedures should also satisfy the contaminant requirements of the remainder of DSP spacecraft surfaces. This will involve (see Section 5.4.1.6) the recommended use of "bidirectional" beam shielding for the PPT thruster so that solar array cover glass surfaces are also protected from the PPT plume.

5.4.1.2 Accretion and Alteration Processes for Spacecraft Surface Contaminant Films

The total procedure by which a deposited film may affect underlying surface properties involves both the accretion and the alteration of the contaminant material. The accretion processes involve both the material source or sources and the method of material transport. Both of these elements in the material accretion involve areas of uncertainty. Considerable uncertainty exists relative to the sources of contaminant material on DSP. For example, a wide range in the estimate of the contaminant may result between a hydrazine unit employing a direct burn of the propellant in the thruster nozzle and a "gas generator" hydrazine unit in which the combustion occurs internally, followed by the storage and ultimate subsequent release, through the nozzle, of the combustion products. For the first type of thruster, unreacted hydrazine may be present to some extent in the exhaust plume during all phases of the burn while in the latter (gas generator) thruster, the storage process is considered to act as a significant reduction method for such unreacted hydrazine release. The status of DSP contamination analyses can become very cloudy, thus, when estimates of the spacecraft surface contamination are based on direct burn hydrazine systems while the DSP spacecraft, in point of fact, employs gas generator hydrazine units.

In addition to the uncertainties in the sources of contaminant material, there are uncertainties in the method of material transport. One method of material transport is line-of-sight between the source and the point of deposition. Material may also be transported, however, in a variety of non-line-of-sight processes (Ref. 16), principally as the result of photoelectric ionization of the material followed by electrostatic reattraction of the (now charged) material to spacecraft surfaces. The line-of-sight transport processes may be expected to produce considerable point-to-point variations in the contaminant density, while the non-line-of-sight processes are expected to produce much more uniformly deposited contaminants. In view of those DSP thermal analyses which indicate significant point-to-point variations in the temperature alterations by contaminant films, it would appear that the principal means for contaminant transport is on a line-of-sight basis, and that non-line-of-sight processes constitute only a minor portion of accumulated surface contaminants.

After the deposition of material occurs on a spacecraft, there are areas of uncertainty in both the dwell time of the material on the surface and upon the properties of those materials which do establish a long term residence on the surface. The dwell time uncertainties occur because sticking coefficients are dependent upon not only the arriving material, but also upon the previously deposited material (whose state and composition are largely unknown). The sticking is expected to increase for very cold surfaces but, it should be emphasized, the accumulation of very thin films (of the orders of tens to hundreds of angstroms in thickness) over very long periods (several years) can be significantly affected by extremely low "vapor pressures" of the material on the surface (for example, a vapor pressure of 10^{-13} torr will remove $\sim 10^{\circ}$ Å of material from a surface in a period of 1 year).

A final area of uncertainty exists in the material properties of those contaminant films which do take up a long term residency on the spacecraft

¹⁶ "Possible Material Transport, Accretion and Alteration Process," Internal TRW Technical Memorandum from J.M. Sellen to DSP Project Office, 1972.

surfaces. Laboratory experiments have been carried out which demonstrate significant darkening of surface contaminant materials by ultraviolet radiation (at wavelengths which are present in the solar spectrum) (Ref. 17, 18, and 19). These studies have also shown, however, that significant differences in the rate of surface film darkening result for differing chemical content in the contaminant. The darkening of spacecraft surface contaminant films by solar radiation (particularly in the UV) should be expected. Rates of darkening and ultimate absorptivity of the darkened contaminant layers may be expected, however, to be material specific and continuing uncertainties in contamination analyses should be expected in this portion of the total contaminant impact assessment.

As a brief summary to this section, it should be re-emphasized that contamination analyses must, of necessity, proceed with many areas of uncertainty, and that contaminant requirements, based on present understandings, cannot be rigorously set or vigorously defended as being hard and quantitative. In view of the spacecraft mission for DSP, however, it appears as prudent that a strict material transport requirement be set. If the PPT thruster can satisfy this conservatively based requirement, there would appear to be only a very small possibility of unacceptable spacecraft or mission impact as the result of PPT plume depositions on spacecraft surfaces.

¹⁷ P.F. Jones and E.N. Borson, "The Effects of Deposition and Irradiation of Contaminants from the Outgassing of Silastic 140 RTV," Aerospace Report TOR-0059 (6129-01)-56, February 10, 1971.

¹⁸ "Contamination of Second Surface Mirrors I. Prelaunch Cleaning Procedure, α Radiation Study," Memorandum from P.D. Fleischauer and A.R. Calloway to D.W. Moore, The Aerospace Corporation, Technical Memorandum 73-4070-CP-682, February 21, 1973.

¹⁹ P.D. Fleischauer and L. Tolentino, "The Far Ultraviolet Photolysis of Polymethylphenylsiloxane Films on Quartz Substrates," Proceedings of the 7th Conference on Space Simulation, NASA SP-336, p. 645 November 1973.

5.4.1.3 Estimated Levels of Surface Film Buildup for DSP Flight 4

The use of the Quartz Crystal Microbalance (QCM) on the DSP has allowed an estimate of material film buildup during the DSP orbital period. Recognizing that some differences may exist between the sticking coefficients to the QCM surface and the sticking coefficients to various spacecraft surfaces, an estimate may be made that ~ 4 micrograms/cm² of material accretion occurs over a 3-year period (Ref. 20). For an assumed density of 1 gram/cm³, this mass density would represent a surface film thickness of ~ 400 Å, after 3 years of orbital life. Temperature measurements at the DSP sensor have indicated approximately 4°C rise in temperature over this 3-year period as the result of the accretion and alteration of this surface film. From the indicated temperature rise and the film buildup, a "linearized DSP temperature effects factor" has been defined as

$$F_T = \frac{\Delta T}{\Delta h \Delta t} = \frac{40^{\circ}\text{F}}{(400 \text{ Å}) (3 \text{ years})} = 0.033 \frac{^{\circ}\text{F}}{\text{Å-year}}$$

In a separate analysis (Ref. 21), estimates have been made of the contaminant sources on DSP. From that analysis it has been estimated that 68% of the contaminant build up is the result of sensor electronic enclosure venting and that 28% of the contaminant is from the hydrazine thrusters, in a Mode 6 operation over the 3-year orbital period. There have been differing viewpoints as to the accuracy of the analysis of the thruster derived contaminants because these Mode 6 calculations were based on hydrazine combustion in the thruster nozzles and not in a plenum tank (see the Section 5.4.1.2 discussion of the gas generator hydrazine thruster). For present purposes, however, the estimate of 28% of the contaminant buildup as thruster related is retained. From this, it follows that the propulsion contaminant is estimated as ~ 1 mg/cm² (~ 100 Å in thickness) for a 3-year period of DSP orbital flight.

²⁰ "Contamination Analysis/Design," Report 5359, Section 4, AESC.

²¹ C.R. Maag, Jr., "Status of the SPADS Contamination Analysis Program," AESC Technical Interchange Meeting 3, October 11, 1977.

5.4.1.4 Recommended Material Deposition Requirements for the Pulsed Plasma Thruster

The recommended material deposition requirements will be considered as a three-tiered approach. For the first of these tiers, Level I, the material deposition will be limited to that same value presently estimated to result from the operation of the propulsion system. For a Level I requirement, then, the substitution of the PPT for a hydrazine system would be neither advantageous nor disadvantageous from a contaminant standpoint. The tradeoffs between the PPT system and a hydrazine system would, for a Level I requirement condition, be determined along other system parameter lines. For the second tier of requirements, Level II, the PPT thruster would be required to deposit 0.5 of the presently estimated hydrazine system contaminant, thus improving the propulsion related contamination by a factor of 2. For the final tier of the requirement, Level III, the allowed PPT material buildup would be 0.25 of the presently estimated hydrazine system contaminant. Table 35 summarizes these requirements.

Table 35. PPT Mass Deposition Requirements

Level	PPT Mass Buildup per 3 Years *	Estimated Sensor ΔT per 3 Years
I	1 $\mu\text{g}/\text{cm}^2$, 100 Å	10.0°F
II	0.5 $\mu\text{g}/\text{cm}^2$, 50 Å	5.0°F
III	0.25 $\mu\text{g}/\text{cm}^2$, 25 Å	2.5°F

*The point-of-location for the satisfaction of the deposition requirement is the present location of the DSP Type II radiators.

The requirements of Table 35 may also be restated in the nomenclature of the normalized efflux coefficient, ϵ . For the present requirement the ϵ value will be determined as PPT mass deposited and retained on the unit surface area (1 cm^2) normalized to the total thruster mass throughput. For a total mass release from the PPT thrusters of 4×10^4 grams, the

allowable ϵ for a Level I condition is $(10^{-6} \text{ grams/cm}^2)/(4 \times 10^4 \text{ grams}) = 2.5 \times 10^{-11} \text{ cm}^{-2}$. The Level II requirement will call for a reduction in ϵ to $1.25 \times 10^{-11} \text{ cm}^{-2}$, and the Level III requirement will call for a reduction in ϵ to $0.625 \times 10^{-11} \text{ cm}^{-2}$. These allowable ϵ values are stated at the location of the present Type II radiators on the DSP sensors.

5.4.1.5 Recommended Pulsed Plasma Thruster Placement on DSP Spacecraft

The total complement of three PPTs is to be located at a single azimuthal position (for a cylindrical coordinate system (r, z, ϕ) in which the Z-axis is the spin axis of the DSP) and with an appropriate spacing, in the Z direction, about the spacecraft CG. It is recommended that the thrusters be located at the intersection of the -T axis (using here the DSP sensor axis notation) with the spacecraft body shell. This PPT placement produces the following advantages:

- (1) Large azimuthal angular separation (~ 90 and ~ 180 degrees) between the PPT cluster and the DSP star trackers
- (2) Large angular separation (greater than 90 degrees) between the PPT cluster and the various RADEC sensors
- (3) Angular separation of ~ 90 degrees between the PPT cluster and the Type I radiators in closest proximity to the cooling inputs for those sensor elements for which there are maximum cooling requirements.

If it is desired to locate the PPT cluster at a greater azimuthal angular separation from the Link I antenna (for the -T axis placement of the PPTs the angular separation is ~ 45 degrees), an acceptable direction of movement of the cluster is toward the -X axis (here using the DSP spacecraft axis notation). Location of the PPT cluster within the angular band from the -T axis to the -X axis will retain the material deposition advantages of position outlined above.

5.4.1.6 Bidirectional Beam Shielding for the Pulsed Plasma Thruster

The PPT will be equipped with a beam shield to reduce material transport from the PPT to the DSP surfaces. The recommended beam shield for the PPTs to be placed on the DSP will be "bidirectional" — that is, will be such as to create umbra regions in two principal directions. The first of these umbras will be cast (primarily) in that Z direction for which the

DSP sensors are located, and the second of the umbras will be cast (primarily) in the opposite Z direction. The second umbra region created by the beam shield is to reduce the PPT material transport to the body mounted solar array cover glasses.

5.4.2 Electromagnetic Compatibility of the 1-Millipound Pulsed Plasma Thruster on DSP

This section presents several observations based on currently available data and recommends future work needed to fully evaluate the electromagnetic compatibility (EMC) situation since there is insufficient data available to fully establish the EMC of the pulsed plasma thruster with the DSP satellite.

The DSP satellite requires a minimum +6 dB electromagnetic compatibility safety margin between all interface circuits and their environment. This requirement has been achieved and demonstrated by computerized compatibility analysis and actual satellite tests. The proposed pulsed plasma thruster presents a severe electromagnetic interference (EMI) environment to DSP. In fact, the tested environment exceeds MIL-STD-461 and MIL-STD-1541 radiated environment limits in some frequencies by as much as 100 dB (Ref. 22).^{*} The fact that MIL-STD limits are exceeded does not mean that there is an incompatibility with a satellite. Many circuits can withstand environments well above MIL-STD limits. The actual levels, however, that circuits can tolerate are determined by analysis and/or test. The approach that should be taken to assure successful integration of the flight configured thruster with DSP is outlined below.

The purpose of computerized EMC analysis is to analytically determine the effects of radio-frequency (RF) fields generated by the thruster. An existing DSP computer model may be used for this purpose. A SEMCAP

^{*} The approach described here is also applicable to DSCS-III. A computer model of DSCS-III that can handle transient interference and threshold devices (the SEMCAP computer model does so for DSP) will be required for compatibility analysis.

²² "Pulsed Plasma Radio Frequency Interference Studies," AFRPL-TR-77-85, September 1977.

(Specification and Electromagnetic Compatibility Analysis Program) model of DSP was developed and implemented for predicting EMC response of the spacecraft. An overview of what SEMCAP does is shown in Figure 36. Basically, SEMCAP resorts to a computerized analysis because of the huge amount of terminal-to-terminal wiring involved in any spacecraft system. After all of the system descriptions such as the source and receptor characteristics and the wiring layout are put into the computer, the coupling is computed via four types of coupling matrices. Fortunately, since many of the wires run in common bundles or cable harnesses, the size of the matrices is not comparable to the number of terminals. The outputs of SEMCAP are given in several ways:

- Voltages at each receptor terminal
- Margin of immunity in dB
- Alphabetical indicators of negative immunity margins

The additions to SEMCAP to model EMI from the pulsed plasma thruster are small in comparison to the effort required to implement SEMCAP originally. After the pulsed plasma thruster EMI is modeled, a SEMCAP analysis will identify these circuits having an EMC safety margin less than +6 dB. In addition to identifying these circuits, their exact safety margin will be computed.

Following the initial analysis described above, the thruster EMI model can be modified to achieve +6 dB safety margin. These data can then be used to specify the EMI requirements for the thruster, if it is to be compatible with DSP.

It should be emphasized that the recommended analysis is one which uses an existing EMC computer model of DSP. The computer analysis consists of interference generator models, receptor circuit models, and coupling media transfer models. The receptor models include any interface circuit which is capable of being susceptible. These circuits include equipment for signal interfaces (both analog and digital), timing and control circuits, command circuits, receiver RF input, and sensitive power interfaces. The receptor circuits are modeled in terms of their effective bandwidth

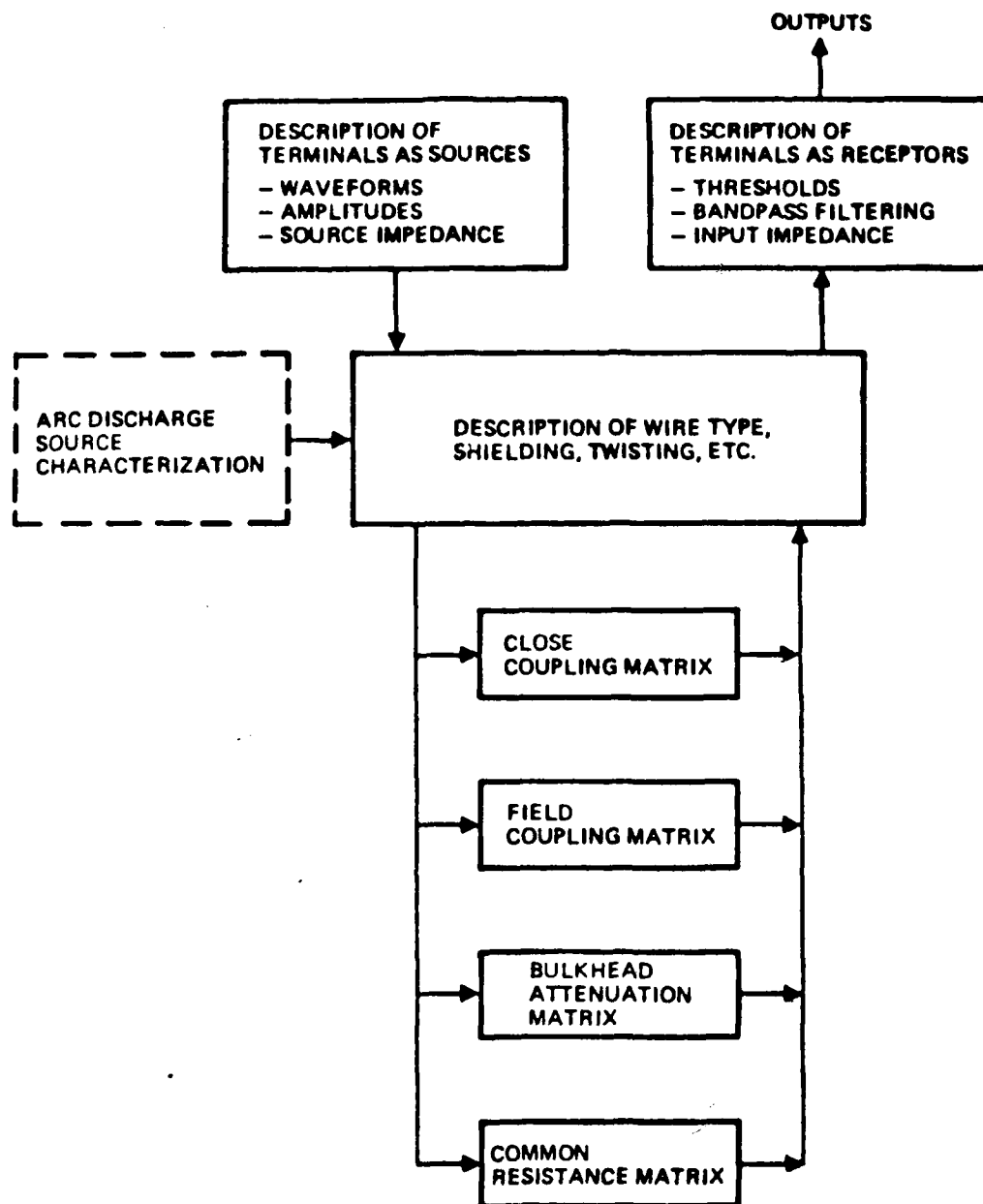


Figure 36. SEMCAP Overview

and threshold of sensitivity which is required to cause an operational malfunction or degrade performance. The coupling transfer media consist of a mathematical model of the satellite cable harness, including type of wire shielding, shield termination, and effects of utilizing satellite structure as a circuit return. New models will have to be generated to describe measured electric and magnetic fields from the thruster.

In addition to the available data, the following data are required to fully evaluate the potential impact to DSP:

- E-Field Data: primary discharge from 1.6 GHz to 10 GHz, and trigger noise from 1 GHz to 10 GHz
- H-Field Data: from 20 Hz to 15 kHz

Some analysis can be performed without these data. In this event, the results will indicate how important these data would be. If the effects of the fields are diminishing in those frequencies where data are not available, the data would not be as important as if the effects are increasing.

5.4.3 Interaction with DSP Communications

DSP has three space/ground S-band communication links for telemetry from and command of the satellite:

<u>Link No.</u>	<u>Power</u>	<u>Bit Rate</u>	<u>Role</u>
1	3.5 W/20 W	1.024/2.048 MHz	Payload data
2	2.5 W	128/1 kHz	Status and health ranging data
3	--	--	Command, ranging

All three links are protected by encryption, and link 1 has available rate 1/2 convolutional encoding for error detection and correction. In general, the data rates are sufficiently low and the data content sufficiently redundant that periodic 30-microsecond outages would not pose a significant problem. It is possible that a worst-worst, very low probability orbital situation could exist where a critical piece of data could be endangered, but the risk with the new engine is well within the range of risks currently experienced. These conclusions are discussed briefly below.

The command link, link 3, is especially well protected. The data rate is low, and the command message received at the satellite must meet many conditions and pass several tests before it can become effective; while pulsed plasma thruster firing might in a worst case distort one or two bits of the message, the impact would be a rejection of the message rather than an incorrect execution. A major protection is that the command process is basically closed loop: the on-board effects, the decoder test results, etc., are communicated back to the ground via telemetry so that the ground can verify correct command execution. Finally, DSP uses dedicated ground stations that could, if necessary, track the engine firing pattern and issue commands during the 5 or 6 second minimum interpulse time.

The satellite health and status telemetry, link 2, is not mission critical. At low bit rate (1 kbps), a firing would typically be transparent, even in a worst case. At high bit rate (128 kbps), a 30-microsecond firing could conceivably distort one or two bits of the downlink; the decryption mechanism could cause several words to be lost. If the lost words happened to occur at the worst possible time (perhaps the main frame synchronous words) a whole 8-millisecond main frame might be garbled, but relock would occur on the next main frame. There is no data on either the main frame or a subframe where an 8-millisecond loss would be significant. On ground station displays, which use a 7-second data refresh cycle, a particular data value may be in error for 7 seconds, but would then be corrected. Reference data, missing at most the 8 milliseconds, are available on tape if an operator should wish to investigate the anomalous readout. The status and health nature of the data, however, is such that this problem would not be expected during the life of the satellite.

The only possible problem would occur on link 1. At the 1 or 2 megabit data rate, a firing could mask 30 to 60 bits of payload data. When decryption effects are considered, the impact could extend to about 2 milliseconds. In almost all cases, such an outage would cause no impact and operators would be unaware of it. There could occasionally be an annoying indication on the display that some data might be questionable (the result of a short term loss of lock), but there are a number of other, more effective annoyances.

In the worst-worst case, a critical measurement could be transmitted once and only once just as a firing occurs. Since the engine duty factor is less than 30 microseconds in 5 seconds (6×10^{-6}) and the extended impact period duty factor of 2 milliseconds per 5 seconds (0.4×10^{-3}), if the engine were completely effective in destroying data it would only affect less than 0.04%. The likelihood of a critical measurement occurring during this period and being masked is thus extremely remote. Even if it did occur, the impact would be softened by the fact that most such measurements occur in pairs by design, and by the fact that repeat measurements will occur within seconds. If tests should verify that the engines can impact the measurement data, corrective action is feasible at the ground station by modifying data processing algorithms. Discussions with contractor ground station personnel indicate that they believe even the worst case impact would be in the noise level.

The above discussion indicates that DSP could tolerate the worst case pulsed plasma thruster impact on its satellite communication links. However, it is desirable that no adverse effects exist whatsoever on the communication links. If future testing of actual plume impacts does not further allay fears, the on-board transmissions software could be modified to eliminate the link 1 concern. For example, an attitude control subsystem signal that fires the thrusters could be used to inhibit data transmissions for 30 microseconds to 1 or 2 milliseconds. The loss in effective data rate would be negligible.

5.5 RELIABILITY ANALYSIS FOR DSP

A reliability assessment of the solid Teflon pulsed plasma propulsion subsystem for DSP was performed utilizing a computerized Monte Carlo simulation technique. In this technique, the computer program runs a large number of mission simulations with the time-to-failure (TTF) changing from one simulation to the next, but distributed according to established failure rates. The failure rate data were obtained from the DSCS-III reliability study.

The DSP analysis consisted of 5000 simulated missions. In each of these simulations TTFs were generated for each thruster based upon an exponential distribution about each thruster's mean time-to-failure. The

mission simulations were performed until a thruster failure occurred, at which time the redundant thruster was activated, its appropriate duty cycle defined and time-to-failure generated, and the simulation continued. In this manner each mission simulation continued through either the failure of a second thruster or the completion of the 7-year mission. Therefore, the reliability predictions presented in Table 36 are the cumulative results of 5000 simulated missions and are representative of the results which might anticipated from the actual testing of 5000 identical sets of thrusters.

5.6 COST ANALYSIS

Cost estimates have been generated for comparing the standard DSP hydrazine subsystem with the combination hydrazine/pulsed plasma. The basic cost assumptions used for the DSCS-III study (Section 4.7) were retained. All estimates are presented in 1979 dollars at the cost level exclusive of contractor's fee. For comparison purposes, start-up costs have been excluded from the estimates shown. It is assumed that similar hardware will be in production at the time the subsystem is needed for application.

Tables 37 and 38 present recurring cost estimates for DSP. Table 37 is for the existing hydrazine subsystem. Table 38 is for a combined hydrazine/pulsed plasma subsystem containing three 1-millipound thrusters. Nonrecurring cost estimates for implementing pulsed plasma propulsion on DSP are shown in Table 39.

From the cost comparison (Table 40), it is seen that the recurring cost of the combination hydrazine/pulsed plasma system is \$727K more than the all hydrazine system.

Table 36. Parametric Reliability Assessment, Pulsed Plasma Propulsion Subsystem for DSP

$(\lambda_{PDA})_A$ (bits)	$\frac{(\lambda_{PDA})_S}{(\lambda_{PDA})_A}$	Reliability (Years On-Orbit)						
		1	2	3	4	5	6	7
500	0.1	0.999+	0.991	0.980	0.972	0.964	0.956	0.947
1500	0.1	0.999+	0.983	0.969	0.954	0.936	0.923	0.913
2500	0.1	0.999+	0.972	0.952	0.932	0.911	0.888	0.876
3500	0.1	0.999	0.968	0.943	0.917	0.892	0.864	0.848
500	0.5	0.999+	0.988	0.977	0.965	0.954	0.943	0.934
1500	0.5	0.999+	0.969	0.948	0.930	0.904	0.882	0.867
2500	0.5	0.999	0.962	0.931	0.899	0.871	0.840	0.815
3500	0.5	0.999	0.957	0.912	0.869	0.829	0.791	0.757
500	1.0	0.999+	0.984	0.971	0.957	0.942	0.928	0.915
1500	1.0	0.999	0.964	0.935	0.903	0.877	0.847	0.823
2500	1.0	0.999	0.952	0.903	0.863	0.816	0.776	0.736
3500	1.0	0.998	0.932	0.872	0.818	0.764	0.714	0.672

$(\lambda_{PDA})_A$ = Active failure rate, propellant-discharge assembly

$(\lambda_{PDA})_S$ = Standby failure rate, propellant-discharge assembly

Table 37. Recurring Cost Breakdown, Hydrazine Propulsion Subsystem for DSP

Item	Unit Cost (\$ Thousands)	Quantity	Total (\$ Thousands)
HARDWARE			
High Level Thruster Assembly	26	4	105
Low Level Thruster Cluster	76	2 sets	153
Propellant Tank	37	2	74
Gas Generator Assembly	32	1	32
Plenum Tank	18	1	18
Valves	--	(a)	54
Valve Driver Electronics	3	24	79
Other Fluid Components	--	As Req'd	35
Structure	--	As Req'd	50
Thermal Control	--	As Req'd	20
Integration & Assembly	--	As Req'd	258
PROGRAMMATIC			
Subsystem Engineering			144
Reliability & Quality Assurance			100
Project Management			100
TOTAL			1222

(a) 4 latching valves, 4 solenoid valves, 2 fill and drain valves

Table 38. Recurring Cost Breakdown, Pulsed Plasma/Hydrazine Propulsion Subsystem for DSP

ITEM	Unit Cost (\$ Thousands)	Quantity	Total (\$ Thousands)
PULSED PLASMA PROPULSION HARDWARE			
Thruster & Fuel Supply	36	3	108
Capacitors	60	3	180
Power Converter	149	3	447
Gimbal Assembly	25	3	75
Gimbal Drive Electronics	16	6	96
Structure	--	As Req'd	15
Thermal Control	--	As Req'd	10
Integration & Assembly	--	As Req'd	22
HYDRAZINE PROPULSION HARDWARE			
High Level Thruster Assembly	26	4	105
Propellant Tank	31	2	62
Valves	--	(a)	54
Valve Driver Electronics	3	8	26
Other Fluid Components	--	As Req'd	18
Structure	--	As Req'd	35
Thermal Control	--	As Req'd	15
Integration & Assembly	--	As Req'd	131
PROGRAMMATIC			
Subsystem Engineering			230
Reliability & Quality Assurance			160
Project Management			160
TOTAL			1949

(a) 4 latching valves, 4 solenoid valves, 2 fill and drain valves

Table 39. Nonrecurring Cost Breakdown, Pulsed Plasma Propulsion Subsystem for DSP

ITEM	\$ THOUSANDS
PULSED PLASMA PROPULSION SUBSYSTEM	
Thruster Development	2500
Subcontract Control	200
Subsystem Qualification	935
Design of Gimbal Drives & Drive Electronics	<u>175</u>
Subtotal	3810
SYSTEM INTEGRATION RETROFIT	
Control Subsystem Analysis	50
Structural Design	50
Thermal Design	80
Electrical Design Integration	50
Ground Segment	60
System Test & Evaluation	<u>125</u>
Subtotal	415
RELIABILITY & QUALITY ASSURANCE	120
PROJECT MANAGEMENT	755
TOTAL	5100

Table 40. Recurring Cost Comparison Summary (DSP)

Subsystem	Cost (\$ Thousands)
Hydrazine	1222
Hydrazine/Pulsed Plasma	1949

VI. GLOBAL POSITIONING SYSTEM MISSION

The NAVSTAR Global Positioning System (GPS) is a space-based radio frequency navigation system which will provide signals for precise determination of position, velocity, and system time by users having proper equipment (Ref. 23). The navigation signals will be provided by a constellation of 24 three-axis stabilized satellites uniformly distributed around three 12-hour orbits, each inclined 55 degrees relative to the equator. This configuration will allow any user, anywhere on earth and at any time, to be within line-of-sight of at least four satellites as required for determining three components of position and system time. Implementation of the system is currently scheduled in three phases as indicated in Figure 37 (Ref. 24). The Phase I space segment consists of eight navigation development satellites (NDS). The goal is to maintain a minimum of five on orbit at all times, using four at a time for precision navigation. The Phase II space segment calls for three additional satellites to be launched on a replenishment basis as needed to maintain a basic six satellite configuration. The 18 satellite Phase III space segment is scheduled for initial operational capability in the mid-1980s.

The purpose of the present study was to investigate application of the pulsed plasma thruster as part of an autonomous control loop to minimize in-track position error for Phase III satellites. At the present time, the GPS ground segment performs satellite tracking and control functions which include daily orbit calculations. The ephemerides data from these calculations are uploaded daily and superimposed on coded satellite navigation signals. In addition, the GPS is limited in its ability to predict satellite location within a 24-hour period. Random solar radiation pressures are the primary contributors to this limitation which amounts to an in-track error of >2 meters. Thus, implementation of an autonomous control system will reduce the requirements for expensive daily orbit calculations and ephemerides loading. An autonomous system will also permit improved

²³Navigation, Vol. 25, No. 2, Summer 1978.

²⁴L. Jacobson and L. Huffman, "Satellite Navigation with GPS," Satellite Communications, 16, July 1979.

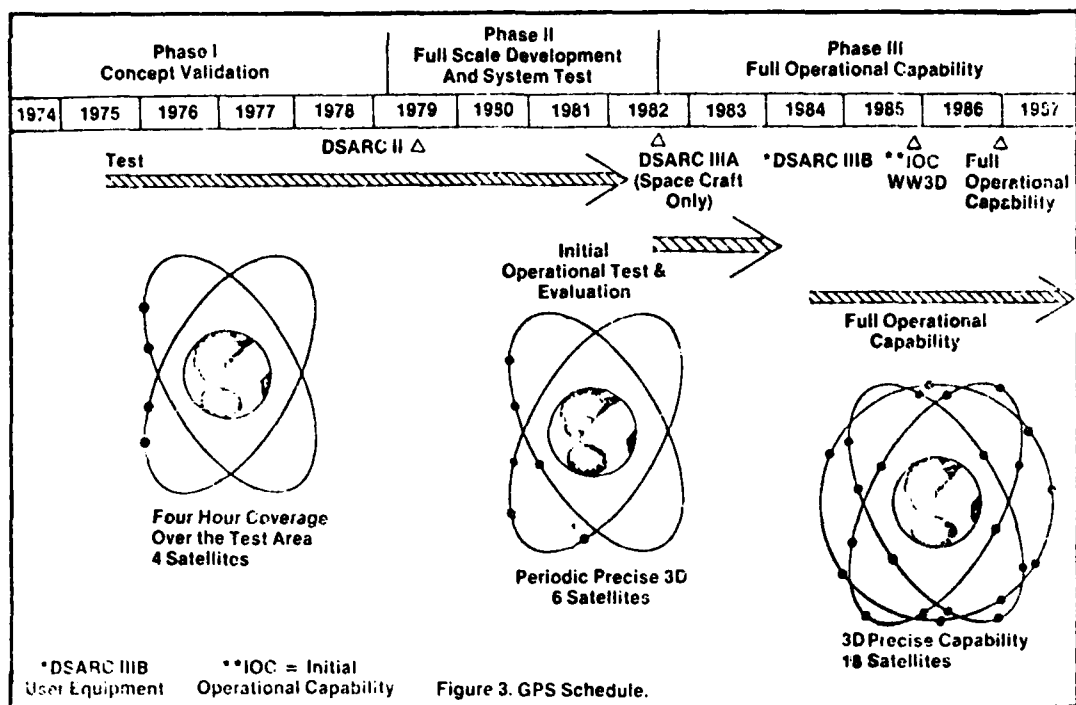


Figure 37. Overview of NAVSTAR GPS (Ref. 24)

position accuracy. At present, advanced hydrogen maser clocks are planned for future operational use. However, the capability of these advanced clocks will be of no avail unless improved positional accuracy is achieved.

This study concentrated on the ability of a pulsed plasma propulsion system, used in conjunction with a single axis disturbance compensation system (DISCOS) sensor to automatically compensate the in-track component of solar pressure, to improve the accuracy with which the satellite position can be predicted. The major mission parameters are summarized in Table 41. Figure 38 shows the planned Phase III design (Ref. 25).

The present study has been performed maintaining the basic Phase III design features as much as possible. However, as discussed later, several major changes were required.

²⁵"GPS Phase III Space Vehicle Systems Engineering Study," Final Report, SSD-79-0108, Rockwell International, 27 April 1979.

Table 41. Global Positioning System Mission

Payoff with Pulsed Plasma Propulsion	Improved position accuracy
Orbit	Half-synchronous, circular
Altitude	10,900 nautical miles
Inclination	55 degrees
Period	12 hours
Mission Life	10 years
Spacecraft Power Load (end of life)	1000 watts
Satellite Weight	~1650 pounds
In-Track Position Accuracy	<1 meter

The GPS satellites uses monopropellant hydrazine for performing the following maneuvers:

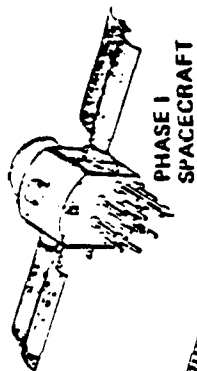
- Spacecraft spin (0-25 rpm) and despin
- Velocity changes in the spin mode
- Reorientation of the spin axis (precession)
- Three-axis control and stabilization
- Velocity changes under three-axis control

The subsystem contains 53 pounds of propellant operating in a blowdown mode. The 16.5-inch diameter tanks provide potential propellant loading up to 121 pounds while maintaining thruster inlet pressures of 90 psia at end of mission. For the present study the basic hydrazine system will be retained. Pulsed plasma propulsion will be added solely to provide the DISCOS propulsion function.

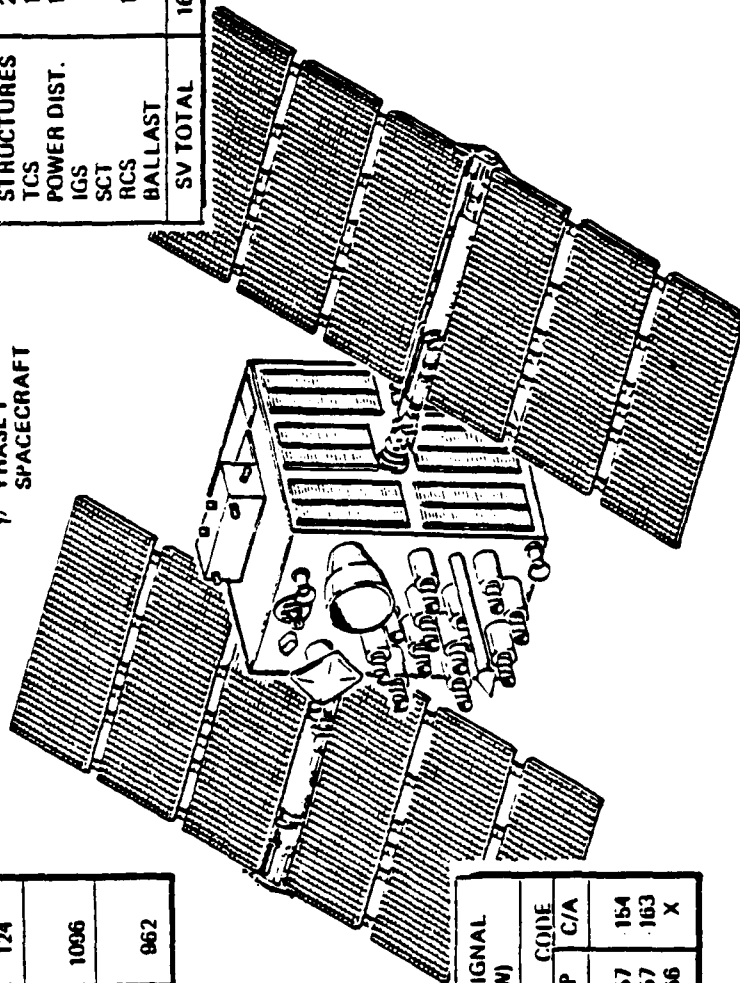
Autonomous control of navigation satellites has been previously demonstrated on the experimental TRIAD satellite (Ref. 26). Its control loop incorporated a DISCOS sensor and cold gas reaction jets. The basic idea

²⁶"A Satellite Freed of All but Gravitational Forces: TRIAD I," Journal of Spacecraft and Rockets, Vol. 11, No. 9, September 1974, pp. 637-644.

WEIGHT	
SUBSYSTEM	WT (LB)
NAVIGATION	212.7
TT&C	137.3
AVCS	72.8
EPS	386.3
STRUCTURES	256.0
TCS	100.0
POWER DIST.	152.6
IGS	74.3
SCT	93.6
RCS	140.5
BALLAST	20.7
SV TOTAL	1646.8



ELECTRICAL POWER	
ARRAY AREA (FT ²)	124
10 YR EOL POWER (WATTS)	1096
AVERAGE LOAD (WATTS)	962



RECEIVED L-BAND SIGNAL STRENGTH (dBW)			
SIGNAL	FREQ (MHz)	CODE	
		P	C/A
L1	1575.42	167	154
L2	1227.60	167	163
L3	1381.06	166	X

Figure 38. Baseline GPS Phase III Space Vehicle Design (Ref. 25)

is that a very small satellite is completely enclosed in a cavity of a larger satellite. The inner satellite, or proof mass, is shielded from all external surface forces, drag, and radiation pressure. As part of the design, it is necessary to:

- Eliminate all possible force interactions, including mass attraction between the two bodies (an exhaustive list of these forces, the relationships governing them, and calculations of representative magnitudes, has been published in Ref. 27)
- Sense the relative displacement between the two bodies
- Use this displacement to modify the motion of the (outer) satellite. As a result, the satellite is constrained to the orbit of the proof mass, which is free of all external forces

Pulsed plasma thrusters have been used on navigation satellites in conjunction with DISCOS sensors to provide autonomous drag compensation. This concept was used on the TIP II and TIP III satellites (Ref. 28). A single-axis DISCOS (Figure 39), as described in Reference 29, was integrated with fore and aft firing thrusters for realizing drag compensation. Solid Teflon pulsed plasma thrusters were employed. An identical arrangement is being implemented for the NOVA spacecraft series.

6.1 CONFIGURATION STUDIES

The 55-degree orbit inclination imposes unusual configuration/attitude control requirements for maintaining proper orientation of the solar arrays and thermal control surfaces. This is because the 55-degree orbit plane may be inclined by as much as 78.5 degrees with respect to the ecliptic.

²⁷ B.O. Lange, "Control and Use of a Drag Free Satellite," Stanford University SUDAAR, June 1964.

²⁸ W.J. Guman and S.J. Kowal, "Pulsed Plasma Propulsion System for TIP-III Satellite," JANNAF Propulsion Meeting, 1975.

²⁹ F.F. Mobley, et al, "Electromagnetic Suspension for the TIP-III Satellite," IEEE Transactions on Magnetics, Vol. MAG-11, No. 6, November 1975.

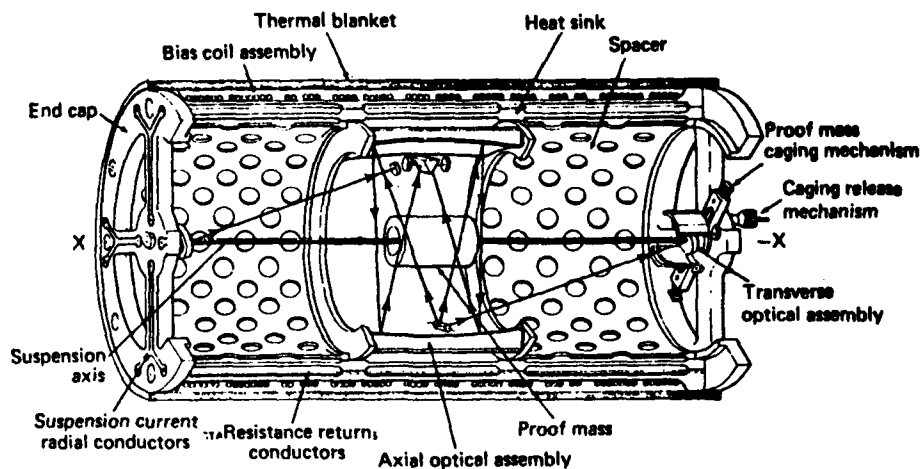


Figure 39. Single-Axis DISCOS Concept

By way of comparison, a synchronous equatorial orbit is inclined by only 23.5 degrees with respect to the ecliptic plane and it is adequate to maintain the array booms parallel to the north-south direction. The high declination GPS orbits require essentially a 2 degree of freedom solar array control and additional control maneuvers for avoiding solar incidence on thermal control surfaces. The present NAVSTAR concept provides the additional degree of freedom and attitude control by seasonal yaw maneuvers. A similar strategy for a DISCOS system would be undesirable because of the requirement to maintain the DISCOS axis and thrust direction parallel to the velocity vector. Because of the severity of this requirement, a major part of the study effort was to select and evaluate alternate spacecraft configuration/maneuver strategies which could simultaneously satisfy thermal, solar array, and DISCOS requirements.

6.1.1 Candidate Configurations

Initially five candidate GPS/DISCOS configurations were considered:

- (1) Spherical spinner (around earth-pointing axis) with body mounted solar cells
- (2) Cylindrical spinner (around earth-pointing axis) with body mounted solar array

- (3) Three-axis stabilized rectilinear with 2 degrees of freedom deployed solar array
- (4) Three-axis stabilized, seasonal yaw adjustments to allow single degree of freedom deployed array
- (5) Cylindrical spinner (axis parallel to earth spin axis) with body mounted array

These configurations are discussed in greater detail in the following paragraphs.

6.1.1.1 Configuration 1 — Spherical Spinner

This configuration is a spherical spacecraft with the external surface covered with solar cells. The spacecraft attitude in orbit requires that the spacecraft spin about the Z-axis with +Z-axis always pointed at nadir.

Thermal comments regarding configuration 1 include:

- (1) The solar array will act as a temperature sink for the internal components. Component dissipation will be radiated to the solar array and then reradiated from the solar array to space. Therefore, the solar array must be of a minimum area to radiate the internal heat dissipation based on an average solar array temperature.
- (2) Minimum sizing of the sphere is based on the hot case conditions of 1000 watts internal dissipation at mid-life and winter solstice solar flux (simplified analysis)

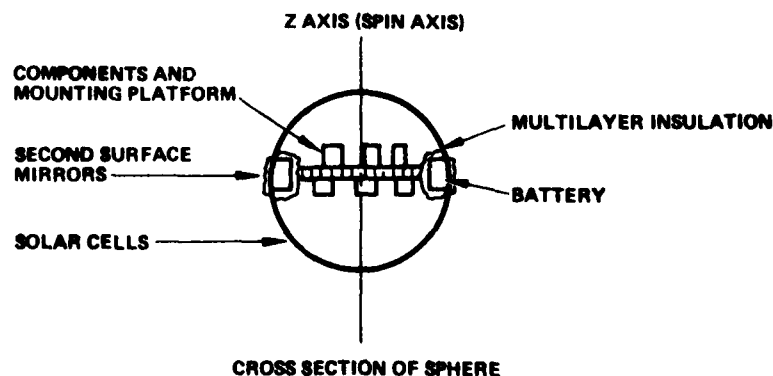
$$R_{MIN} = \sqrt{\frac{Q (3.414) \left[1 + \frac{\epsilon_{S/A} F_{S-SP}}{\epsilon_1 \epsilon_2 F_{S-P/L}} \right]}{4\pi \left(\epsilon_{S/A} F_{S-SP} \sigma_{T_{P/L}}^4 - \frac{\alpha_{S/A} G}{4} \right)}}$$

$$R_{MIN} = \sqrt{\frac{1000 (3.414) \left[1 + \frac{(0.83)(1.0)}{(0.9)(0.9)(0.5)} \right]}{4 (3.14) \left[(0.83)(1.0)(145) - \frac{(0.72)(450)}{4} \right]}}$$

$$R_{MIN} = 4.6 \text{ ft}$$

where

- Q = Internal dissipation = 1000 watts
- $\alpha_{S/A}$ = Effective absorptance of solar array = 0.72
- $\epsilon_{S/A}$ = Emittance of solar array = 0.83
- ϵ_1 = Emittance of components = 0.9
- ϵ_2 = Emittance of solar array back side = 0.9
- G = Solar constant = 450 Btu/hr-ft²
- $T_{P/L}$ = Component temperature = 27°C
- F_{S-SP} = View factor of solar array to space = 1.0
- $F_{S-P/L}$ = View factor of solar array back side to components = 0.5
- R = Radius of sphere (ft)
- (3) Average hot temperature of solar array is $\sim 9^\circ\text{C}$ when solar vector is normal to spin axis
- (4) Long life batteries require lifetime temperatures in the 0° to 16°C range. This requires mounting batteries directly to a second surface mirror radiating area on external surface of the sphere at mid-position along the spin axis. They require thermal isolation (and heaters) from the remainder of spacecraft.



Disadvantages of Configuration 1 include:

- (1) During certain portions of the orbit the solar vector will be collinear (or near) with the spin axis causing higher temperatures on the constantly illuminated solar array and may cause excessive temperature gradients affecting

component temperature control. Detailed transient thermal analyses will be needed to verify this. Average temperature of the sun side of the array will be 490C during this condition.

- (2) During portions of the orbit when the solar vector approaches the spacecraft +Z axis (where the antenna farm will be located), less solar array area will be isolated
- (3) To accurately determine power available from the solar arrays in this configuration requires additional thermal analysis. Season, inertial location of orbit, orbit life and internal power dissipation should be considered.
- (4) Would require despun DISCOS

6.1.1.2 Configuration 2 - Cylindrical Spinner

The cylindrical spacecraft has solar cells covering the external surface of the cylinder. The spacecraft attitude in orbit has the spacecraft spin about the Z axis (axis of revolution of the cylinder) with the +Z axis always pointed at nadir.

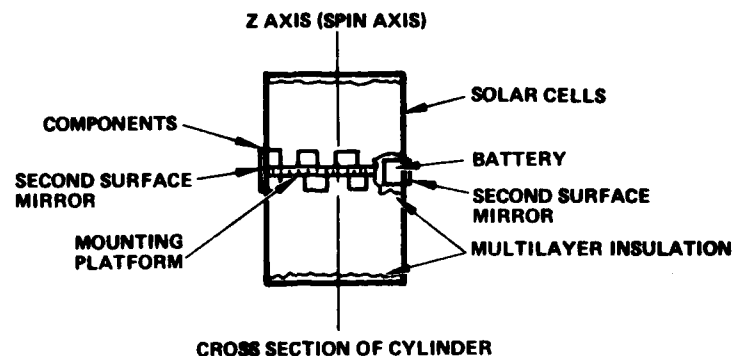
Thermal comments regarding configuration 2 include:

- (1) The cylindrical solar array will act as a temperature sink for the internal components. Component dissipation will be radiated to the solar array and then reradiated from the solar array to space.
- (2) Minimum sizing of the cylindrical solar array sink is based on the hot case conditions of 1000 watts internal dissipation at mid-life and winter solstice solar flux (sun normal to spin axis).

$$A_{MIN} = \frac{Q (3.414) \left[1 + \frac{\epsilon_{S/A} F_{S/A-SP}}{\epsilon_1 \epsilon_2 F_{CYL-P/L}} \right]}{\epsilon_{S/A} F_{S/A-S/P} \sigma T_{P/L}^4 - \frac{\alpha G}{\pi}}$$

The minimum area required to maintain the payload at 27°C is 706 ft². This transforms into a cylinder 16 feet in length with a radius of 7 feet which is prohibitively large. The average hot case temperature of the solar array is ~180C when the solar vector is normal to the spin axis.

- (3) To reduce the size of the cylinder for thermal reasons will require partial mounting of components to a band of second surface mirrors around the cylinder. Heaters, internal louvers, and/or variable conductance heat pipes will be required to maintain acceptable component temperatures during cold case conditions (i.e., when the solar vector is highly inclined relative to the spacecraft spin axis).
- (4) Batteries will require mounting directly to external second surface mirror radiating area, and isolation from the remainder of the spacecraft and heaters.



Disadvantages of configuration 2 include:

- (1) Thermal control subsystem will require heater power, variable conductance heat pipes, and/or louvers when the sun angle is highly inclined relative to the spin axis and when the power from the solar array will be marginal.
- (2) During portions of the orbit when the solar vector is collinear with the spin axis, there will be no insulation on the solar array unless the cylinder ends are covered with solar cells.
- (3) Will require a despun DISCOS.

6.1.1.3 Configuration 3 — Three-Axis Stabilized Rectilinear

Spacecraft configuration 3 can be rectangular, hexagonal, octagonal, etc., with boom-mounted 2 degree of freedom rotating solar arrays. The spacecraft attitude in orbit requires that the spacecraft be three-axis stabilized with the +Z axis always pointed at nadir and the +X axis always in the velocity vector. This configuration is inherently the most compatible with a DISCOS system and has been selected as the baseline design.

Thermal comments regarding configuration 3 include:

- (1) In the orbit being considered and with the spacecraft attitude maintained as described above, all external spacecraft surfaces will receive nearly a one sun solar flux during some period of an orbit.
- (2) Thermal control can be maintained by mounting components directly opposite second surface mirrors (SSM) on these surfaces but is somewhat inefficient. The SSM area requires sizing for hot conditions of full sun, but will require some heater power for cold conditions when there is no solar impingement considering a constant power component. The spacecraft Y surfaces which can see normal sun for an extended period can maintain acceptable temperatures on components which have a power/mirror area density of approximately 12 W/ft² of SSM. The spacecraft X surfaces can maintain component temperatures with a power/mirror area density of approximately 17 W/ft² SSM.
- (3) Heater power requirements can be reduced by using variable conductance heat pipes between the component and the radiator or using constant conductance heat pipes to distribute heat from an insulated SSM radiator to a shaded SSM radiator.
- (4) The boom mounted solar array average temperature at end-of-life is ~380C.
- (5) A nonilluminated thermal control surface can be provided by a 180-degree yaw maneuver every 6 months.

Disadvantages of configuration 3 include:

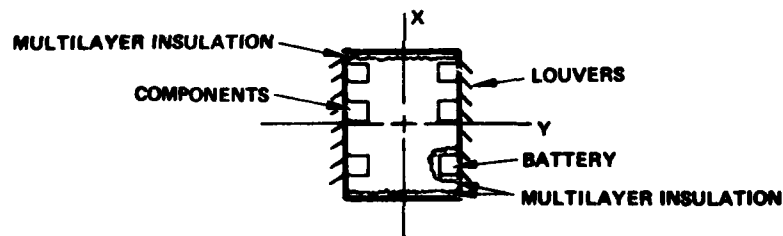
- (1) The thermal control subsystem will require heater power variable and/or fixed conductance heat pipes.
- (2) There is no preferred spacecraft surface to mount batteries which require lifetime temperatures in the 0° to 16°C range. To obtain these battery temperatures, the batteries require direct mounting to an SSM area which receives less than 45% of full sun solar impingement. An X spacecraft surface may be acceptable by relying on the battery thermal mass to minimize orbital temperature variations. Transient thermal analysis is required for verification.
- (3) Will require biaxial solar array drives. Booms must be long enough to prevent the main body shadowing solar array.

6.1.1.4 Configuration 4 — Three-Axis Stabilized Rectilinear

This spacecraft configuration is rectangular solid or cubical with a boom-mounted single-axis rotating solar array. The spacecraft attitude in orbit has the spacecraft +Z axis always pointed at nadir and the spacecraft yawed in orbit to maintain the solar vector always in the spacecraft Z-X plane.

Thermal comments regarding configuration 4 include:

- (1) This spacecraft attitude will provide two sides of the spacecraft (Y surfaces) which will receive little or no solar impingement. Component mounting density can be approximately 30 W/ft² of radiating area on these Y surfaces.
- (2) For a constant internal power dissipation, no on-orbit heater power will be required. If the payload power varies, louvers can be employed on the Y surfaces to maintain component temperatures without heater power.
- (3) Batteries can be mounted on the Y surfaces of the spacecraft and isolated from the remainder of the spacecraft structure for their special thermal control requirements.



CROSS SECTION OF COMPARTMENT

Disadvantages of configuration 4 include:

- (1) The disadvantages for this system are primarily in subsystems other than thermal. The ACS system is more complex and the propulsion system will not have thrusters or DISCOS axis continuously in the velocity vector.

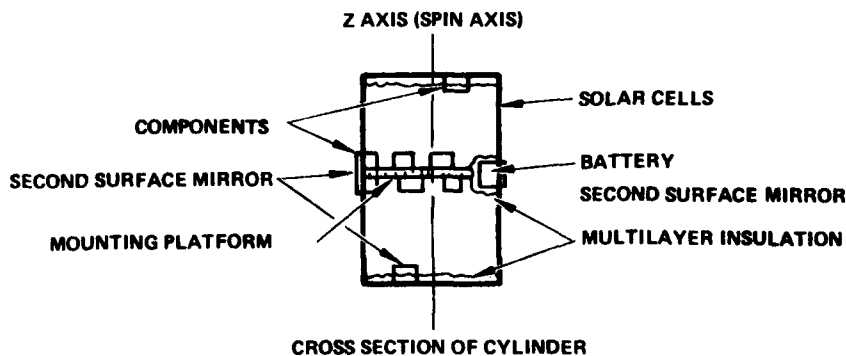
6.1.1.5 Configuration 5 — Cylindrical Spinner

This configuration is a cylindrical spacecraft with the external surface of the cylinder covered with solar cells. The attitude in orbit has

the spacecraft spinning about the Z-axis (axis of revolution of the cylinder) with the Z-axis maintained normal to the equatorial plane.

Thermal comments regarding configuration 5 include:

- (1) The solar vector will remain ± 23.5 degrees from normal to the spin axis, providing a relatively benign thermal environment. The solar array temperature will vary between approximately 0° to 16°C during the on-orbit life of the spacecraft.
- (2) To use the solar array as a radiative temperature sink for the payload components (1000 watts) will require a minimum solar array area of approximately 706 ft^2 as stated for configuration 2.
- (3) Mounting components directly opposite second surface mirror radiating areas can reduce the solar array area required for thermal. Components can be mounted to these SSM areas at a power density of 25 W/ft^2 of SSM area. Heaters should not be required during cold conditions for this configuration.
- (4) Batteries can be mounted on the cylinder or cylinder ends for thermal control since the solar vector will not impinge at an angle greater than 23.5 degrees. Batteries will require direct mounting to the external SSM area and thermal isolation from the remainder of the spacecraft and heaters.



Disadvantages of configuration 5 include:

- (1) The spacecraft Z axis is not earth pointing; therefore, the antenna farm will possibly require a despun platform. Also, the antenna will require gimbaling to maintain earth pointing.
- (2) The DISCOS system will require a despun platform.

6.1.2 GPS/DISCOS Configuration

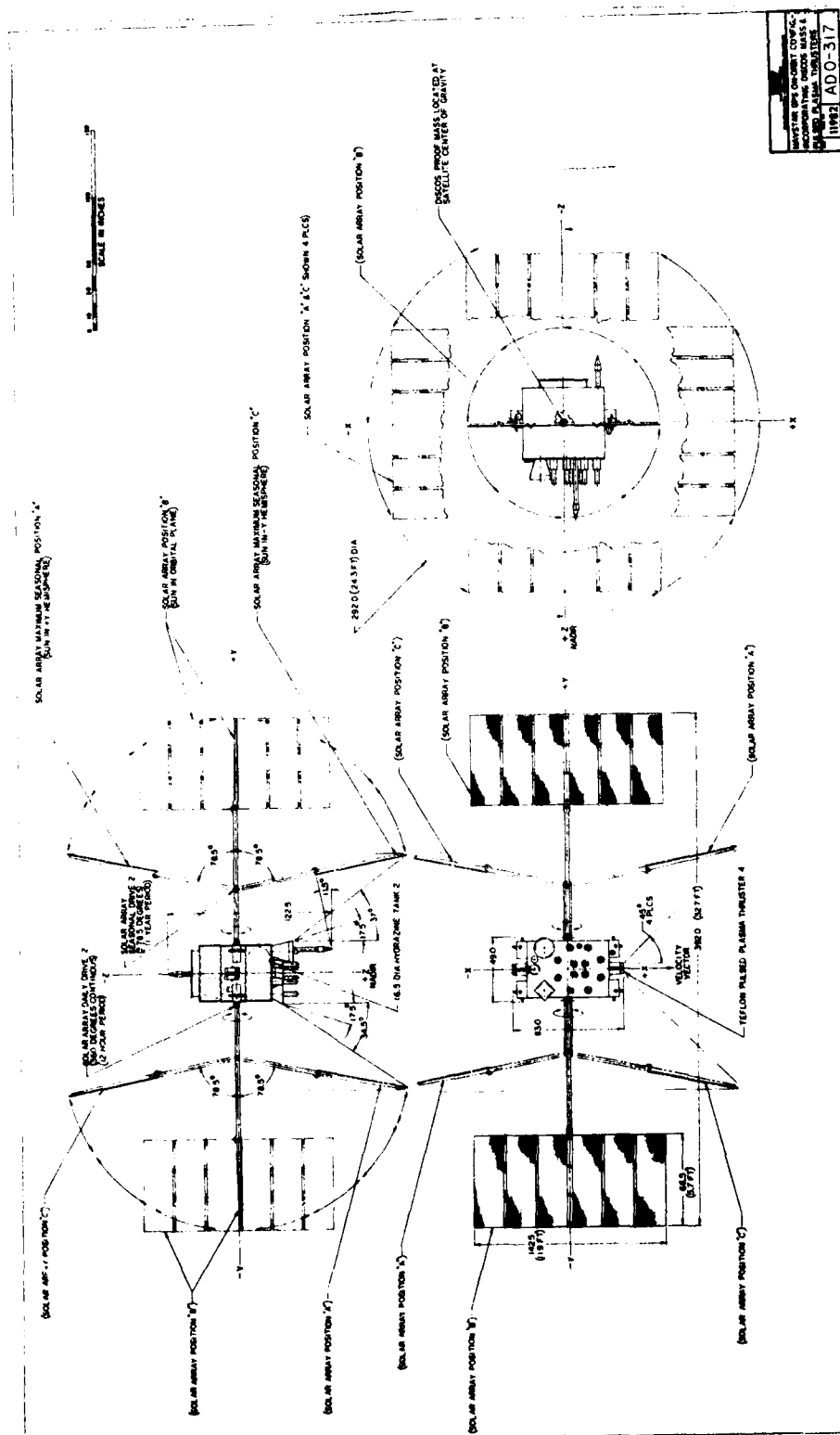
Figure 40 shows the layout for the GPS/DISCOS baseline (configuration 3). Complete redundancy is provided by four-pulsed plasma thrusters located in pairs on the east and west satellite faces, in line with the satellite center of mass. The configuration adheres as closely as possible to the present Phase III GPS design. However, in order to accommodate DISCOS, the following design modifications would have to be implemented:

- Two degree of freedom solar array. The present GPS concept utilizes a single axis solar array drive combined with seasonal yaw maneuvering to maintain proper sun orientation for the planned 55-degree inclination orbits. In this configuration, a second array degree of freedom was used in order to avoid the yaw requirement. This was necessary to maintain the DISCOS sensing and thrusting axis (i.e., the satellite X axis) collinear with the velocity vector at all times. The required array articulations are described in Figure 40.

The array booms are sized, articulated, and driven so as to avoid shading each other or the spacecraft and to maintain constant centers of gravity and pressure. To accomplish this the main array drive rotates the array with a 12-hour period about the Y axis. The seasonal drive provides yearly back and forth articulation of the array boom hinge to keep the array perpendicular to the sun line. The maximum articulation ($\pm\theta_m$) required is equal to the declination of the orbital plane. A semiannual 180-degree yaw maneuver can be employed to limit the articulation to one quadrant (i.e., $0 \leq \theta \leq \theta_m$). The yaw maneuver will also allow a thermal control surface that does not receive full sun incidence.

The overall configuration keeps the array outside a 45-degree cone half-angle with respect to the thruster exhaust. Figure 40 presents further details of the solar array configuration.

- Existing hydrazine thrusters moved to new locations. This was necessary to allow the DISCOS thrusters to be mounted in-line with satellite CG.
- Redistribution and symmetrization of mass distribution. A volume of approximately 4 inches in diameter by 8 inches in length (along X axis) must be made available at the satellite CG. The satellite mass must be distributed to reduce mass attraction forces on DISCOS to $<10^{-11}$ g along X axis and $<10^{-8}$ g in Y-Z plane. In order that the gravitational forces remain sufficiently low throughout the range of DISCOS travel, it is also necessary that the gradient of mass attraction forces be less than 10^{-11} g/mm along the X axis.



- Redesigned satellite thermal control. In addition to the usual thermal control requirements for battery and electronics, GPS Phase III will have a thermal control requirement of $\pm 0.10^\circ\text{C}$ for its Cs and Rb clocks.

The present Phase III design uses yaw maneuvers to maintain the solar vector in the X-Z plane. This allows the Y faces to be used for thermal control since they never receive direct sun. Because the DISCOS GPS will not yaw, all external spacecraft surfaces will receive nearly one sun solar flux during some period of an orbit. Thus, more radiator area (and potentially more heaters) will be required. It is possible to provide one surface that never receives direct sun by performing a 180-degree yaw maneuver twice a year, at local noon, when the sun is in the orbit plane. This maneuver will also reduce the total annual solar array reticulation by 50%.

- Possible redesign of antenna farm. The biaxial solar array drive allows the array to penetrate the forward hemisphere relative to the plane of the antenna farm (+Z face). Although the arrays remain well out of the direct line of transmission, more detailed study is needed to determine the impact on antenna radiation patterns. If interference exists, further redesign will be needed to narrow the unidirectional beam patterns, and it may be necessary to relocate the S-band omnidirectional antenna.

6.2 PROPULSION REQUIREMENTS

The study results of the impact of DISCOS and pulsed plasma on the orbital and attitude control functions of GPS are summarized below. Solar pressure on GPS is quantified and provides the basis for defining a propulsion system for DISCOS (in this case, pulsed plasma). The nonideal effects of out-of-orbit plane thrust vector misalignments and satellite gravitation changes are studied, and the impact on the attitude control system is summarized.

The most significant results of the study include:

- Thruster impulse bits must be ≤ 1.8 mlb-sec
- 3200 lb-sec of impulse required for mission life
- Out of orbit plane thrust considerations constrain yaw control
- Satellite mass properties are probably controllable to the tolerance required by DISCOS.

6.2.1 Assumptions

The basic satellite mission is that of an advanced GPS mission. It is required to maintain track of the satellite with sufficient accuracy to tell a user its orbit path to within 1 meter precision. This has traditionally been done by elaborate modeling of orbital parameters and updating these parameters with almost continuous tracking data. Ultimate tracking precision is limited by relatively high frequency (with respect to multiple orbits) perturbations to the orbit caused primarily by external disturbances — chiefly solar pressure and the errors induced by the hydrazine system when orbital corrections are made. The role of DISCOS is to exactly compensate for these disturbances with a closed loop control via a reference mass which is isolated from external disturbances. In this case, ground control orbital track only needs to compensate for low frequency gravitational perturbations and very low frequency DISCOS bias uncertainties. Since orbital control is continuously exerted, large hydrazine corrections are less frequently required. Because these disturbances affect primarily the orbital velocity and not precession of the orbit plane, DISCOS only need provide a single axis of control (along orbit path).

Since this study relates to the possible use of pulsed plasma for this mission, it was decided to assume minimal modifications for other hardware. In the case of DISCOS, the flight tested unit used for TIP-II was assumed (Ref. 29, 30):

- Single active axis
- Although the total travel allowed is larger, it is desired to maintain velocity control to within a 2 mm deadzone
- 10^{-7} g suspension force
- 10^{-11} g sensitivity along active axis
- 10^{-8} to 10^{-11} g biasing capability along active axis

Figure 39 shows the basic system.

³⁰S.J. Kowal, TRW Applied Physics Laboratory Memo, S4S-10-001, 2 February 1973.

The satellite is assumed to be an advanced GPS mission as reported by Reference 25 with the minimal changes necessary to implement a DISCOS-pulsed plasma system. The layout is shown in Figure 40. The basic changes to the configuration of Reference 25 include:

- Placement of DISCOS at the satellite center of mass
- Location of four small pulsed plasma thrusters along orbital velocity axis (two plus and two minus)
- Stabilizing the yaw axis to orbital coordinates so that the DISCOS and pulsed plasma thrusters are always pointing properly
- Adding a second solar array drive to the solar panel booms so that the arrays can be sun pointing during all seasons. Satellite mass is assumed to be 51.5 slugs (1648 pounds).

6.2.2 Solar Pressure Model

The basic equation for predicting solar pressure on a satellite is:

$$F = \sum_{i=1}^n V_F A_i |\cos N_i| (1 - V_i) \int_s^{\hat{}} + (2V_i) (\cos N_i) \hat{N}_i$$

where

V_F = solar pressure on satellite ($\sim 9.4 \times 10^{-8}$ lb/ft²)

A_i = area of particular satellite body (ft²)

N_i = angle between sun vector and normal to body face

V_i = coefficient of reflectivity for body

$\int_s^{\hat{}}$ = sun vector

\hat{N}_i = body face normal vector

The satellite consists of primarily the solar array panels (124 ft²) plus the body whose area changes with aspect angle of sun but is approximately 30 ft². The coefficient of reflectivity is ~ 0.23 for front face of solar panels, 0.5 degree for kapton insulated surfaces, and 0.89 for

mirrored surfaces (10-year average). $N_i = 0$ degree for solar panels and varies for body faces (always <90 degrees for portions facing sun). Considering all of these factors, the average solar force is 2×10^{-5} pounds directed along the sun vector.

This force must be resolved into satellite orbital parameters so that the effects of each component can be evaluated. Defining the inclination of the sun with respect to the orbit plane as β and orbit rate as ω_0 , then the sun vector in orbital coordinates is:

$$\hat{s} = \sin \beta \hat{y} + \cos \beta [(\sin \omega_0 t) \hat{x} + (\cos \omega_0 t) \hat{z}]$$

where $-78.5 \text{ degree} < \beta < +78.5 \text{ degree}$ (yearly variations of ± 78.5 degree to 31.5 degrees, depending on time of year and specific orbit).

$$\omega_0 = \frac{2\pi}{12 \text{ hr}} \text{ (rad/hr)}$$

\hat{x} = vector along orbital velocity path (roll axis)

\hat{y} = out of orbit plane vector (pitch axis)

\hat{z} = vector direct toward earth (yaw axis)

Note the solar pressure is constant in the out-of-orbit plane component and varies with orbit orientation. Because this is a constant around the orbit and earth's gravitational forces keep the orbit centered about the earth, this produces a coning or wobbling motion. This coning motion is bounded at 17 feet for the worst case sun inclination angle.

The in-plane \hat{z} component of solar pressure merely perturbs the orbit eccentricity and, since the forces are cyclical, little effect is seen on ground track. The in-plane \hat{x} component is the one that produces significant orbital drift and is the reason for incorporation of DISCOS. This component is:

$$F_{\hat{x}} = (2 \times 10^{-5}) \cos \beta \cos (\omega_0 t)$$

It is now necessary to calculate an average F for a GPS mission. Since ω_0 is constant, the average of $\cos \omega_0 t$ over an orbit is $2/\pi$. $\beta = (55 \pm 23.5 \text{ degrees}) \sin y t$ where $y = 365/t$ (days). The choice of where in the 31.5 to 78.5 degree span a particular year's excursion lies depends on the particular geometry of the orbit plane relative to the ecliptic. The net average is $\sim 10^{-5}$ pounds. For 10 years, this totals 3150 lb-sec.

6.2.3 Propulsion Requirements for DISCOS

It has now been shown that DISCOS on GPS requires a propulsion system capable of providing impulse along the plus and minus orbital velocity vectors totaling 3150 lb-sec and approximately equally distributed between the two directions. All that remains is to define the range of acceptable impulse bits and alignment requirements. Impulse bit sizing is presented below; the alignment discussion is presented in the next section.

The basic constraint on impulse bit is that it not be so large as to cause fuel-wasteful two-sided limit cycling for small disturbances and not be so small as to cause loss of control.

6.2.3.1 Upper Impulse Bit Bound

The normal control concept is to allow the DISCOS reference mass drift within an acceptable region (given as 2 mm or 0.0066 ft). When the boundary of this region is reached, a pulse is fired, moving the satellite so that the reference mass remains centered. This impulse imparts a Δ velocity to the satellite that would cause the reference mass to eventually reach the opposite end of the dead zone were it not that a disturbance acceleration is driving the satellite back to the original side of the dead zone, causing a repetitive control pulse. When this occurs, the control impulse equals the disturbance impulse over an extended period of time and control is 100% efficient (until the slowly changing disturbance force reverses polarity which usually happens only four times a day). If the control impulse bit is too large, the reference mass will reach the other end of the dead zone before the disturbance drives the satellite back and a superfluous control pulse of the same polarity as the disturbance force is generated. This increases the number of control pulses required at the original end of the dead zone and wastes propellant. Of

course, if no disturbance torque exists and only finite control pulses are available, two-sided limit cycling must exist. It should be noted that two sided limit cycling is perfectly acceptable except that it uses extra propellant.

Since the current disturbance pressure model does have periods of time when this disturbance is quite small, a compromise must be reached allowing occasional two-sided limit cycling. In this case, the crossover level arbitrarily selected is two-sided limit cycles no greater than 10% of the time for the orbit plane/sun vector geometry, which produces minimum in-plane disturbances ($\beta = 78.5$ degrees). The disturbance at this threshold is 1.2×10^{-6} pounds causing an acceleration of 2.33×10^{-8} ft/sec². Since the dead-zone is 0.0066 feet, the allowable impulse bit ΔI is that which produces a Δ velocity = $2V_0$ where

$$\text{and } \left. \begin{array}{l} d = -1/2 at^2 + V_0 t \\ at = V_0 \end{array} \right\} (a = \text{disturbance, } V_0 \text{ defined above})$$

Solving the above yields $\Delta I = 1.8 \times 10^{-3}$ lb-sec as the upper limit to the impulsed bit with a pulse occurring every 1506 seconds.

6.2.3.2 Minimum Impulse Bit

The only constraints on the lower impulse bit are that the thruster be able to maintain an average thrust level greater than the disturbance forces and not require an excessive number of pulses. The assumptions here are that a pulse repetition rate of one pulse every 5 seconds and total number of pulses per thruster of 10^7 are reasonable bounds. Since the peak average disturbance force is 2×10^{-5} pounds, this translates into 2×10^{-4} lb-sec (including a x2 safety factor). Since the propellant is equally spread in the plus and minus directions, two thrusters must be capable of 3150 lb-sec. The 10^{-7} pulse thruster requirement sets the lower bound of 1.575×10^{-4} lb-sec. The controlling lower bound is 2×10^{-4} lb-sec.

6.2.4 Orbit Plane Precession Due to Misalignment

In-orbit plane solar pressures are periodic (with respect to orbital coordinates). This means that alternate plus and minus thrusters will fire over an orbit. If a thruster is misaligned, it will create an out-of-plane component for approximately one-half an orbit. This is unfortunate, since, if the same out-of-plane component existed for the entire orbit, a bounded wobble of the orbit plane would occur. In this case, the precession can add up each orbit. A bias in the attitude control system which would cause a steady state yaw pointing error would produce the same problem in that the plus and minus thrusters would produce opposite out-of-plane thrusting around orbit and their effects would be additive in precessing the orbit plane. Also, a satellite misalignment between the attitude control yaw sensors and DISCOS-pulsed plasma thruster axis would produce the same effect. These misalignments are not known, and a tolerable precession for GPS is not known. However, for an average misalignment over the entire orbit (plus and minus thrusters) of 1 degree, the total out-of-plane precession is 0.73 feet when the sun is in the orbit plane. Since this is additive per orbit, it can become significant and must be taken into consideration when specifying and controlling out-of-plane misalignments.

6.2.5 Effects of Mass Shifts Within Satellite

Ideally, DISCOS is placed at the center of gravitational attraction of the satellite so that it is impervious to these forces. The mass will then react only to orbital gravitational forces and provide the desired reference. It is essential that these mass attractions from the satellite be $<10^{-8}$ g. For precise operation, it is desired that the sensitive axis (\hat{x}) satellite attraction be $\leq 10^{-11}$ g. However, if fixed attractions are greater than this, it is possible (but undesirable) to bias them out electrically after in-orbit tracking data determines the appropriate value. However, changes in mass distribution of the satellite during flight are more difficult to determine because they are not constant. The requirement then exists that changes in gravitation attraction on DISCOS of the satellite not exceed 10^{-11} g.

The principal sources of gravitation shift are in the solar array panels (while rotating) and hydrazine consumption. These two units are

built in pairs symmetrically located about DISCOS, hence ideally produce no net g shifts. The purpose of the calculations below is to provide tolerances on how far from ideal they may travel.

The basic gravitational attraction equation is

$$F = G \frac{M_1 M_2}{R^2}$$

where

F = gravitational force on either mass

M_1, M_2 = mass of two objects attracting each other

G = universal gravitational constant

R = separation of centers of mass of two objects

The g attraction is

$$g = G \frac{M_1}{R^2}$$

In terms of slugs mass and foot distance, 1 slug at 1 foot separation is approximately 10^{-9} g.

The total propellant loaded on the satellite is ~1.6 slugs and $R = 1.75$ feet, providing a net attraction of 0.5×10^{-9} g. These masses are ideally in a plane normal to \hat{x} , passing through the center of DISCOS so that no net force exists. However, if the center of mass of the propellant tanks is offset x feet from this plane along the \hat{x} axis, the net attractive force is (for small \hat{x})

$$g = \left(\frac{x}{1.75} \right) (0.5 \times 10^{-9})$$

constraining g to $\leq 10^{-11}$ yields

$$x < 0.035 \text{ ft } (0.42 \text{ inch})$$

The solar arrays weigh ~3.6 slugs and are separated by 10 feet from DISCOS. The net attraction is then 3.6×10^{-11} g and the allowable offset is 2.8 feet.

6.2.6 Attitude Control Considerations

The use of DISCOS does have a significant impact on the GPS in terms of functions, but little impact on actual equipment. DISCOS is used only for normal mode, in-orbit operation. At all times when hydrazine is used for spin mode operation (if required; acquisition, orbital trim, and occasional out of orbit plane corrections), DISCOS is caged and the pulsed plasma thrusters are inactive. Hence, they have no impact on operation. However, during normal mode the satellite is stabilized to point along the orbital coordinate set. The yaw axis is not rotated to maximize power on the solar panels; instead, the boom holding the panels is tilted to produce the same result. Yaw control must now be exerted via the sun sensor but compensated for the movement of the boom drive. This means that yaw error budgets must include sun sensor errors plus boom drive errors (which can be made very small).

Since a yaw misalignment can produce unacceptable precession of the orbit plane, this causes a tighter yaw pointing accuracy requirement on GPS than originally specified. The requirement should probably be <0.5 degree which should be achievable with the existing GPS ACS equipment. When the sun is near the orbit plane, around orbital noon and midnight, the sun is nearly collinear with the satellite to earth vector and provides a poor yaw reference. Fortunately, little \hat{x} axis solar pressure exists at this time, and the increased yaw errors are not as important since DISCOS activity is small.

The two axis controllable solar panels do offer a minor bonus for ACS. They provide at least two axes (and at times, three axes) of attitude torque capability (by controlling array orientations to modify solar pressure distribution). The capability can be used at least to reduce momentum buildup in the reaction wheels and possibly to unload the wheels. This would reduce the need for magnetics for unloading, and either remove some magnetics requirements or serve as a redundant backup to magnetics.

Pulsed plasma thrusters have such little overall impulse requirements that their total disturbance torques are small compared to other sources of disturbance. They add to momentum wheel unloading requirements less than 50 lb-sec for the 10-year lifetime of the satellite.

6.3 PROPULSION SYSTEM COMPARISON

The characteristics of pulsed plasma and gas propulsion systems for performing the DISCOS functions were evaluated.

6.3.1 Gas Propulsion for GPS/DISCOS

Two candidate gas propulsion systems were sized. The key requirements for this auxiliary system are summarized in Table 42.

The GPS contains a conventional hydrazine propulsion system with 5 and 0.2 lbf catalytic thrusters for acquisition, orbit velocity control and attitude control. However, the DISCOS requirements for impulse bit and number of pulses exceed the qualified capabilities of the existing GPS hydrazine system and other qualified catalytic thrusters. Therefore, only cold gas (nitrogen) and M35 decomposed hydrazine plenum systems were considered as most representative of existing, qualified systems which can easily meet the propulsion requirements.

6.3.1.1 Cold Gas System

A schematic diagram of the gaseous nitrogen system is shown in Figure 41. Two tanks were baselined to facilitate the accommodation of the system into the existing GPS (available spacecraft volume will dictate the tank size and number). The system weight is delineated in Table 43. Weights for both existing qualified tanks and a new tank sized for minimum

Table 42. GPS/DISCOS Propulsion Requirements

Total Impulse	3200 lb-sec
Impulse per Thruster	1600 lb-sec
Number of Thrusters	4 (2 primary - 2 redundant)
Impulse Bit	$\leq 1.8 \times 10^{-3}$ lb-sec per pulse
Duty Cycle	$\leq 1\%$
Number of Pulses	889,000 pulses

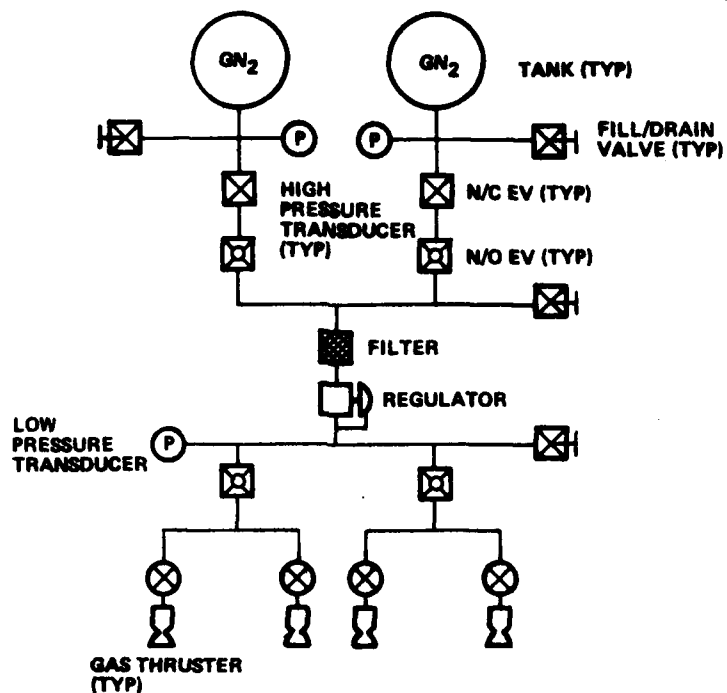


Figure 41. GN₂ System Schematic Diagram

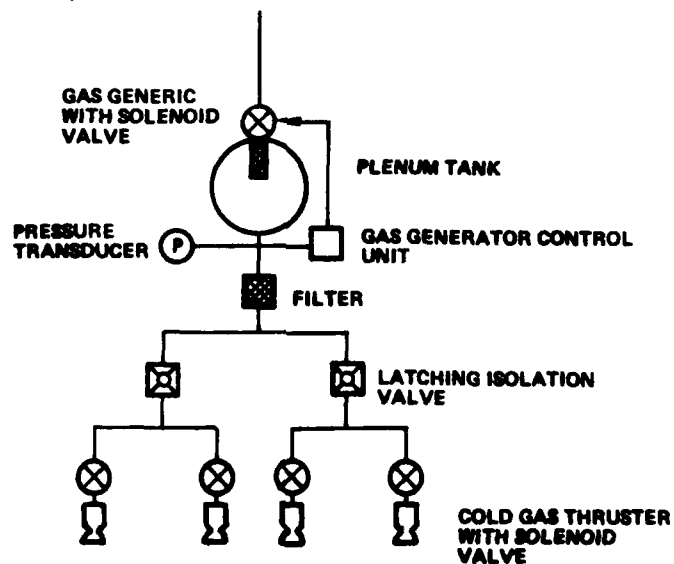


Figure 42. M35 Plenum System Schematic Diagram

Table 43. Cold Gas System Weight Summary

Component	Unit Weight (lb)	Total Weight (lb)
<u>Dry Weight</u>		
Tank (2)	28.6*	57.2*
F/D Valve (4)	0.22	0.9
Pressure Transducers (3)	0.4	1.2
N/C Valve (2)	0.4	0.8
N/O Valve (4)	0.4	1.6
Filter (1)	0.7	0.7
Regulator	1.0	1.0
Thruster Assembly (4)	1.0	4.0
Tubing, Brackets, Misc.	15.0	15.0
		82.4
<u>Pressurant Weight</u>		50.0
Total System Weight		132.4

* Available qualified tank weight = 40 lb/tank. Listed weight is for new tank of minimum weight.

weight are included in the weight summary. The qualified performance capability of the system is shown in Table 44 and compared against the requirements. All requirements have been demonstrated with adequate margin.

6.3.1.2 M35 Plenum System

The M35 plenum system consists of a hydrazine catalytic gas generator, plenum tank for storage of the decomposed hydrazine gas products, a gas generator control unit that maintains plenum tank pressure within a prescribed band, pressure transducer, and associated thrusters and valves as shown in Figure 42. The decomposed hydrazine is delivered at a cool temperature (<100°F for low gas usage) to conventional gas thrusters. For

Table 44. Application Requirements vs Capability Summary for Gas Propulsion for GPS/DISCOS

Parameter	Requirement	Capability	
		Gaseous Nitrogen	M35 Plenum
Total Impulse	3200 lb-sec	>3200 lb-sec	>3200 lb-sec
Impulse per Thruster	1600 lb-sec	>1600 lb-sec	>1600 lb-sec
Impulse Bit	$\leq 1.8 \times 10^{-3}$ lb-sec	0.4×10^{-3} lb-sec at 20 msec pulse width	0.8×10^{-3} lb-sec at 20 msec pulse width and 35 psia inlet pressure
Number of Pulses	$\leq 889,000$	>1,000,000	>1,000,000
Tank Pressure	N/A	4200 psia	0 to 100 psia (35 psia nominal)
Regulator Pressure	N/A	50 \pm 2.5 psia	35 \pm 1.0 psig tank pressure controlled by GGCU
Thrust	N/A	0.018 lbf at 50 psia	0.039 lbf at 35 psia
Average I_{sp}	N/A	65 sec	105 sec
Propellant Throughput	31 lb N ₂ H ₄ for plenum system 50 lb N ₂ for cold gas system	50 lb (function of available tank capacity)	100 lb N ₂ H ₄

this system sizing, it was assumed that hydrazine for the auxiliary propulsion system can be supplied from the existing hydrazine system on GPS, therefore, no additional tanks are required.

The weight breakdown is presented in Table 45. The combination of higher I_{sp} for the decomposition gas products and no additional tanks results in an 85-pound weight saving over the nitrogen system.

The qualified performance capability of the plenum system is shown in Table 43. The plenum system can easily meet all performance requirements without modification.

6.3.1.3 Other System Considerations

For both systems, the following data can be used for evaluating propulsion/spacecraft performance. Each system contains potential single point failures (regulator and gas generator) which can be eliminated with addition of redundant hardware and increased system complexity. However, for this study, configurations with thruster redundancy only were baselined.

- Geometric Thrust Vector. ≈ 0.5 degree for typical nozzle dimension tolerances. May be minimized by greater control of dimension tolerances.
- Impulse Repeatability. $\pm 10\%$ variation. Assumed 5% inlet pressure and valve voltage variation, 5% valve open time variation for a 50 msec nominal electrical pulse width. Thruster-to-thruster impulse matching can be as high as 20% dependent upon thruster dimension and performance variation.
- Minimum Pulse Width. ≥ 20 msec for the dual coil, dual seat valve typically used by TRW for hydrazine and cold gas systems. Single seat valves are available with electrical pulse width capabilities down to 5 msec.

6.3.2 Pulsed Plasma Propulsion GPS/DISCOS

The GPS/DISCOS propulsion requirements can be met by LES-9 type pulsed plasma thrusters operated at 3000 volts. The total system performance is shown in Table 46. In normal operation the thrust would be divided equally between fore and aft thrusters. To guarantee no single point failure will require a total of four thruster assemblies, resulting in a total system weight of approximately 68 pounds.*

*Based on weight estimates supplied by Dr. R. Vondra of AFRPL.

Table 45. M35 System Weight Summary

Component	Unit Weight (lb)	Total Weight (lb)
<u>Dry Weight*</u>		
Gas Generator Assembly (1)	5.0	5.0
Pressure Transducer (1)	0.5	0.5
Filter	0.7	0.7
Latching Isolation Valves (2)	0.6	1.2
Thruster Assembly (4)	1.0	4.0
Lines, Bracket, Misc.	<u>5.0</u>	<u>5.0</u>
		16.4
<u>Propellant Weight</u>		<u>30.5</u>
Total System Weight		46.9 lb

* Assumed no additional tank weight for hydrazine; existing spacecraft RCS tankage can accommodate additional 30.5 pounds of hydrazine.

Table 46. Upgraded LES-9 Pulsed Plasma Performance for GPS/DISCOS

Discharge Voltage	3000 volts
Discharge Energy	80 joules
Impulse Bit	340 μ lb-sec
Specific Impulse	1450 sec
Total Impulse	3400 lb-sec
Number of Pulses	10^7 pulses

The system comparisons with the nitrogen cold gas and hydrazine gas generator propulsion systems are shown in Table 47. It can be seen that the hydrazine gas generator system is the lightest. This weight advantage would disappear if the hydrazine system were required to include completely redundant propellant supply.

Table 47. Propulsion System Comparison for GPS/DISCOS
Application Candidate System

Parameter	Teflon Pulsed Plasma	Gaseous Nitrogen	Hydrazine Gas Generator
Total Impulse (lb-sec)	3200	3200	3200
Impulse Bit (mlb-sec)	0,34	1.8	1.8
Number of Pulses (Total/All Thrusters)	9.4×10^6	1.8×10^6	1.8×10^6
Specific Impulse (sec)	1450	65	105
Propellant Weight (lb)	4.4 ^a	50	31
System Weight (lb)	68	132	47 ^b , 54 ^c

^aIncludes 100% propellant redundancy

^bBased on using excess tankage capacity already available on GPS

^cAssumes 7 lb additional dedicated tankage and valving

6.4 CONCLUSIONS

The GPS Phase III space vehicle is potentially capable of being redesigned to accommodate a DISCOS navigation system. Major modifications required include the following:

- Two degree of freedom solar array
- Relocation of existing hydrazine thrusters
- Redistribution and symmetrization of mass distribution
- Redesign of satellite thermal control system
- Possible redesign of antenna farm

The DISCOS propulsion function can be provided by either a gaseous nitrogen, hydrazine gas generator or solid Teflon pulsed plasma propulsion system (upgraded LES-9 configuration). The pulsed plasma system will produce a payload weight advantage of 64 pounds compared to gaseous nitrogen, and a payload weight penalty of 14 to 21 pounds compared to a hydrazine gas generator.

VII. RECOMMENDATIONS FOR FUTURE DEVELOPMENT

In the course of evaluating the millipound pulsed plasma propulsion system for Air Force missions, several areas requiring future development were identified. These are summarized below.

- Increase Total Impulse Capability. A 68,000 lb-sec capability will provide a no single point failure for the entire 10-year DSCS-III mission. A 55,000 lb-sec capability will provide DSP with 0.12 degree inclination control at the end of a 7-year life with no single point failure.*
- Build and Life Test Prototype Flight Hardware. Long term wearout modes must be evaluated quantitatively and full operation demonstrated before the system can be accepted for operational use.*
- Improve Capacitor Reliability Model. Failure rate and life statistical distribution must be measured for prototype capacitor designs. Theoretical models need to be developed to allow tradeoffs of capacitor size and number versus system weight, cost, and reliability. The technical feasibility of developing capacitor switching and status monitoring hardware should be explored to determine if redundant capacitors can be profitably utilized in thruster assemblies.
- Improve Interactive Effects Data Base. Interactive effects will be a major concern to satellite designers until sufficient data are available to demonstrate the compatibility of pulsed plasma propulsion with sensitive spacecraft subsystems. Specific measurements needed include charged particle measurements down to the $\epsilon = 10^{-11}$ flux level (to improve ability to estimate neutral fluxes), electric field measurements of the primary discharge from 1.6 to 10 GHz and trigger noise from 1 to 10 GHz, and H-field data from 10 Hz to 15 kHz. Finally, it is recommended that shuttle-borne plume effects experiments be performed in order to avoid the facility backscattering problem that exists with laboratory measurements.

*The current updated AFRPL millipound Pulsed Plasma Thruster Development program calls for a 70,000 lb-sec total impulse capability and a confirming life test.

REFERENCES

1. D.J. Palumbo and W.J. Guman, "Continuing Development of the Short-Pulsed Ablative Space Propulsion System," AIAA/SAE 8th Propulsion Specialist Conference, New Orleans, LA, 1972.
2. W.J. Guman and S.J. Kowal, "Pulsed Plasma Propulsion System for TIP-II Satellite," JANNAF Propulsion Conference, 1975.
3. "Mission Integration Study for Solid Teflon Pulsed Plasma Millipound Propulsion System," Appendix A, DSCS-III Data, TRW Report 33775-6002-RE-00, 5 October 1978.
4. B.A. Free, W.J. Guman, B.G. Herron, and S. Zafran, "Electric Propulsion for Communications Satellites," AIAA Paper 78-537, April 1978.
5. D.H. Mitchell and M.N. Huberman, "Ion Propulsion for Communications Satellites," Progress in Astronautics and Aeronautics, Vol. 55, 1977, pp 199-220.
6. D.H. Mitchell and S. Zafran, "Ion Propulsion for Spacecraft Reaction Control," AIAA Paper 78-651, April 1978.
7. S. Zafran, ed., "Ion Engine Auxiliary Propulsion Applications and Integration Study," NASA CR-135312, July 7, 1977.
8. D.J. Palumbo, W.J. Guman, and M. Begun, "Pulsed Plasma Propulsion Technology," AFRPL-TR-74-50, July 1974.
9. W.J. Guman, "Task 1 - Design Analysis Report, Pulsed Plasma Solid Propellant Microthruster for the Synchronous Meteorological Satellite," NASA-CR-122358, December 1971.
10. "Reliability Estimating Procedures for Electric and Thermochemical Propulsion Systems," Booz Allen Applied Research, AFRPL-TR-76-99, February 1977.
11. "Generic Failure Rates for Spacecraft Applications," TRW IOC No. 74-2288-051, July 1974.
12. "Standardized Failure Rate Data," Bureau of Naval Weapons, April 1970.
13. N.H. Fischer and A.E. Tischer, "Study of Multimission Modular Spacecraft (MMS) Propulsion Requirements," NASA-CR-159919, August 8, 1977.
14. F. Etheridge, W. Cooper, and J. Mansfield, "Landsat/MMS Propulsion Module Design," Rockwell International Space Division, Report SD 76-SA-0095-3, September 24, 1976.
15. S. Zafran and J.J. Biess, "Ion Propulsion Cost Effectivity," NASA-CR-159902, December 1978.

16. "Possible Material Transport, Accretion and Alteration Process," Internal TRW Technical Memorandum from J.M. Sellen to DSP Project Office, 1972.
17. P.F. Jones and E.N. Borson, "The Effects of Deposition and Irradiation of Contaminants from the Outgassing of Silastic 140 RTV," Aerospace Report TOR-0059 (6129-01)-56, February 10, 1971.
18. "Contamination of Second Surface Mirrors I. Prelaunch Cleaning Procedure, a Radiation Study," Technical Memorandum from P.D. Fleischauer and A.R. Calloway to D.W. Moore, The Aerospace Corporation, Technical Memorandum 73-4070-CP-682, February 21, 1973.
19. P.D. Fleischauer and L. Tolentino, "The Far Ultraviolet Photolysis of Polymethylphenylsiloxane Films on Quartz Substrates," Proceedings of the 7th Conference on Space Simulation, NASA SP-336, p. 645, November 1973.
20. "Contamination Analysis/Design," Report 5359, Section 4, AESC.
21. C.R. Maag, Jr., "Status of the SPADS Contamination Analysis Program," AESC Technical Interchange Meeting 3, October 11, 1977.
22. "Pulsed Plasma Radio Frequency Interference Studies," AFRPL-TR-77-85, September 1977.
23. Navigation, Vol. 25, No. 2 Summer 1978.
24. L. Jacobson and L. Huffman, "Satellite Navigation with GPS," Satellite Communications, 16, July 1979.
25. "GPS Phase III Space Vehicle Systems Engineering Study," Final Report SSD-79-0108, Rockwell International, 27 April 1979.
26. "A Satellite Freed of All but Gravitational Forces: TRIAD I," Journal of Spacecraft and Rockets, Vol. 11, No. 9, September 1974, pp 637-644.
27. B.O. Lange, "Control and Use of a Drag Free Satellite," Stanford University SUDAAR, June 1964.
28. W.J. Guman and S.J. Kowal, "Pulsed Plasma Propulsion System for TIP-III Satellite," JANNAF Propulsion Meeting, 1975.
29. F.F. Mobley, et al, "Electromagnetic Suspension for the TIP-III Satellite," IEEE Transactions on Magnetics, Vol. MAG-11, No. 6, November 1975.
30. S.J. Kowal, JHU Applied Physics Laboratory Memo S4S-0-001, 2 February 1973.